Weldability

Module 5

Module 5 – Weldability

- 5A – Weld Defect Types
  - 5A.1 – Solidification and Liquation Cracking
  - 5A.2 – Solid-State Cracking
  - 5A.3 – Hydrogen-Induced Cracking
  - 5A.4 – Fatigue and Fracture
- 5B – Corrosion
- 5C – Fractography
- 5D – Case Studies

Module 5 Learning Objectives

- Definition of metallurgical and geometric defects in welds
- Basic understanding of different forms of weld cracking
- Differentiating different types of cracking
- Basic fatigue and fracture principles
- Different forms of corrosion
- Corrosion cracking associated with welds
- Basic aspects of failure analysis

Weld Defect Types

Module 5A

Types of Weld Defects

- Fabrication-related
  - Associated with primary fabrication or repair
  - Can be controlled by combination of metallurgical and welding process factors
  - Use of appropriate inspection techniques is critical
- Service-related
  - Occur upon exposure to service environment
  - Generally mechanically or environmentally induced
  - May result from remnant weld defects or metallurgical phenomena associated with the weld thermal cycle
  - Inspection and design issues are important to control defect formation and monitor propagation

Fabrication-Related Defects

- Process control
  - Lack-of-fusion (LOF)
  - Weld undercut
  - Excessive overbead or drop through
  - Lack of penetration (LOP) or incomplete penetration
  - Slag inclusions
  - Porosity, voids
  - Craters, melt-through, spatter, arc-strikes, underfill
  - Sugaring
    - Oxidation of root pass
  - Cracks
- Other
  - Metallurgical anomalies (e.g., local softening or embrittlement)
  - Geometric defects (design or fitup); e.g., distortion

Lack of Fusion

- Inability to wet the surfaces of the weld joint area completely leaving behind voids
  - Reduced load-carrying capacity
- Detection
  - Radiography and ultrasonic inspection
- Common Causes
  - Improper process parameters
    - Liquid metal too “cold” to fuse to the base material
  - Improper welder technique
    - No weaving
  - Poor access
    - Bad joint design
  - Material composition
    - Viscous flow

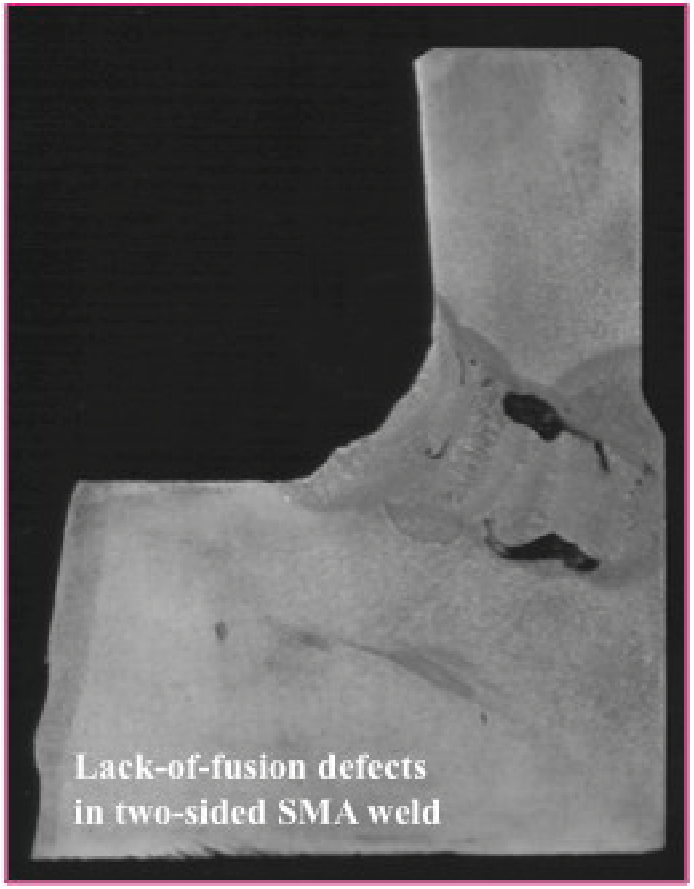

Weld Undercut

- Not efficient tie up of weld metal and base metal region
  - Leads to premature fatigue failure
- Detection
  - Visual and dye penetrant inspection
- Common Causes
  - Improper welding technique
    - Concave weld profile
    - Improper weave technique
  - Improper process parameters
    - Excessive current

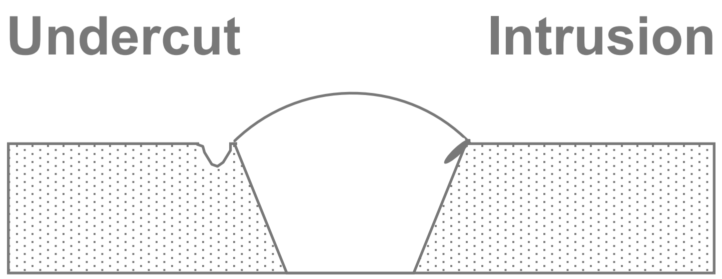

Over-Bead or Drop-Through

- Over-bead (A) happens during capping pass
- Drop-through (B) happens during root pass
- Detection
  - Nondestructive
    - X-ray, visual and dye penetrant inspection
  - Destructive
    - Optical metallographic methods
- Causes
  - Inadequate welder skill
  - Procedure restrictions
  - Joint geometry restrictions

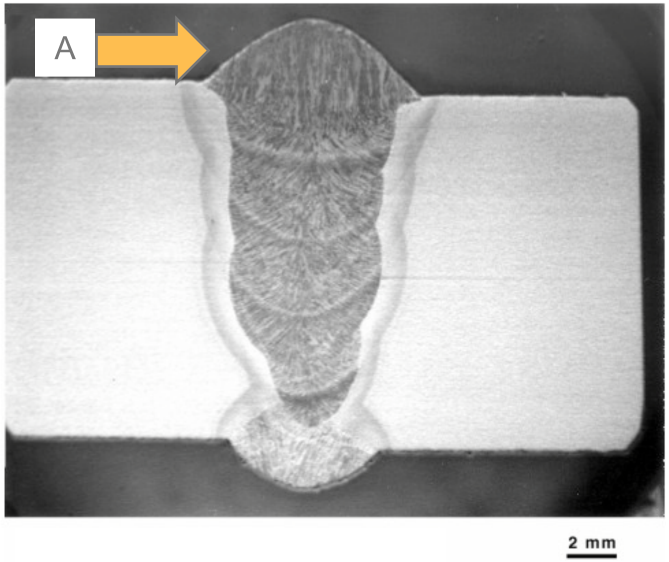

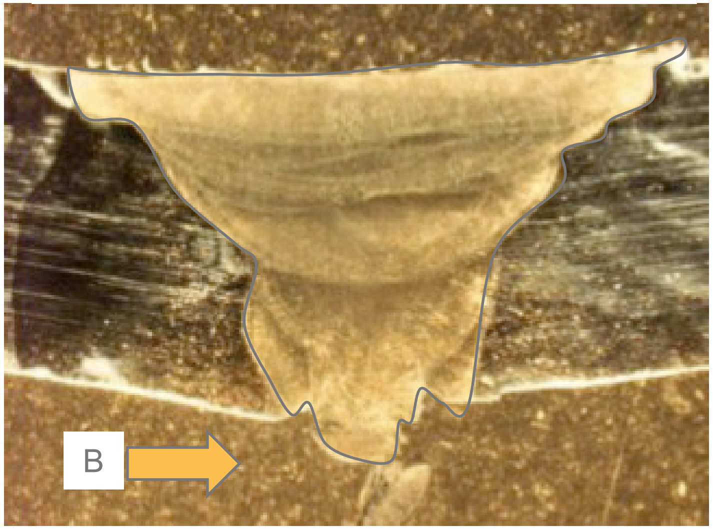

Incomplete Penetration

- Weld pool does not penetrate the whole plate thickness
- Detection
  - Nondestructive
    - Visual, dye penetrant inspection, radiography and ultrasonic inspection
  - Destructive
    - Optical metallographic methods
- Causes
  - Inadequate welder skill
  - Procedure restrictions
  - Joint geometry restrictions
  - Material chemistry changes

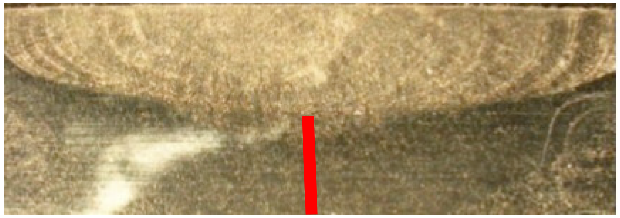

Shallow Penetration

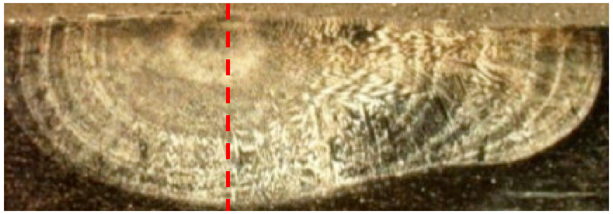

Deep Penetration

Entrapped Slag Inclusions

- This occurs in flux-shielded processes (e.g. SMAW, SAW, and FCAW)
- Detection
  - Radiography and ultrasonic inspection
- Causes
  - Improper welding technique
    - Incomplete removal of the slag from previous bead
  - Poor joint access
  - Inefficient partitioning of inclusions from molten metal

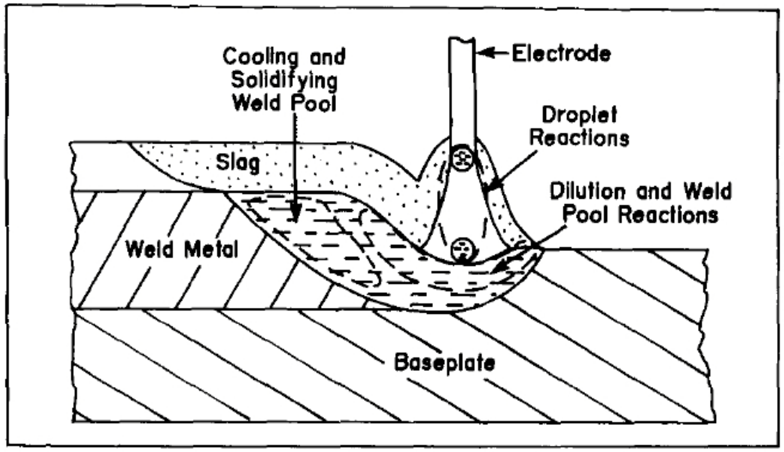

Fig. 1—The three reaction zones which control the chemical composition of the weld metal during SAW.

Ref: Mitra and Eager, 1999

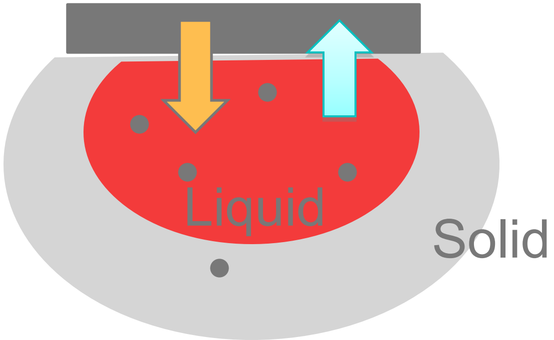

Porosity

- Gas Porosity
  - Molten metals always dissolve more gases than solids so during molten metal solidifies the inability to outgas leads to gas porosity
- Shrinkage porosity
  - Liquid to solid transition in metals leads to shrinkage creating voids and the inability to fill the voids leads to shrinkage porosity
- Detection
  - Visual, dye penetrant inspection, radiography and ultrasonic inspection
- Causes
  - Improper welding technique
  - Improper process parameters
    - Shielding gas, welding conditions, etc.
  - Material composition

Porosity

- Materials – Process interactions are complex during welding
- For similar processing conditions, the change in filler composition leads to a dramatic difference in porosity

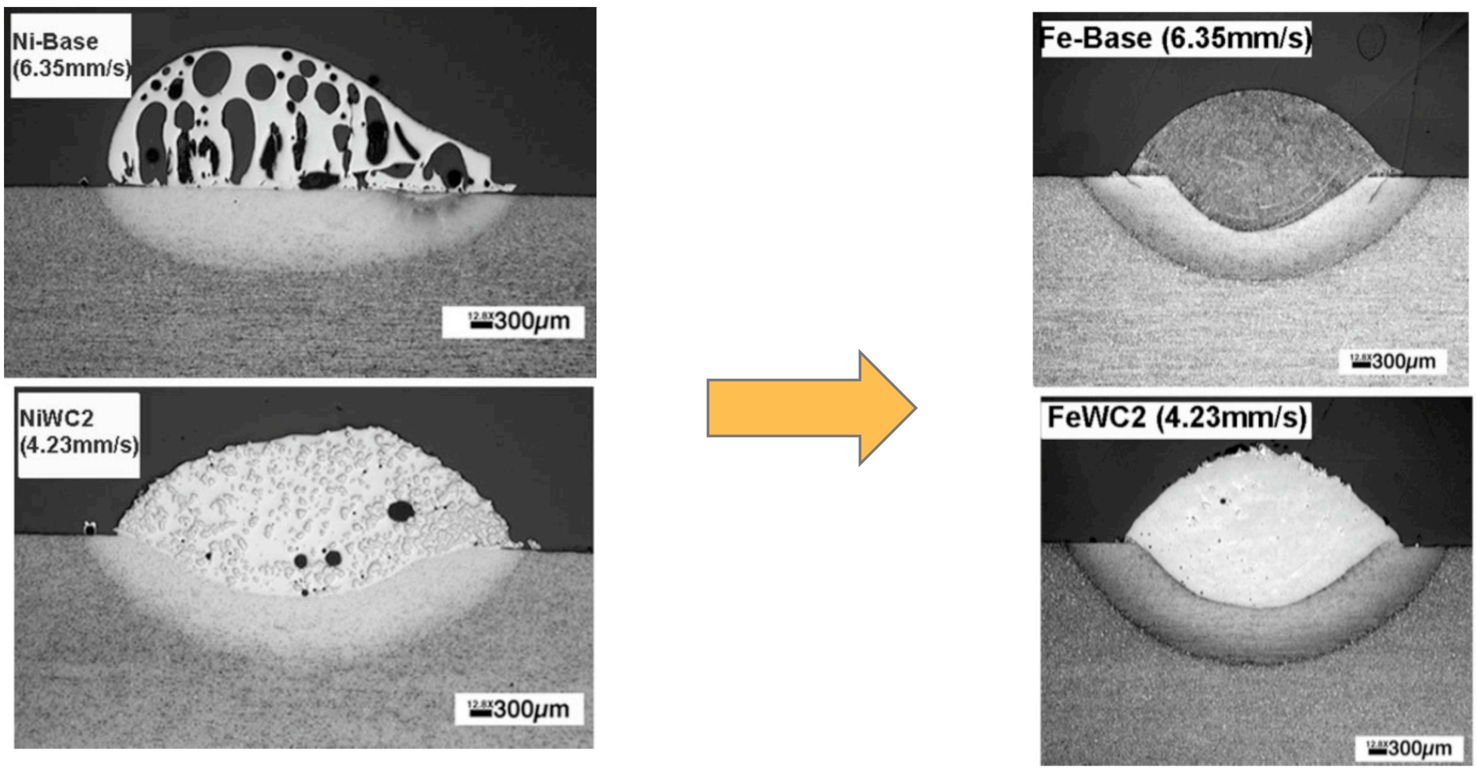

Laser Surface Alloying for hard and corrosion resistance coatings

Oxidation (Sugaring)

- Oxidation at high temperatures removal elements like Cr from the alloy which may lead to preferential corrosion and/or creep failure
- Detection
  - Visual
- Causes
  - Improper welding technique
    - Incomplete shielding of the root pass
  - Poor joint access

Courtesy: CAPSTONE Project by F. Augestine, J. Hurst and J. Rule, OSU, 2009

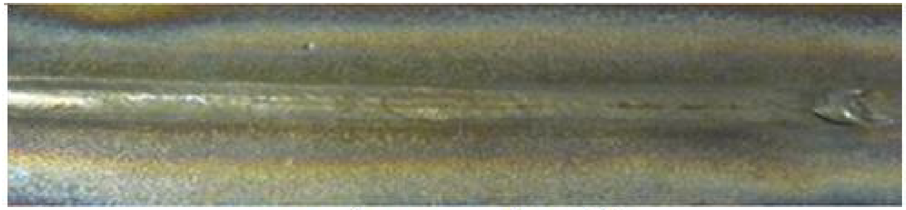

Back Purged Weld

Unshielded Backside Weld

Local Hardening/Softening

- Thermal cycles and material composition may change the local mechanical properties
  - Multi-pass pipeline hardness distributions
    - Blue: soft
    - Red: hard
- Detection
  - Destructive hardness testing
- Causes
  - Material composition
  - Process parameters

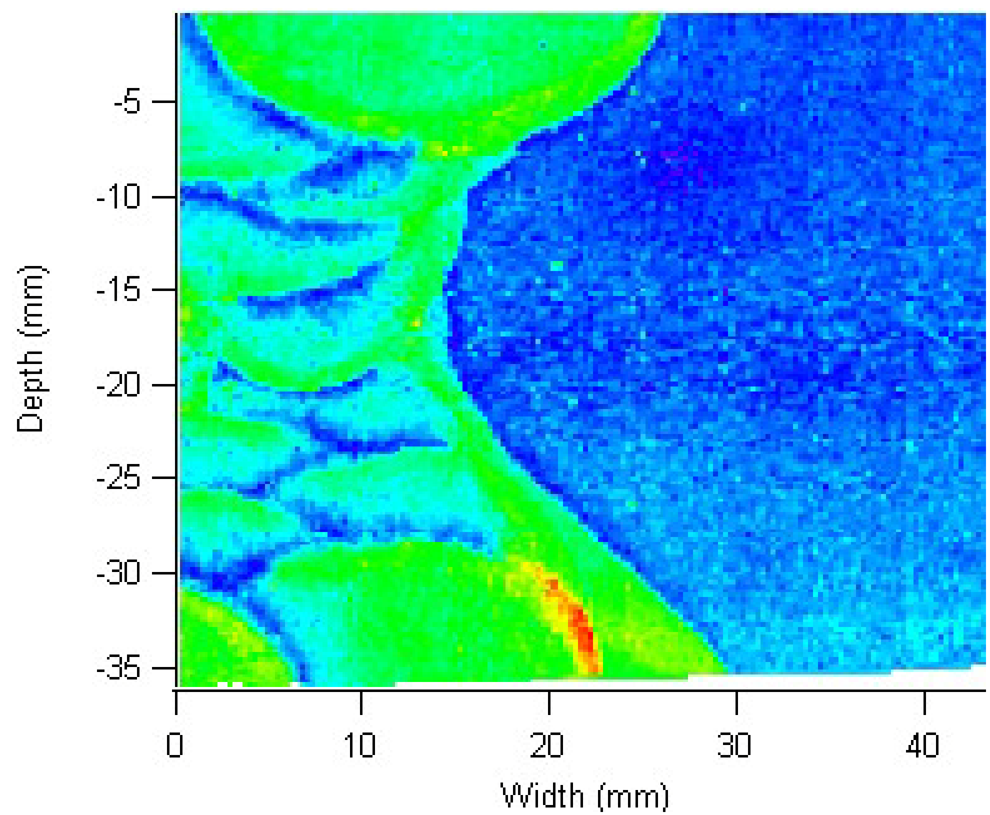

Dimensional Defects: Distortion

- Distortion happens due to localized plastic flow and resulting imbalance of internal stresses
- Main factors are geometry and processing conditions with secondary factors including material microstructure
- This topic is beyond the scope of the present module

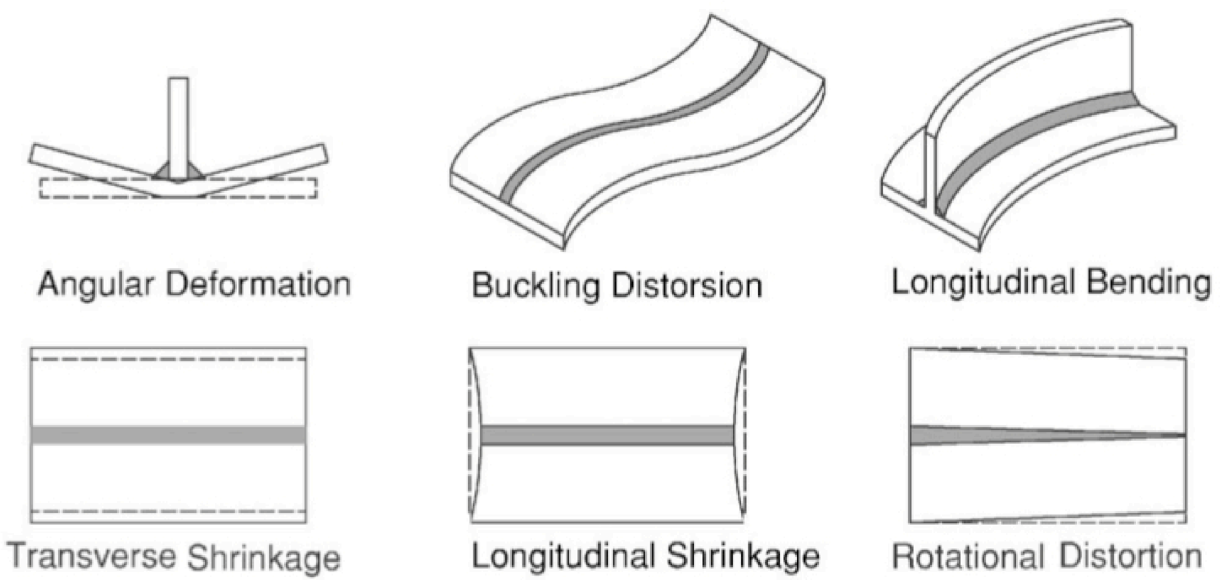

Reference: Masubuchi, 1980

Fabrication-Related Defects - Cracks

- "Hot" cracking
  - Weld solidification
  - HAZ liquation
  - Weld metal liquation
- "Warm" cracking
  - Ductility dip
  - Reheat/PWHT
  - Strain-age
  - Liquid metal embrittlement (LME)
- "Cold" cracking
  - Hydrogen-induced cracking
  - Delayed cracking

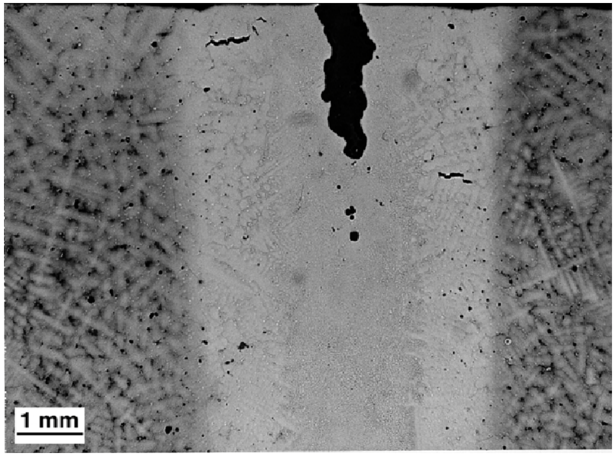

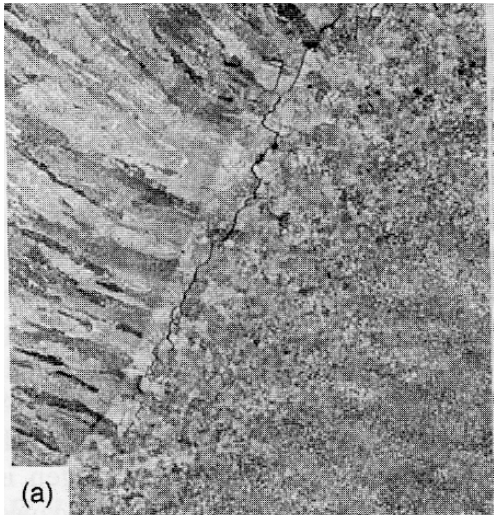

- This module will discuss these defects in more detail

Service-Related Damage Mechanisms

- Hydrogen-induced
- Environmentally-induced (e.g., corrosion)
- Fatigue
- Stress-rupture
- Creep and creep-fatigue
- Corrosion-fatigue
- Mechanical overload

- This module will discuss these defects briefly due to the wide variety and complexity of different service conditions

Solidification and Liquation Cracking

Module 5A.1

Fabrication-Related Defects - Metallurgical

- "Hot" cracking
  - Weld solidification
  - HAZ liquation
  - Weld metal liquation

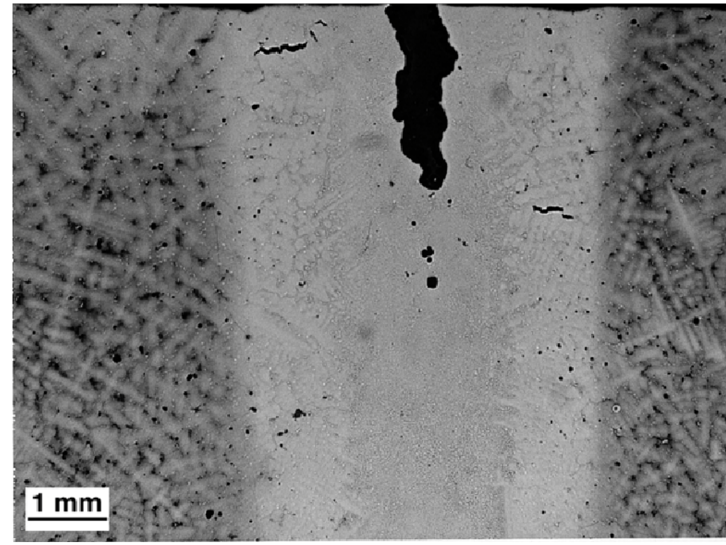

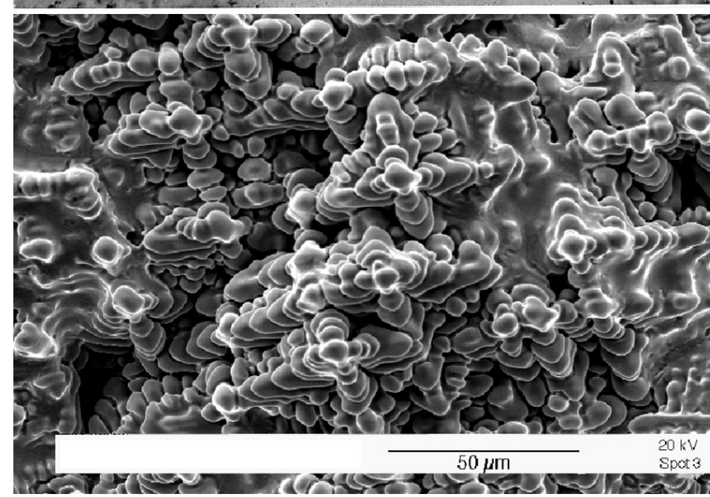

Weld Solidification Cracking

- Two essential elements
  - Susceptible microstructure
    - Large solidification temperature range
    - Liquid films present along solidification grain boundaries
  - Restraint
    - Shrinkage resulting from solidification
    - Thermal contraction
    - Imposed (external) forces

Solidification Cracking Temperature Range

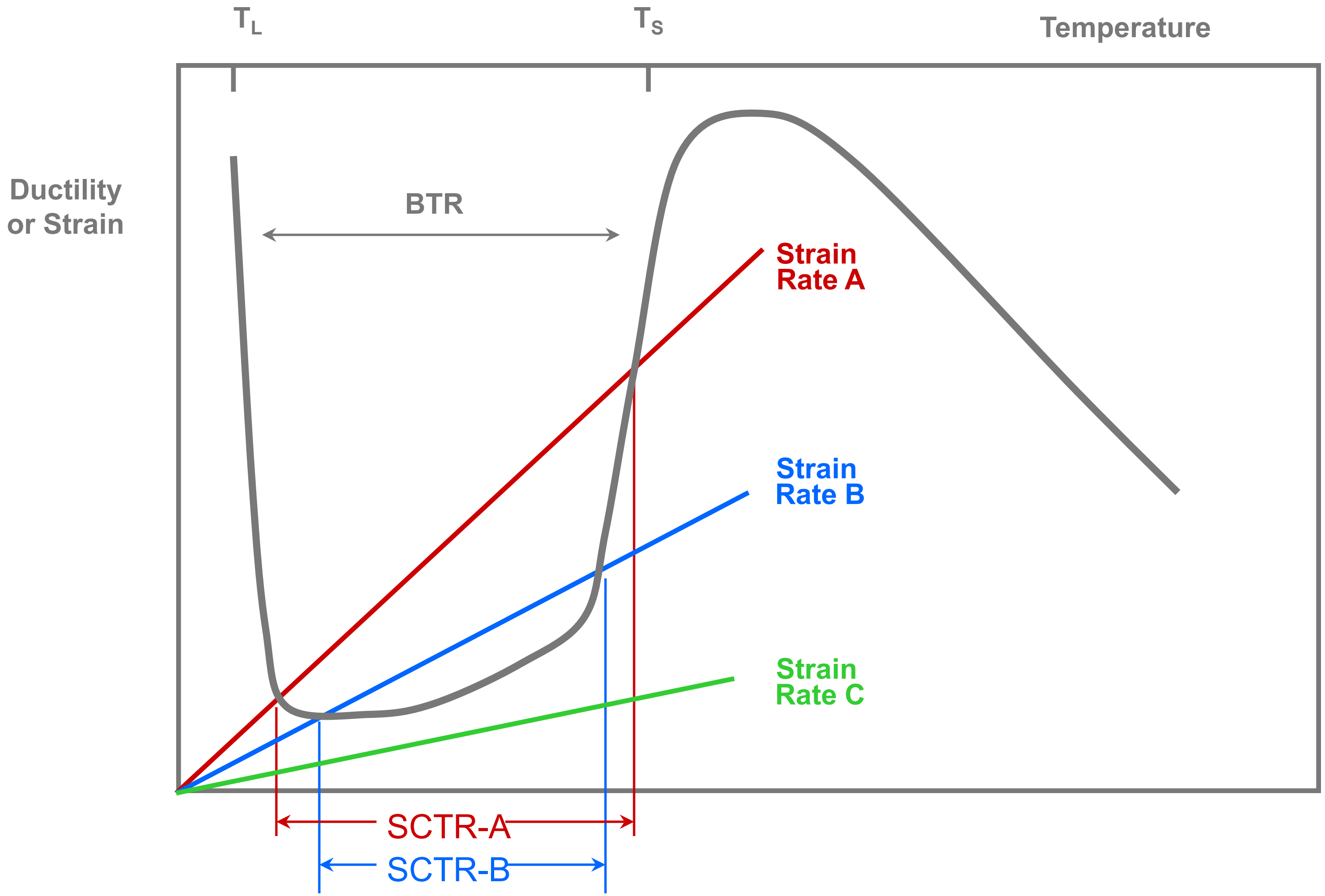

Relative and Maximum Potency Factors for Iron-Based Binary Systems

	Element in Iron-binary System							
	S	B	C	P	Ti	Nb	Mn	Si
Index showing sensitivity for solidification racking	925	917	322	121	14	29	26	2

Demonstration of Phase Diagram

Factors Influencing Weld Solidification Cracking

- Composition
  - Alloying elements
  - Impurity elements
- Nature of grain boundary liquid films
  - Volume fraction
  - Wetting characteristics
- Weld pool geometry
- Weld bead geometry
- Restraint

Circular Patch Test

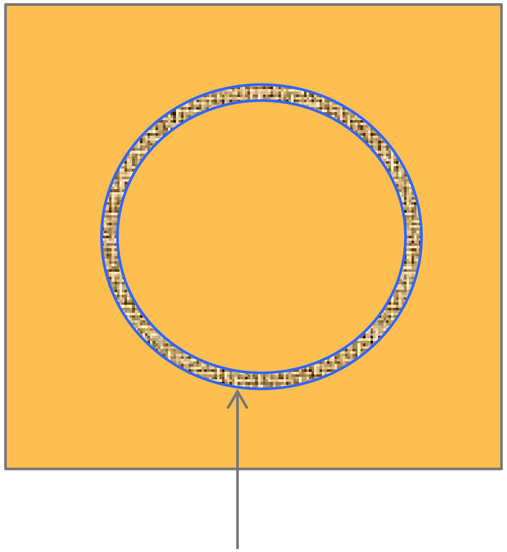

Restraints usually accentuate the solidification cracking, as a result, such geometries are used for evaluating cracking resistance of alloys

Composition

- Alloying elements
  - Effect on solidification behavior (e.g. austenite versus ferrite solidification in steels)
  - Partitioning during solidification may promote eutectic formation (e.g. Al- and Ni-base alloys)
- Impurity elements
  - Partitioning of impurities (e.g., S, P, and B in steels) significantly depresses terminal solidification temperature
  - These elements often enhance the wetting characteristics of the terminal liquid at the SGB

Grain Boundary Liquid Films

- Cracking is associated with liquid films along grain boundaries.
- The nature of these liquid films is controlled by:
  - Volume fraction of liquid
  - Grain boundary area
  - Wetting characteristics

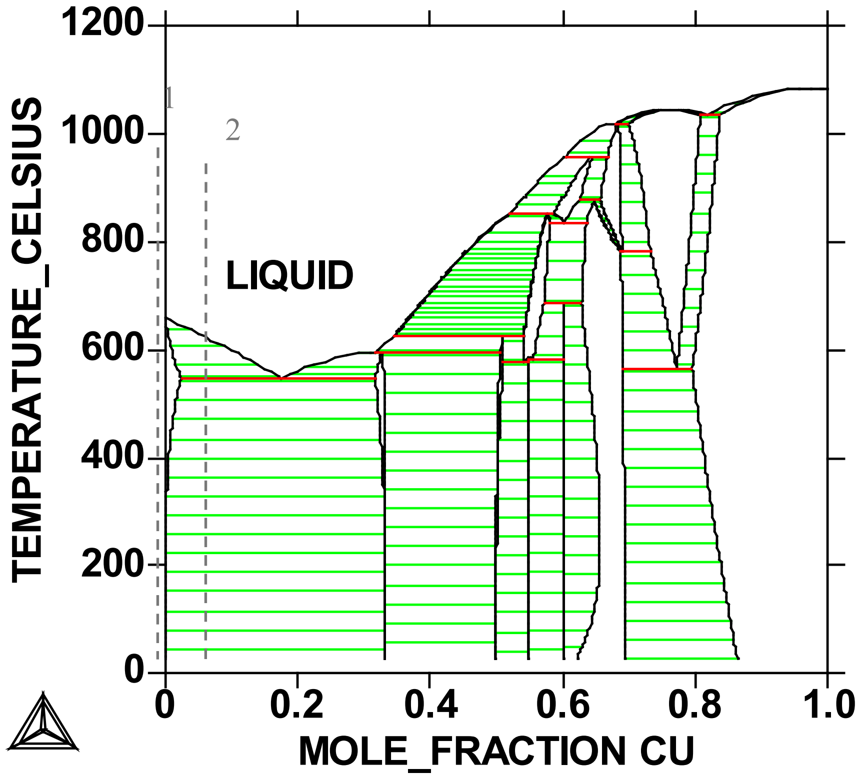

Percent Eutectic Liquid versus Cracking Susceptibility

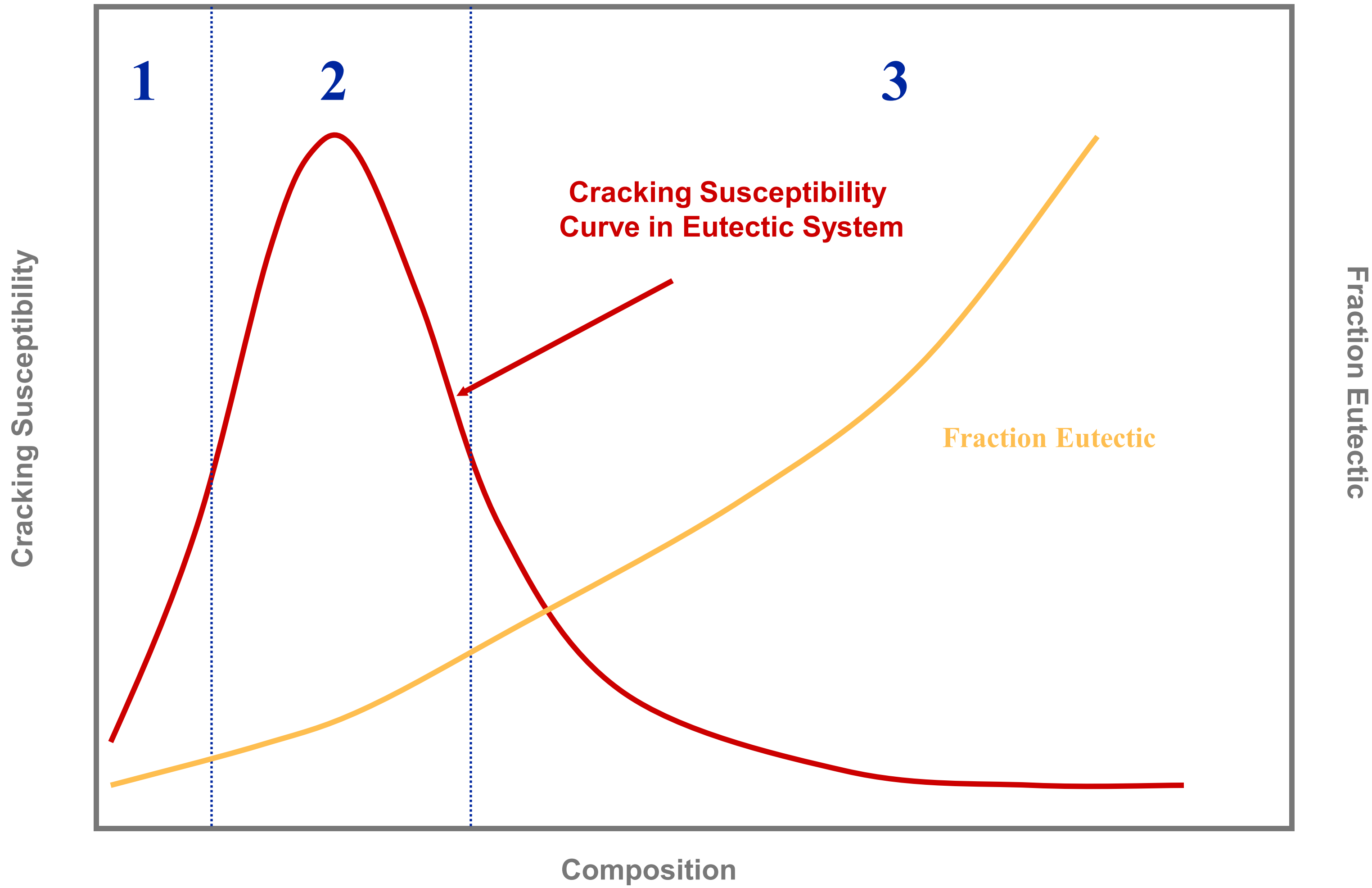

Weld Pool Geometry Also Affects Solidification Cracking

Teardrop Shape

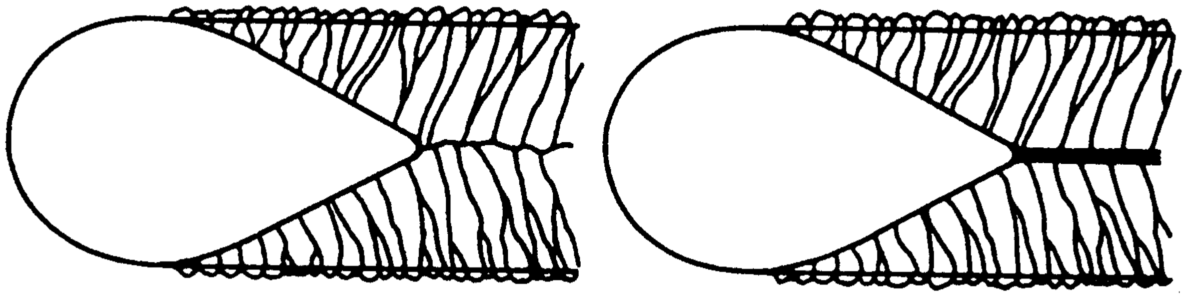

Elliptical Shape

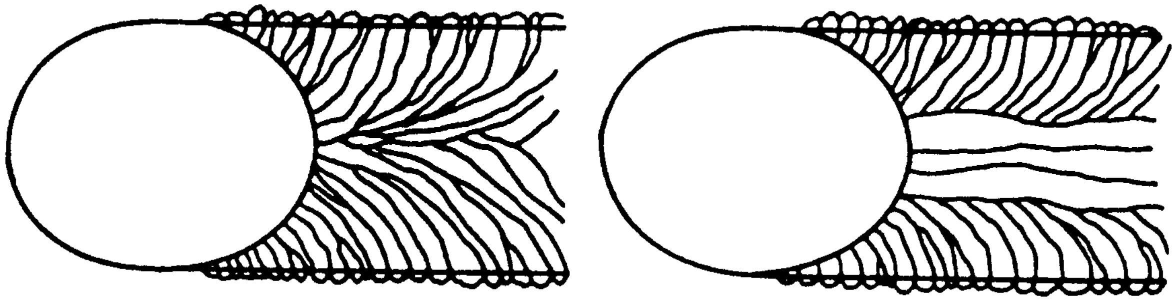

Weld Bead Geometry

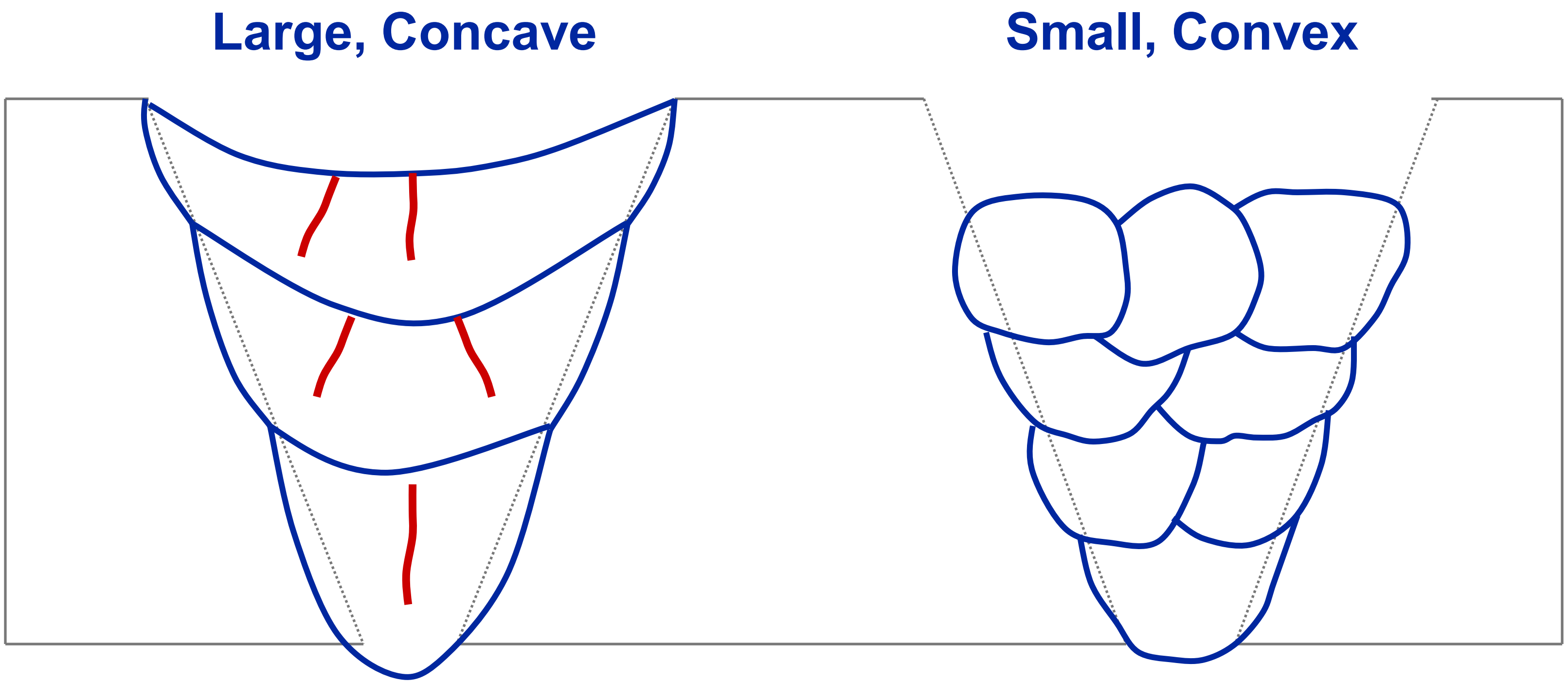

Restraint

- Intrinsic
  - Base metal and weld metal strength
  - Material thickness
  - Joint design
- Extrinsic
  - Fixturing
  - Applied stress

Identifying Weld Solidification Cracks

- Where?
  - Along solidification grain boundaries, occasionally along solidification sub-grain boundaries
- When?
  - During final stages of solidification
- How?
  - Metallography
  - Fractography - exhibit distinct dendritic fracture morphology

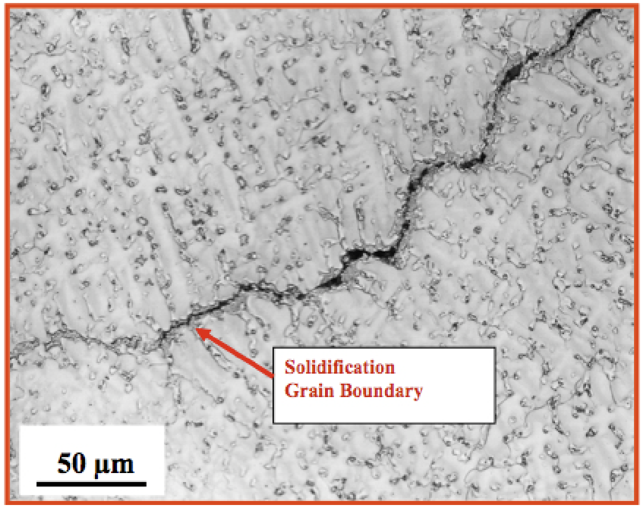

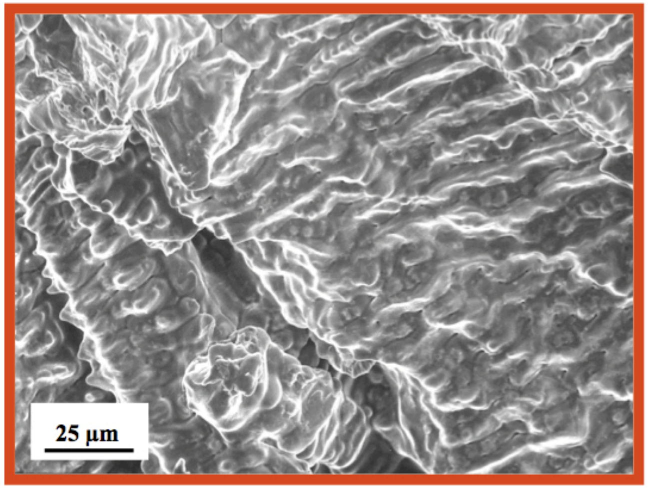

Preventing Weld Solidification Cracks

- Composition
  - Solidification control (BCC vs. FCC)
  - Impurity content
  - Liquid film formation
- Process control
  - Heat input
  - Bead shape
- Restraint
  - Intrinsic
  - Extrinsic

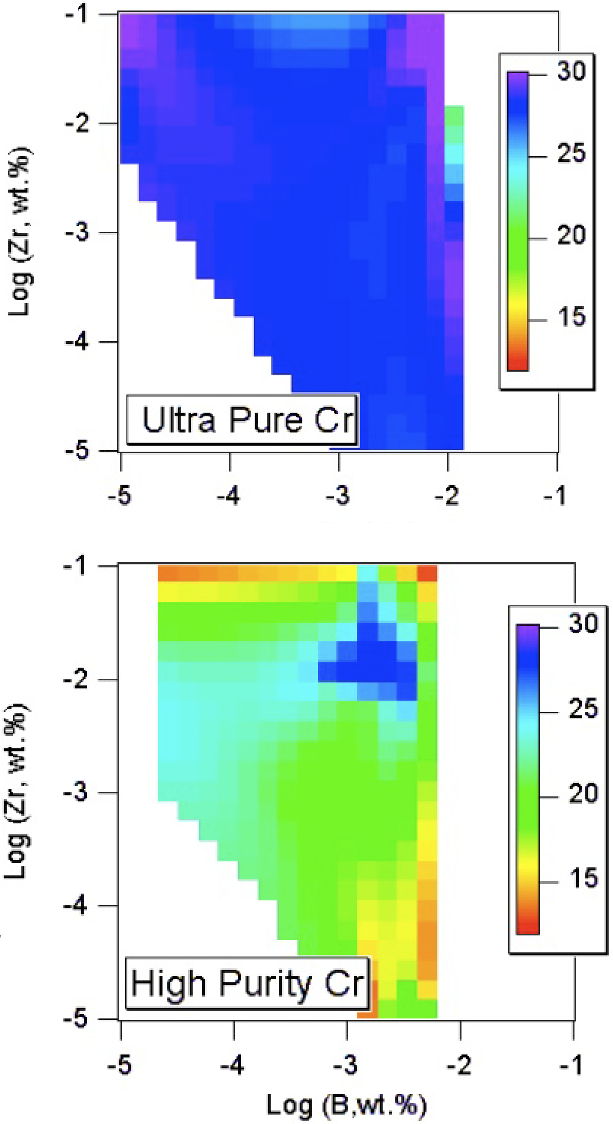

These plots show the stress required to induce solidification cracking in IN939 alloys as a function of raw material source, Zr and B concentrations; Very Purity Raw Material Reduces the Cracking Tendency

Fabrication-Related Defects - Metallurgical

- “Hot” cracking
  - Weld solidification
  - HAZ liquation
  - Weld metal liquation
  - HAZ liquation requires the presence of a liquid, or liquid film
  - Associated with grain boundaries
- Two types
  - HAZ/PMZ liquation cracking
  - Weld Metal (WM) liquation cracking

Liquation Mechanisms

- Penetration mechanism
  - Localized melting
  - Grain boundary migration
  - “Penetration” of boundary by liquid
- Segregation mechanism
  - Segregation of impurity and solute to grain boundaries
  - Gibbsian segregation
  - Grain boundary “sweeping”
  - “Pipeline” diffusion

Penetration Mechanism

- Three elements are required
  - Local liquation phenomenon
    - Segregation melting (BM or WM)
    - Constituent melting (e.g. eutectic)
    - Constitutional liquation
  - Grain boundary motion and intersection
  - Penetration and wetting of grain boundary

Penetration Mechanism

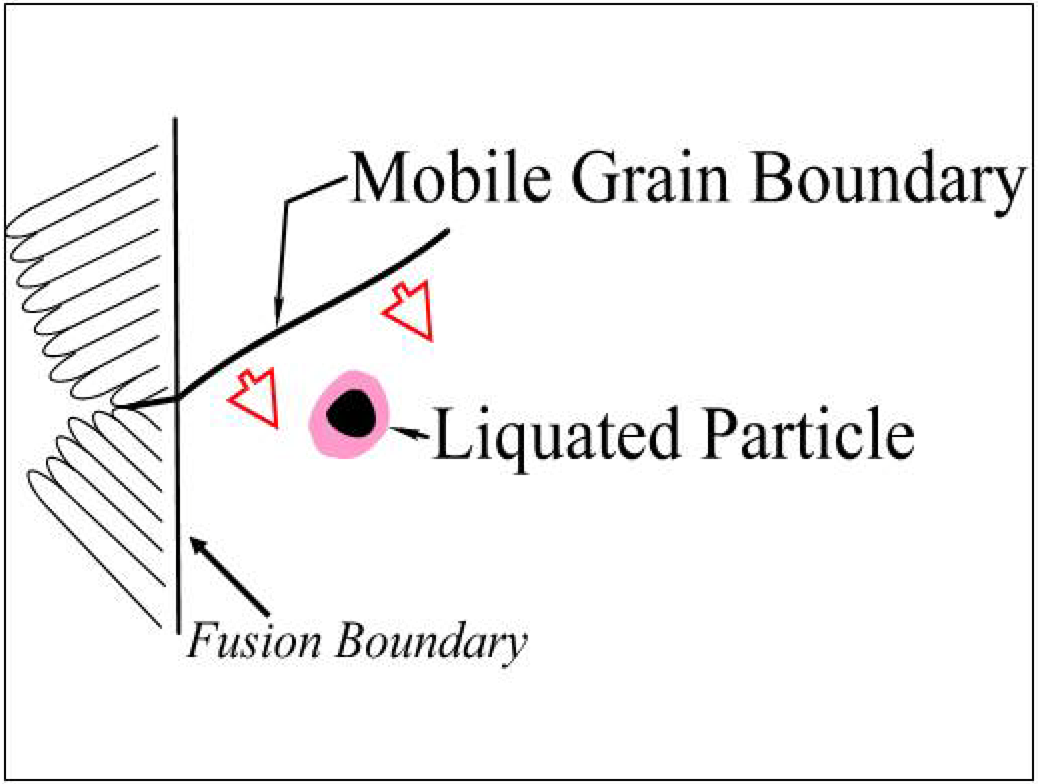

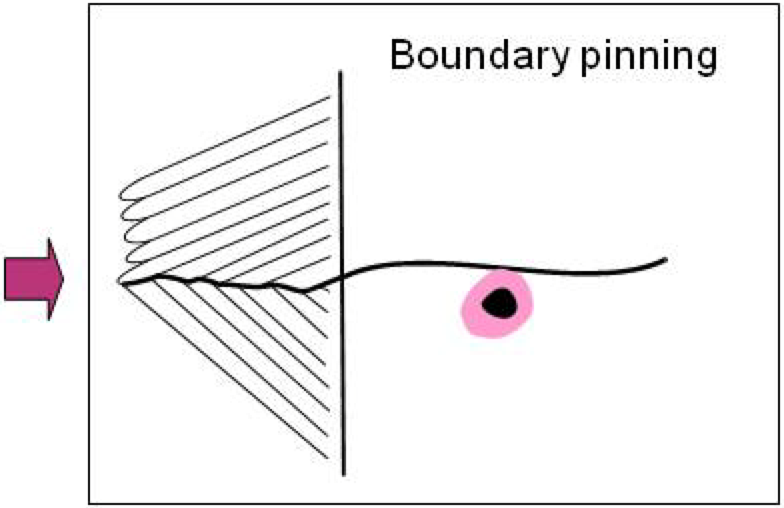

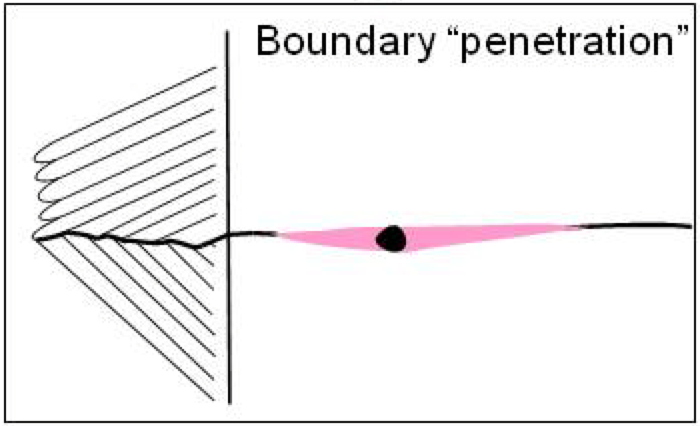

Localized Melting in the PMZ

- Incipient melting
  - Grain boundaries are high energy sites
  - Melting at temperatures a few degrees below bulk solidus
- Solute/impurity banding
  - Local, periodic variations in composition
  - Residual from thermo-mechanical processing
- Constitutional liquation

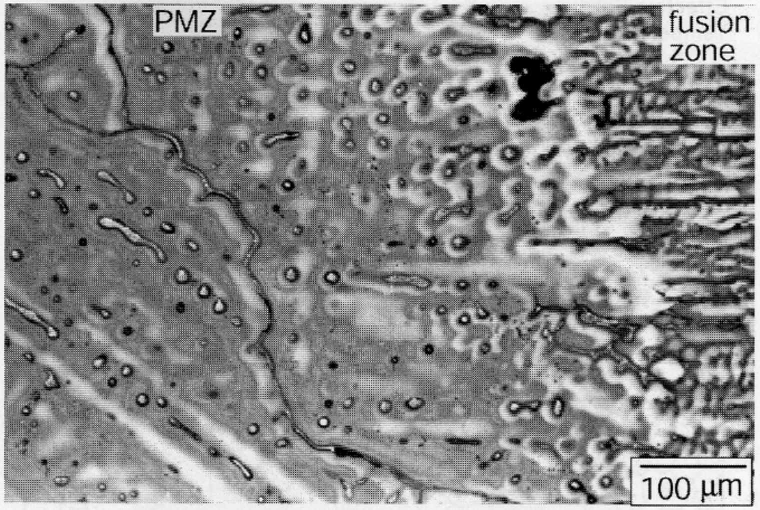

Figure 12.10 PMZ microstructure of gas–metal arc weld in as-cast Al–4.5Cu. Reprinted from Huang et al. (4).

Courtesy: S. Kou, Welding Metallurgy Book, Wiley Interscience

The Constitutional Liquation Mechanism

- Proposed by Savage, et al in the 1960's
- Reaction between a constituent particle and the matrix
- Local melting at the particle/matrix interface

- Note: The particle does not melt, but rather reacts with the matrix prior to the onset of liquation

PMZ in Alloy 718

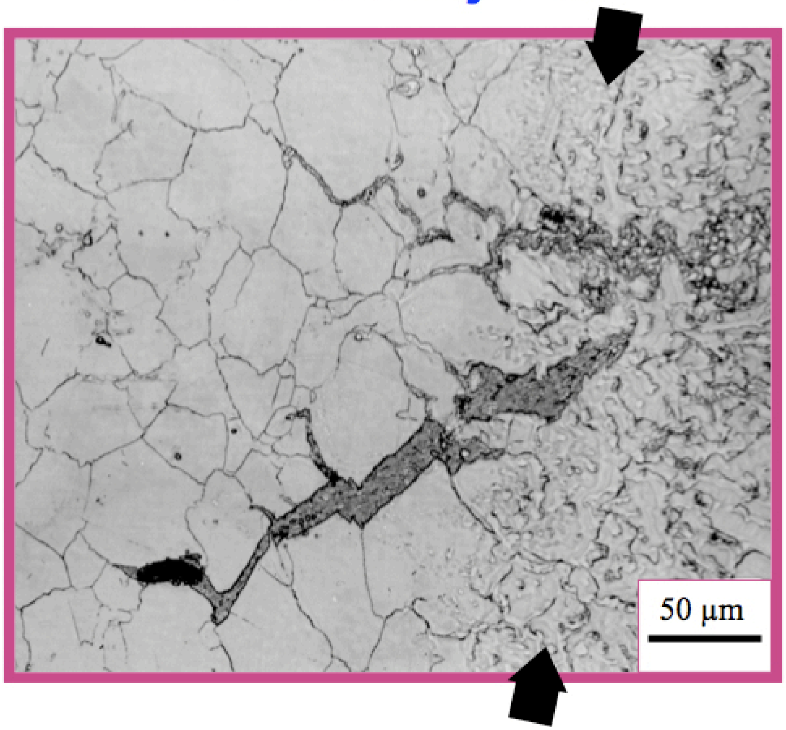

Constitutional Liquation

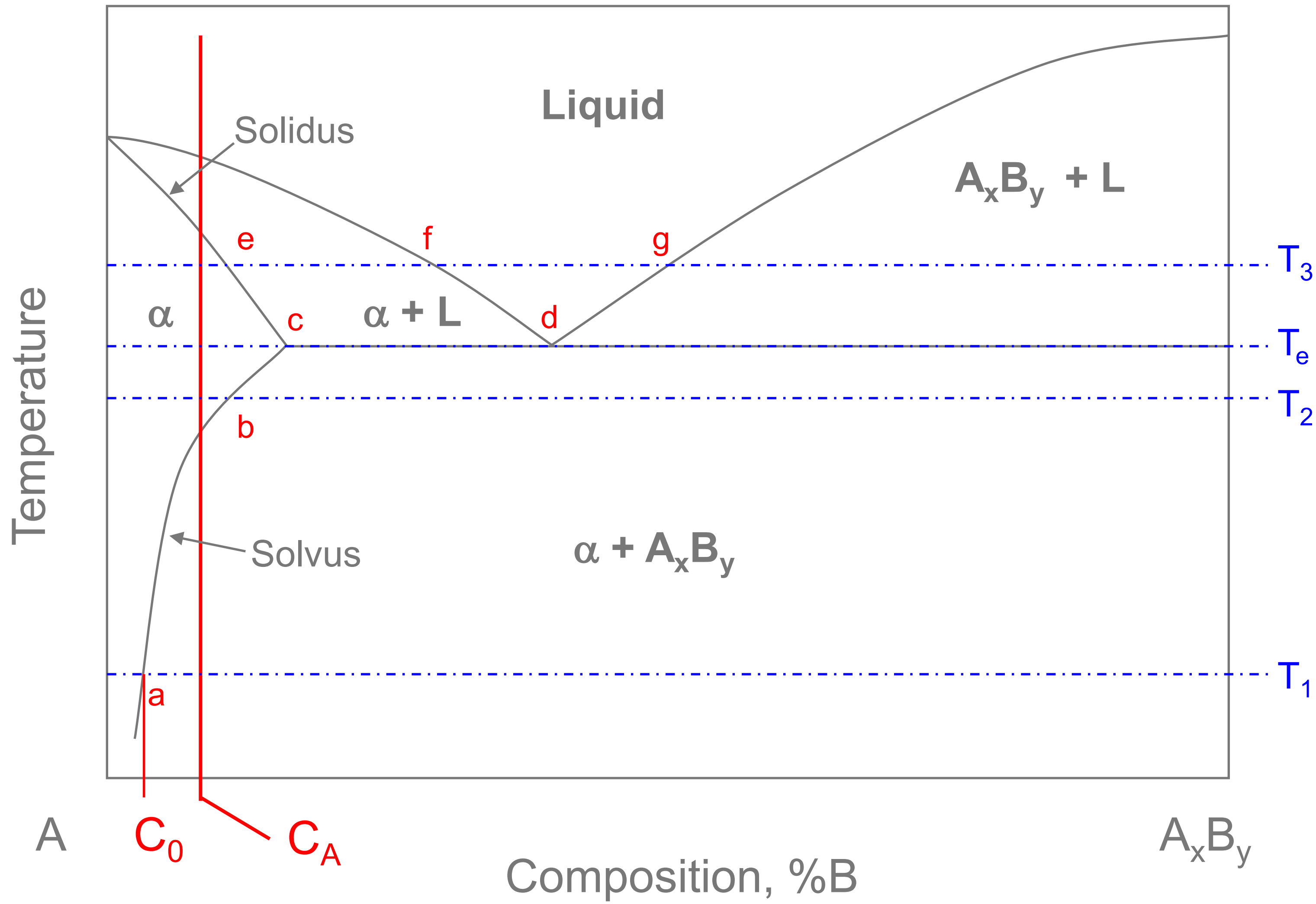

Constitutional Liquation Mechanism

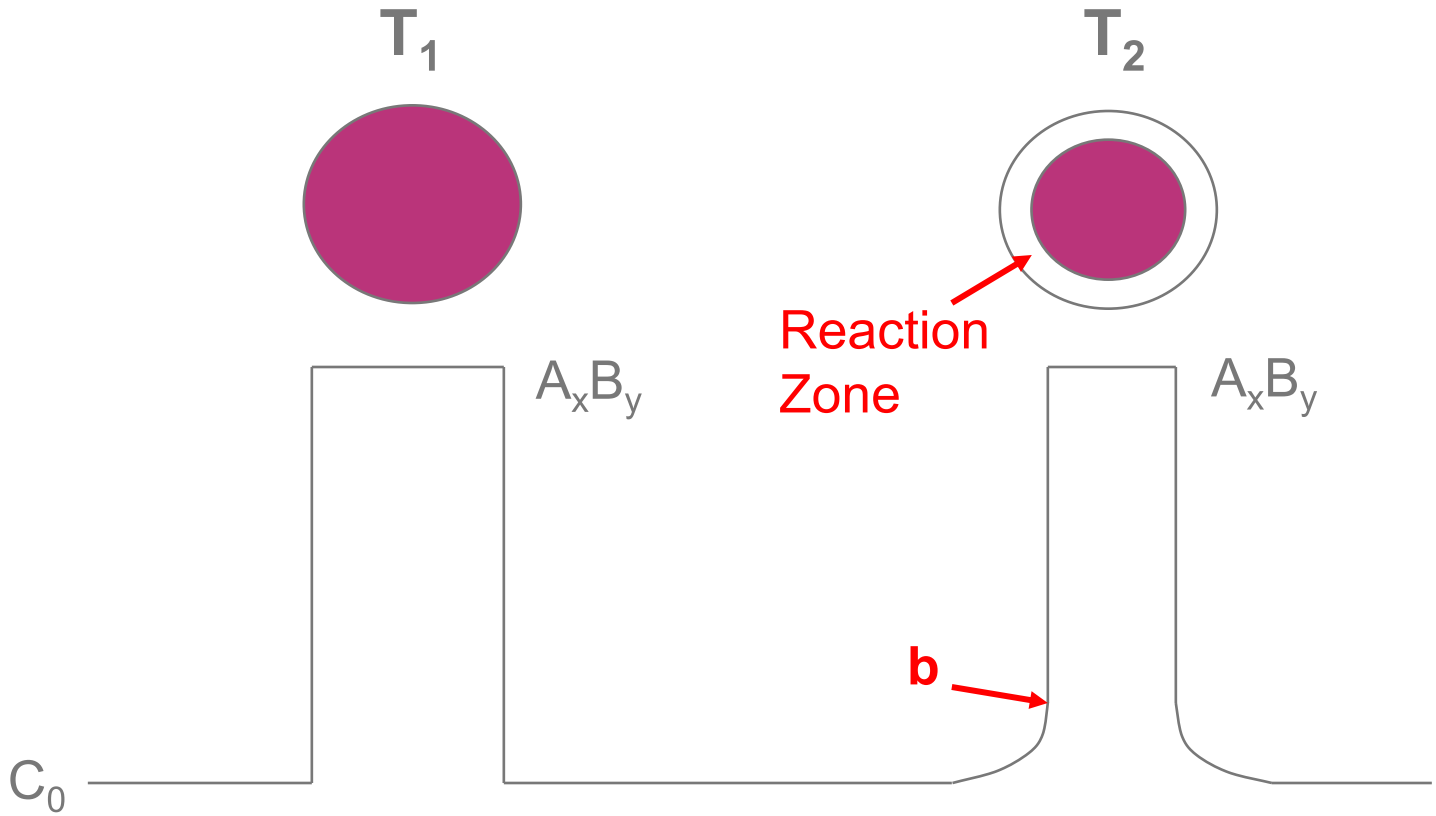

Constitutional Liquation Mechanism

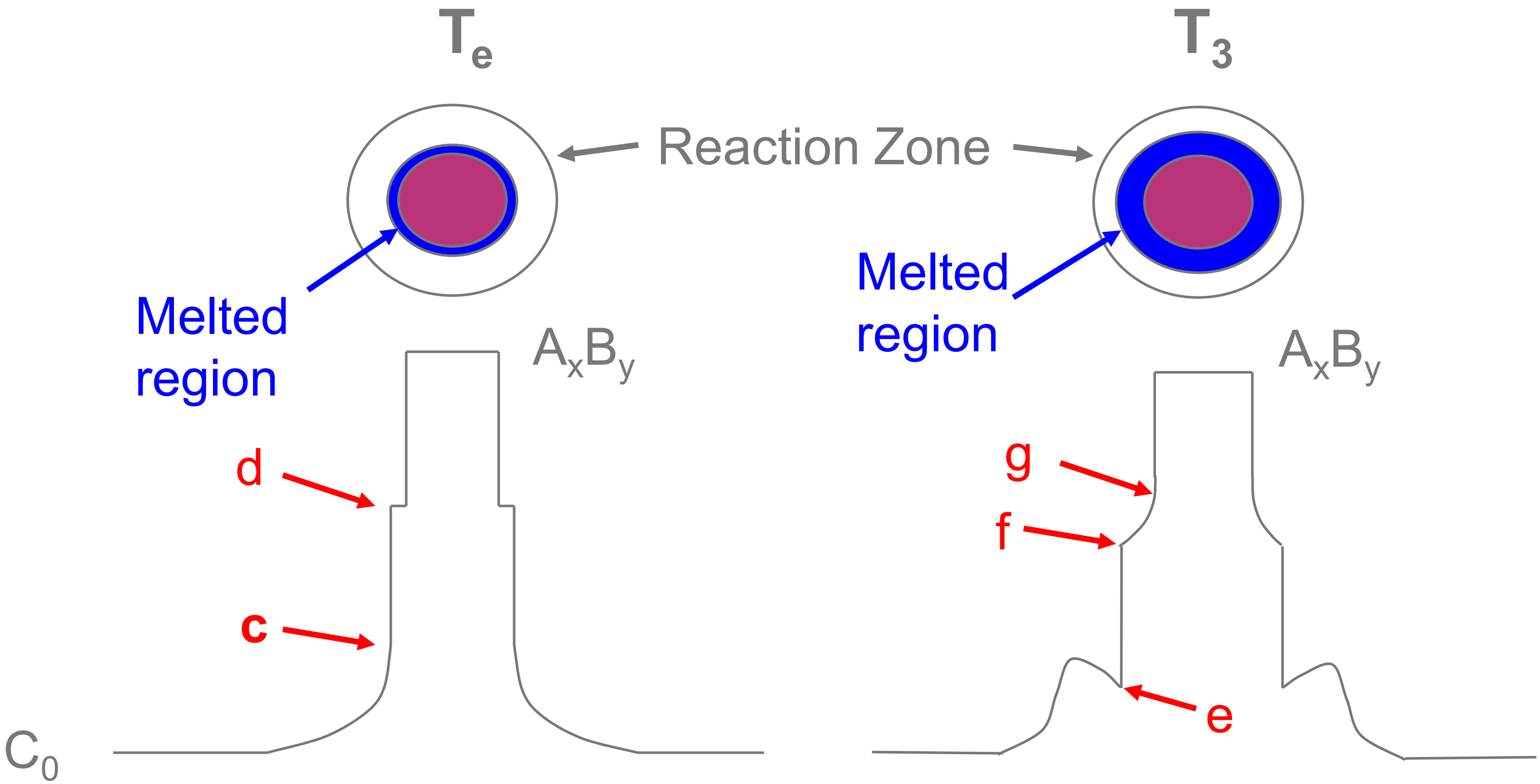

Constitutional Liquation of NbC

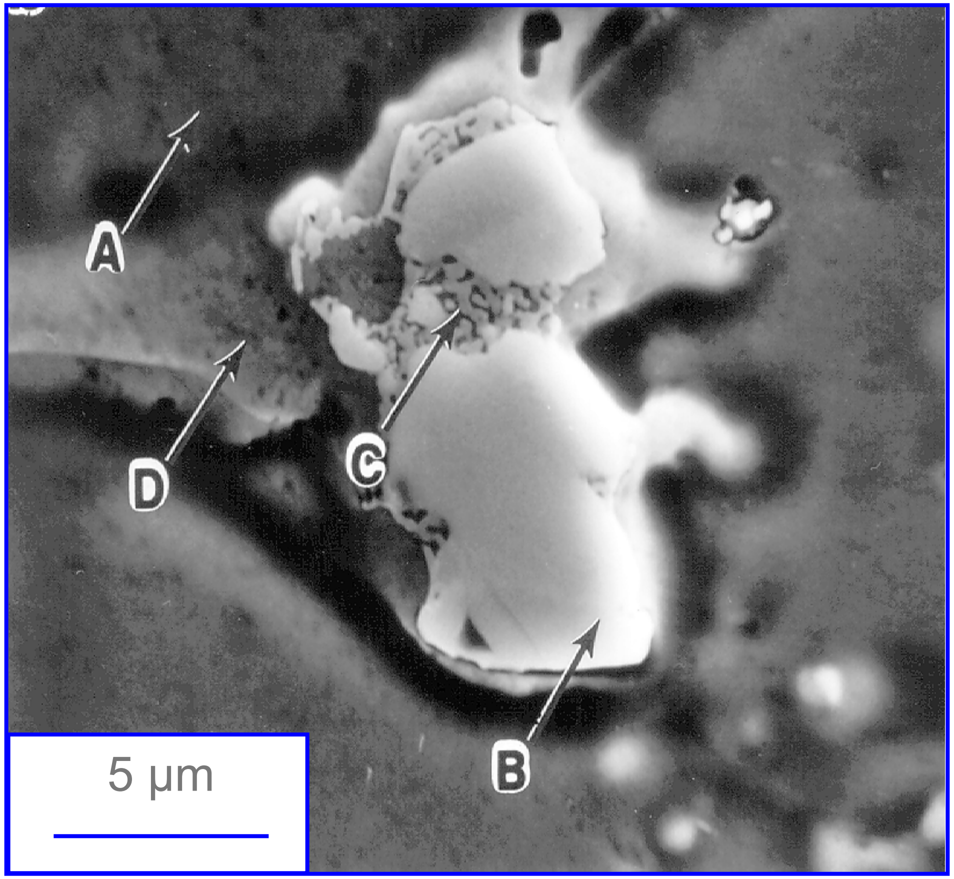

Alloy 907

PMZ Grain Boundary Wetting

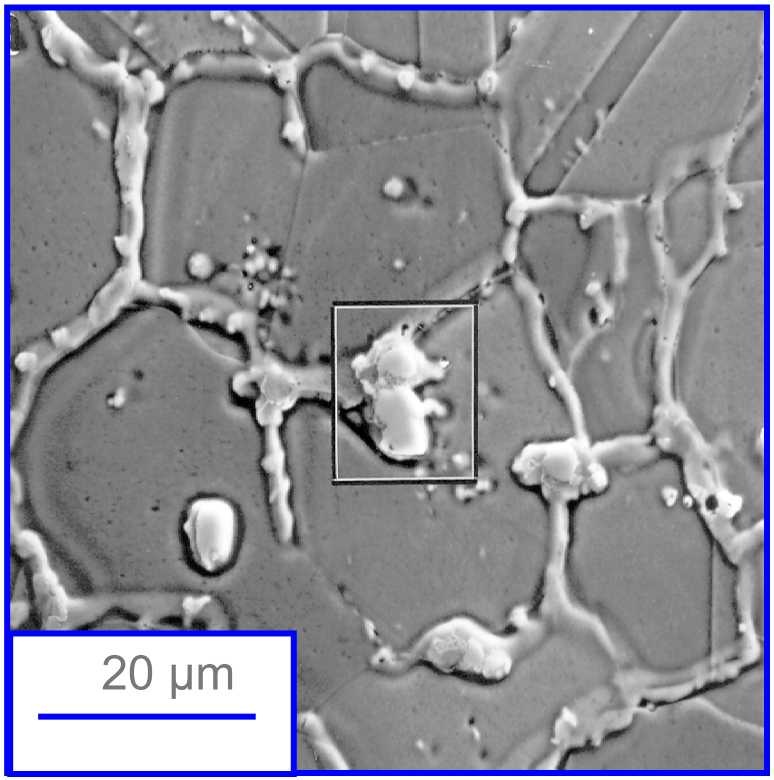

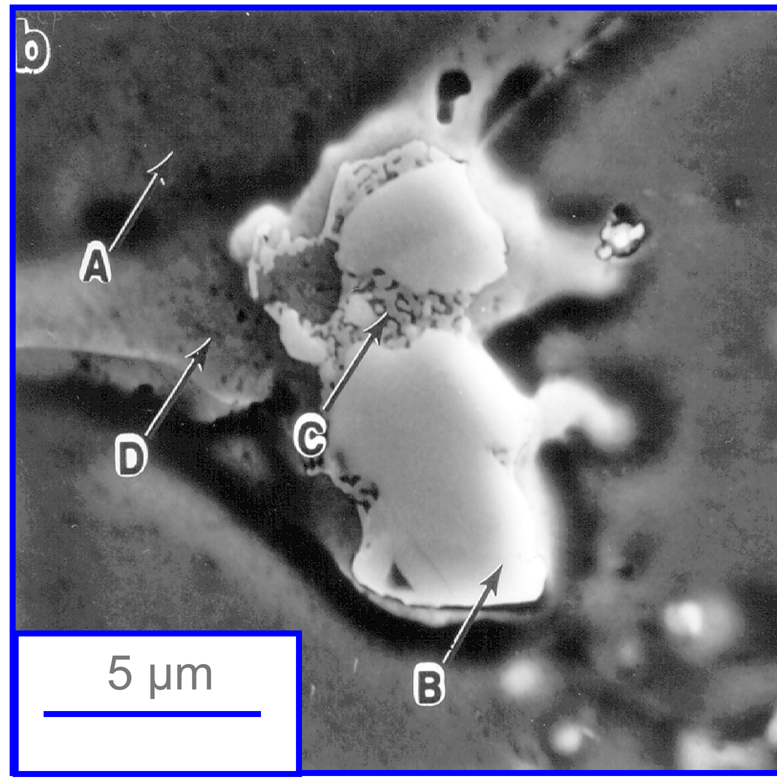

Alloy 907

Constitutional Liquation

Alloy System	*Susceptible Alloys*	*Constituent*
Ni-base	Alloy 718	NbC
	Waspaloy	TiC
	Hastelloy X	TiC
Stainless Steels	Type 347	NbC
	A-286	TiC
	Alloy 800	TiC
Structural Steels	HY-130	TiS

Segregation Mechanism

- This mechanism is used to explain HAZ liquation in alloys that do not undergo liquation in discrete locations. It requires:
  - Diffusion of solute and/or impurity elements to grain boundaries
  - Segregation-induced melting of the grain boundary
  - Grain boundary wetting

Effect of Segregation on Grain Boundary Melting

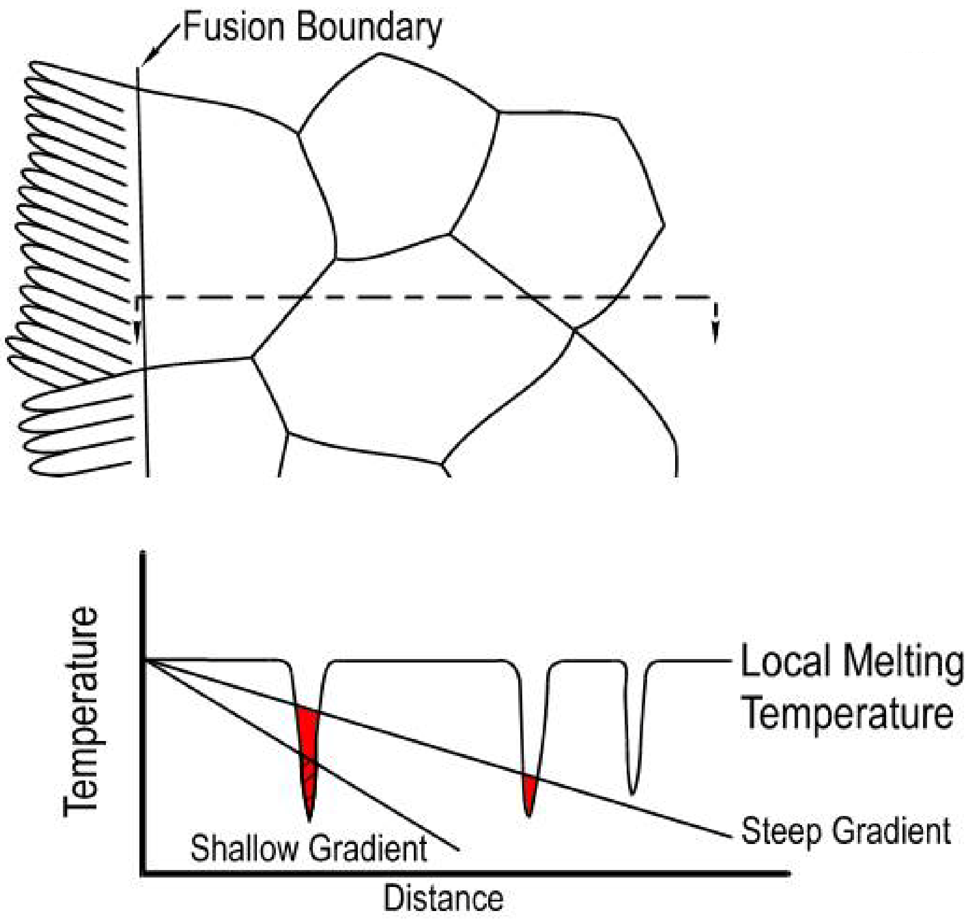

- Segregation of solute/impurities to grain boundaries depresses the local melting point
- Temperature gradient has a strong effect on the extent of melting

Grain Boundary "Sweeping"

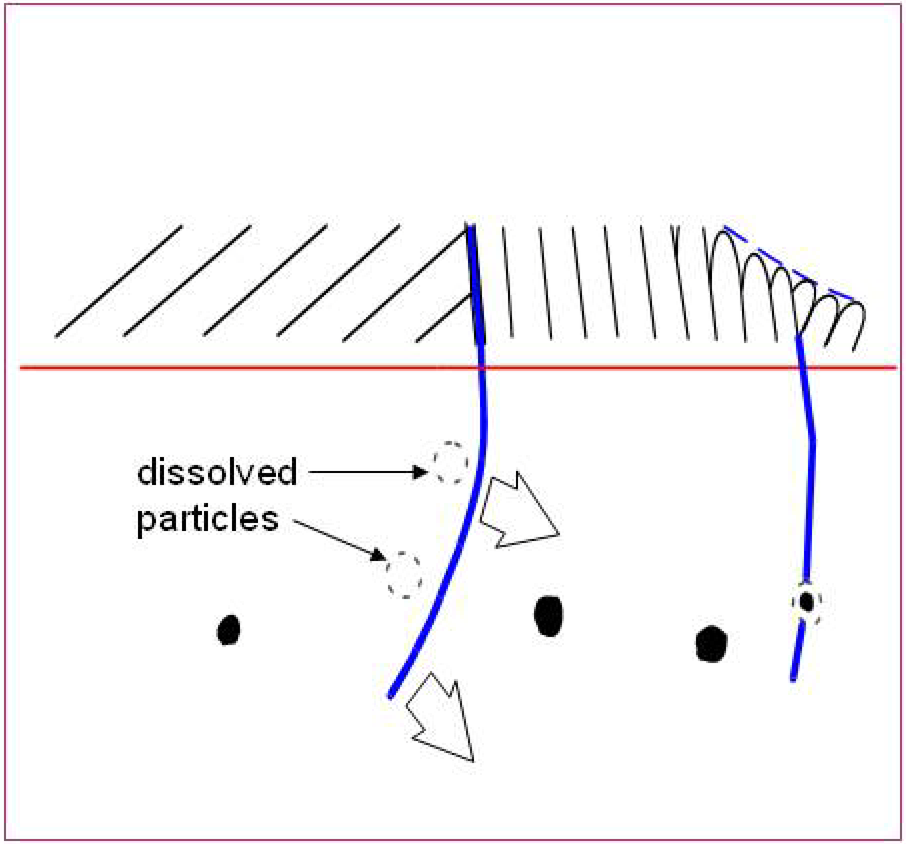

- Thermally-induced grain boundary motion in HAZ
- High affinity of some elements for grain boundaries
    - Impurities – S, P, B
    - Solutes – Ti, Si
- Elements "swept up" and move with boundary

Pipeline Diffusion

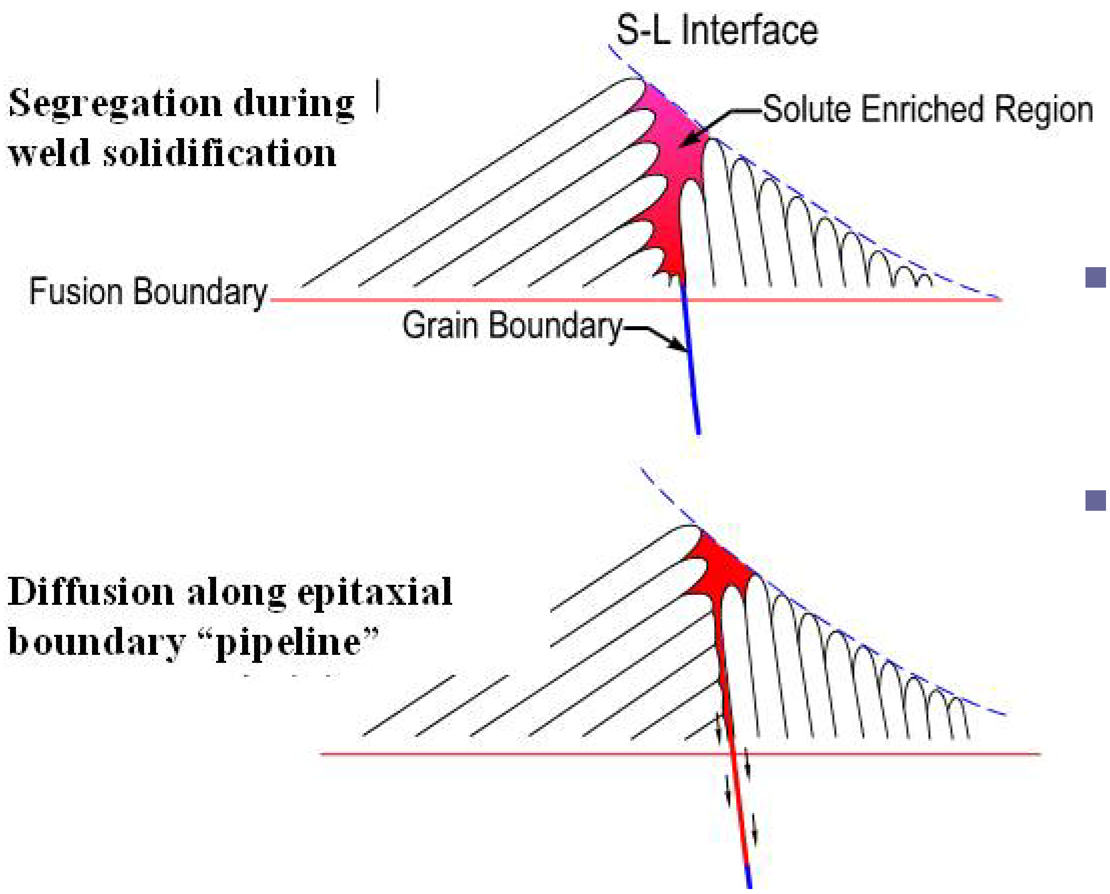

- Solute segregation in fusion zone along solidification grain boundaries (SGBs)
- Grain boundary "pipeline" due to epitaxy
- Rapid grain boundary diffusion

Weld Metal Liquation Cracking

- Often referred to in literature as “microfissuring”
- Restricted to reheated weld metal (multipass welds)
- Not associated with constitutional liquation
- Locations
  - Solidification grain boundaries (SGBs) due to segregation during initial solidification (Case 3)
  - Migrated grain boundaries (MGBs) due to a segregation or penetration mechanism
- Most often observed in single phase, austenitic weld metal

Weld Metal Liquation Cracking

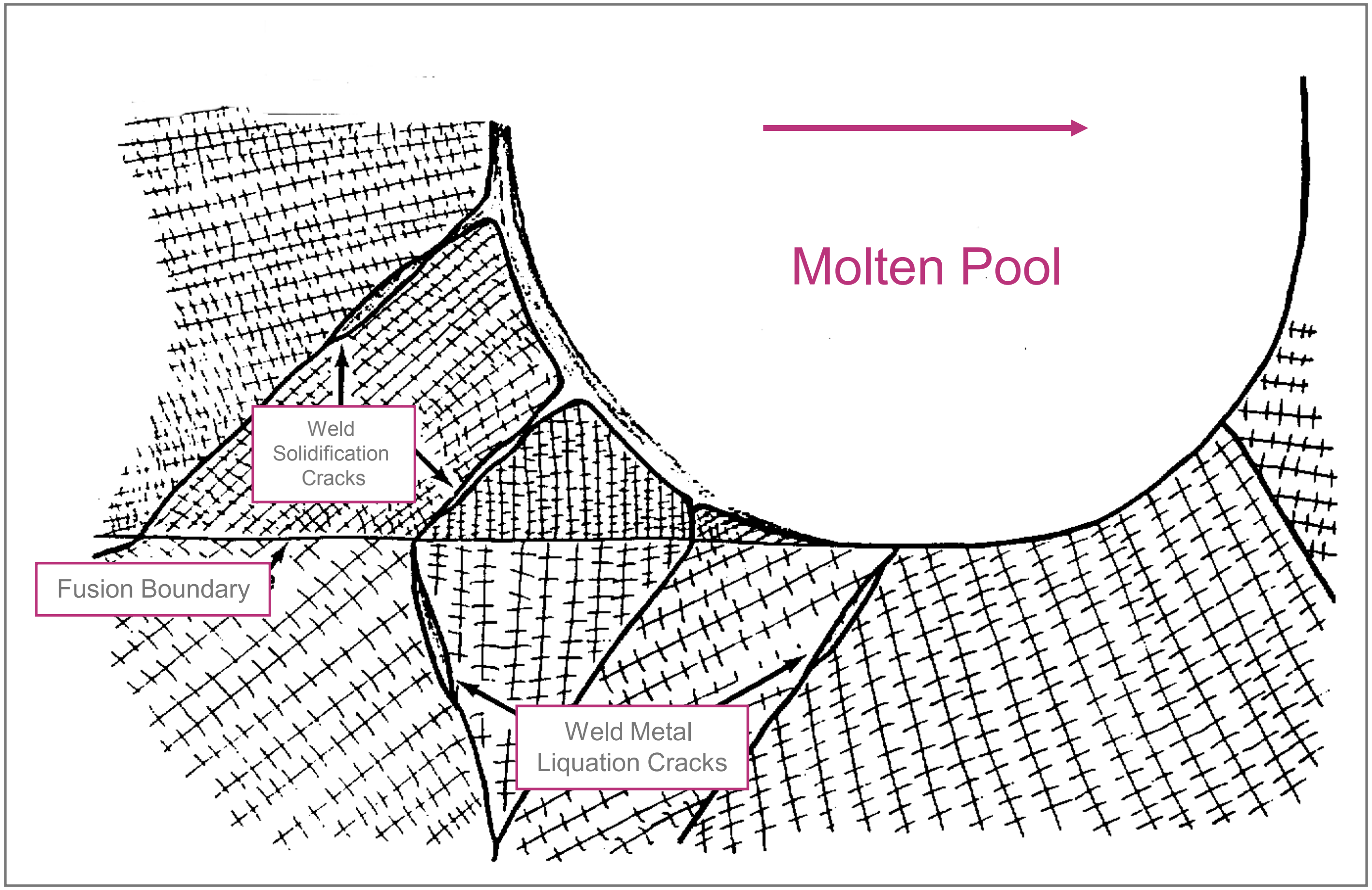

Variables which Influence HAZ/WM Liquation Cracking

- Microstructure
  - Grain size
  - Phases and constituents
- Heat treatment
- Composition
  - Alloying elements (Ti, Nb, etc.)
  - Impurities
- Welding conditions
  - Heat input
  - Filler metal

Effect of Grain Size on HAZ Liquation Cracking

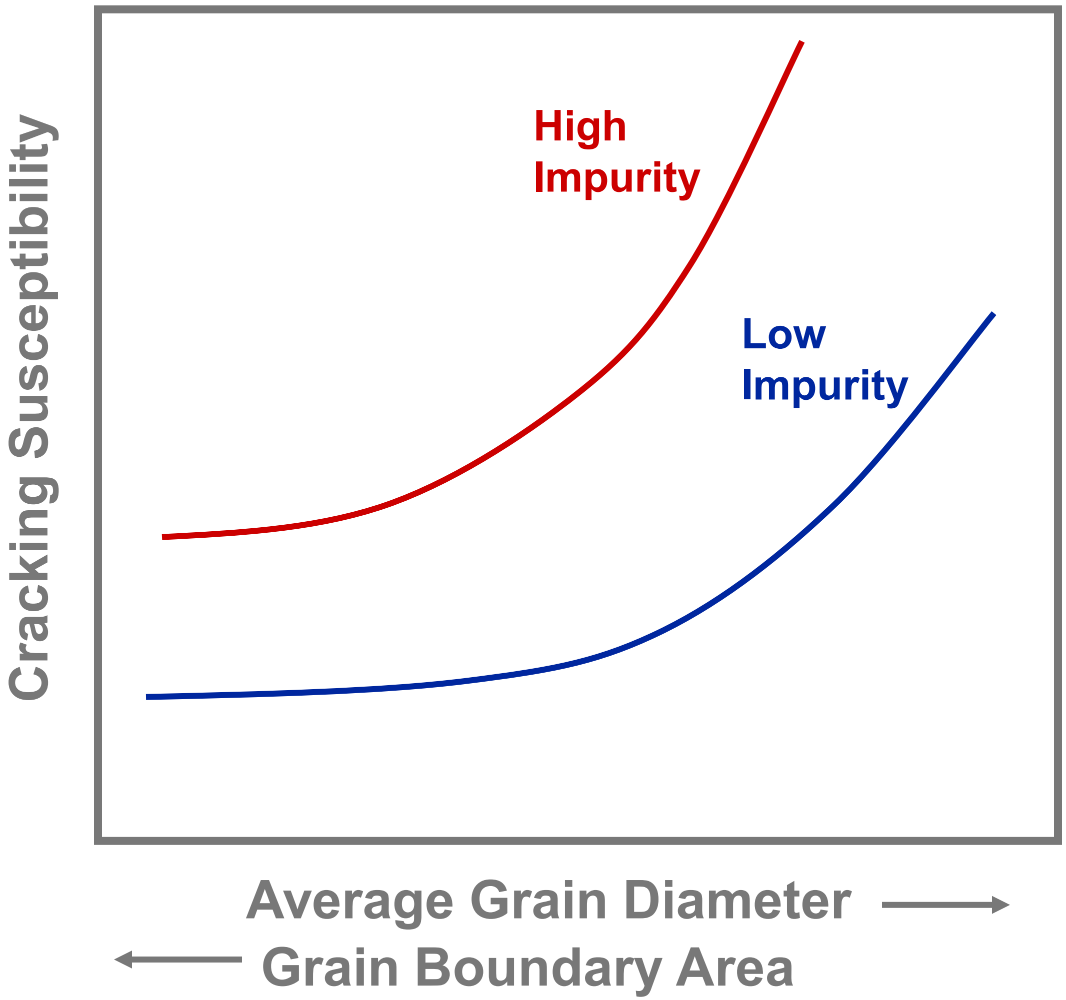

- Grain boundary liquid films
- Less liquid film coverage with finer grain size
- Liquid film strength
- Strain localization

Susceptible Alloy Systems

- Generally fully austenitic (FCC) microstructure
- Austenitic stainless steels
  - Types 347 and 321
  - Type 310
- Nickel-base alloys
- High-strength steels

Identifying HAZ/PMZ Liquation Cracks

- Where?
  - Grain boundaries
  - Close proximity to fusion boundary
  - May be continuous across fusion boundary
- When?
  - On-cooling in region subject to liquation
- How?
  - Always intergranular
  - Fracture surface may be decorated with liquid films

Identifying WM Liquation Cracks

- Where?
  - Reheated weld metal
  - Solidification grain boundaries and/or migrated grain boundaries
- When?
  - On-heating or on-cooling in regions heated above liquation temperature
- How?
  - Always intergranular
  - Smooth or dendritic fracture surface

Preventing Liquation Cracking

- Microstructure control
  - Minimize grain size
  - Introduce second phases (ferrite)
  - Control boundary mis-orientation
- Composition
  - Reduce impurities
  - Avoid local melting and constitutional liquation
- Restraint
  - Weld in solution annealed condition
  - Multi-bead techniques
  - Design and fixturing

How Do We Evaluate Weldability Under Controlled Conditions?

- Some laboratory tests for evaluating weldability:
  - Varestraint Cracking Test (Linear and Spot)
  - SigmaJig®
  - Gleeble Thermomechanical Simulation
- Due to the limited scope, we will see how we do the SigmaJig test with a case study
- However, the general framework is same, temperature, stress and evaluate the material sensitivity

SigmaJig® Test

- Perform welding (similar conditions) with different applied stress on similar thickness sample
- Identify the critical stress at which you initiate cracking
- If the stress to induce cracking is higher, then the alloys are resistant to weld solidification cracking

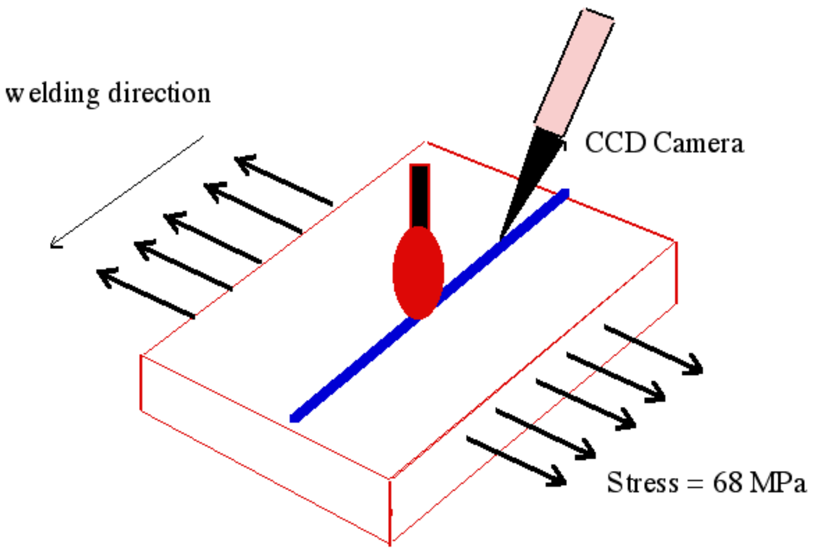

Courtesy: ORNL

An Example of Weld Crack Monitoring

- Let us see the crack dynamics

Sub-Solidus Crack Formation in a Stressed Weldment was Observed

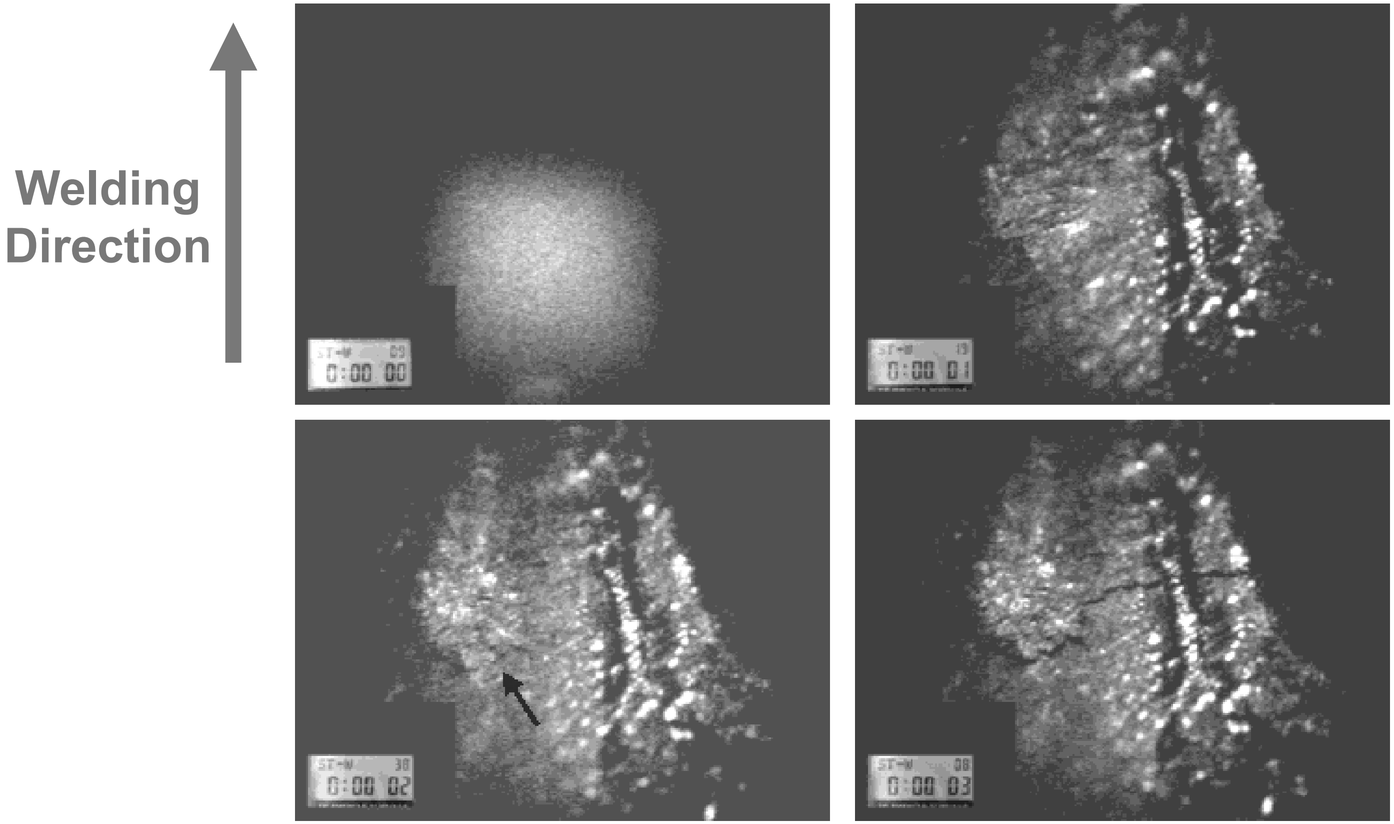

- Weld cracks in M738 (~IN738) was transverse in nature
- The cracking is attributed to the presence of low-melting eutectics and the presence of longitudinal stress

Let Us See the Real-Time Movie of Cracking

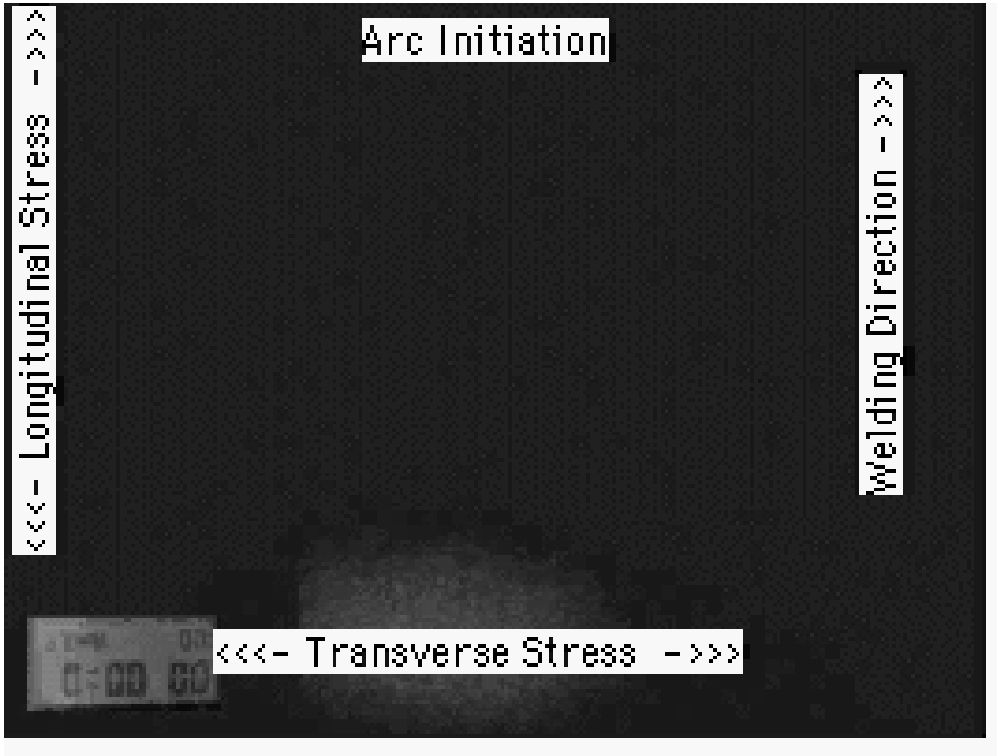

- What is the significance of this test for nuclear/energy construction applications?

Threshold Cracking Stress in IN939 Linked to Minor Element Concentrations (B, Zr & S)

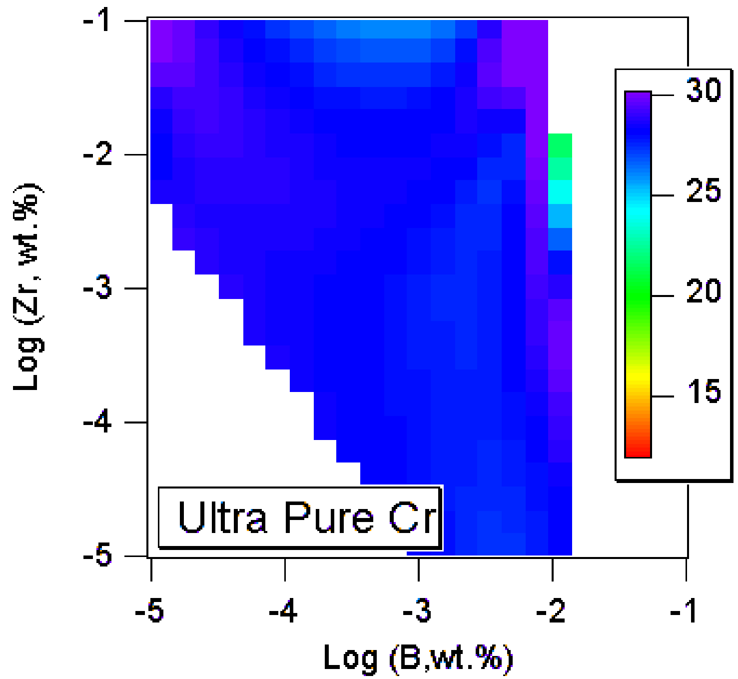

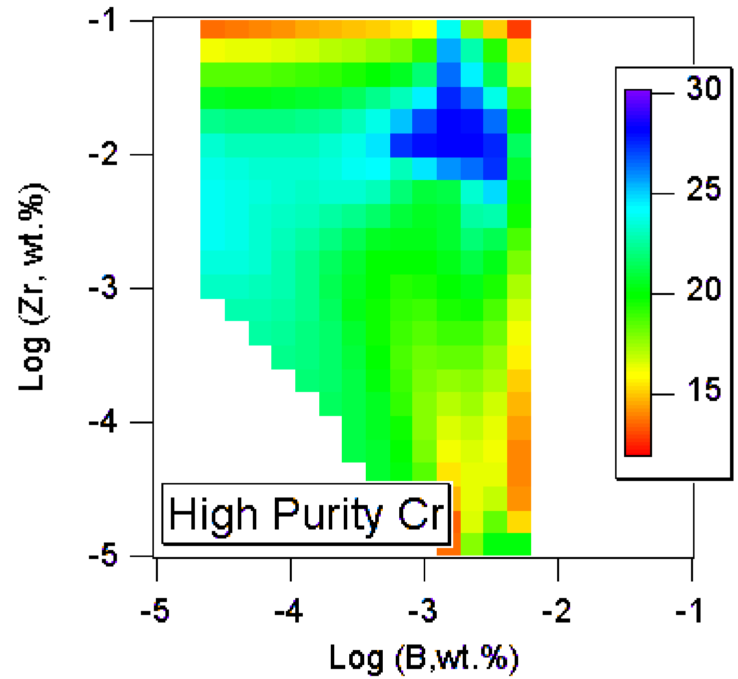

- The above results lead to tightly controlled IN939 alloy composition for better weldability
  - E. P. George, S. S. Babu, S. A. David, and B. B. Seth, Proceedings of the BALTICA V conference in Helsinki, 2001)

Solid-State Cracking

Module 5A.2

Fabrication-Related Defects - Metallurgical

- “Warm” cracking
  - Ductility dip
  - Reheat/PWHT
  - Strain-age
  - Liquid metal embrittlement (LME) (Cu contamination)

Ductility-Dip Cracking

- Severe loss in ductility below the solidus temperature
- May occur on-heating or on cooling
- Observed in both weld meta and base metal HAZ
- Always intergranular
- Austenitic (FCC) microstructure

Ductility Dip Cracking Range

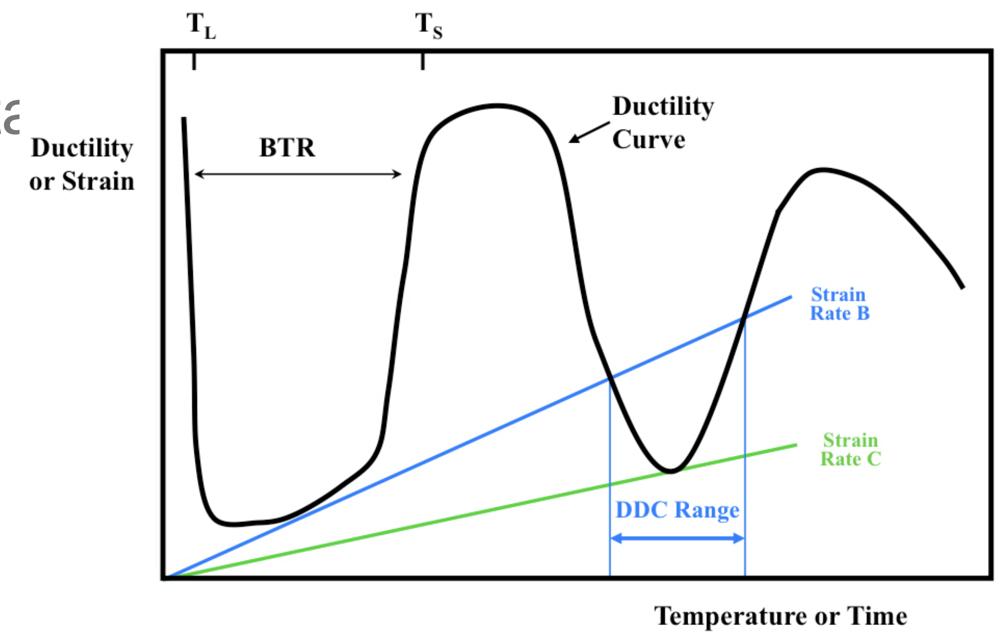

Ductility-Dip Cracking

- Susceptible materials
  - Austenitic stainless steels
    - Fully austenitic base metals and filler metals
    - High purity grades
  - Ni-base alloys
    - Solid-solution strengthened
    - Multipass weld metals
- Characteristics
- Along solidification grain boundaries and migrated grain boundaries in the weld metal
- Associated with boundary mobility and large grain size

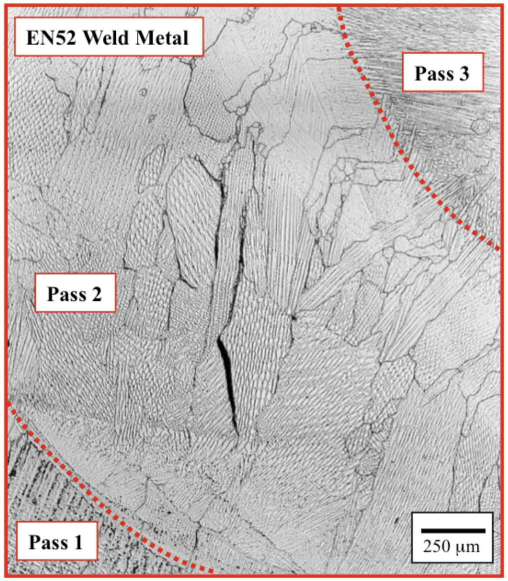

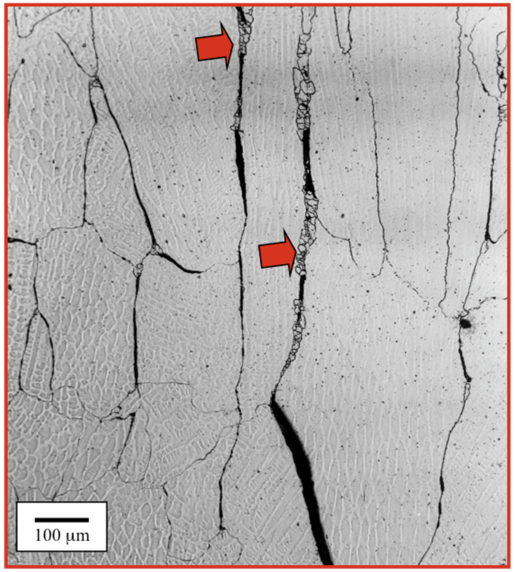

Reheat Cracking

- Low alloy steels and some stainless steels are susceptible
- Occurs during PWHT and stress relieving
- Associated with austenite or prior austenite grain boundaries
- May occur during cladding of structural steels

Conditions for Reheat Cracking

- During welding
  - In low alloy steels, transformation to austenite
  - Dissolution of alloy carbides
  - Segregation of impurity elements
- During reheating
  - Reprecipitation of alloy carbides
  - Relaxation of stresses

Susceptible Materials

- Low alloy steels with secondary carbide formers
  - A508, A517, A533
  - Cr-Mo or Cr-Mo-V steels
- Austenitic stainless steels (Type 347)
- Other alloys with strong precipitation reactions

Alloying Elements (from Haure and Bocquet)

G = 10C + Cr + 3.3Mo + 8.1V

for G<2, steel is resistant

Impurity Elements (from Brear and King)

I = 0.2Cu + 0.44S + 1.0P + 1.8As + 1.9Sn + 2.7Sb

Mechanism for Reheat Cracking

- On-heating transformation to austenite
  - Alloy carbides dissolve
  - Austenite grain growth
  - Segregation of impurities to grain boundaries (optional)
- Upon reheating to PWHT temperature
  - Strong intragranular precipitation response
  - Stress relaxation occurs simultaneously
  - Strain localization at prior austenite grain boundaries
  - Failure at, or near, grain boundaries

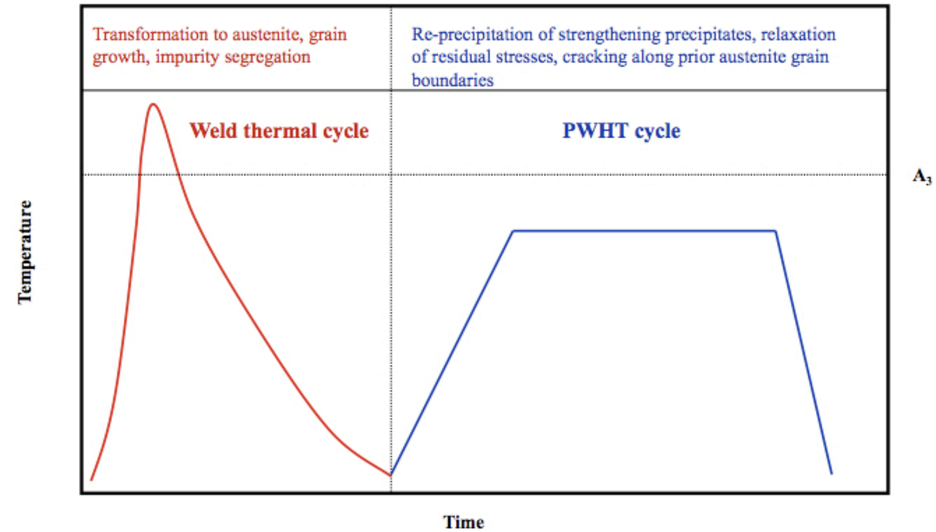

Mechanism for Reheat Cracking

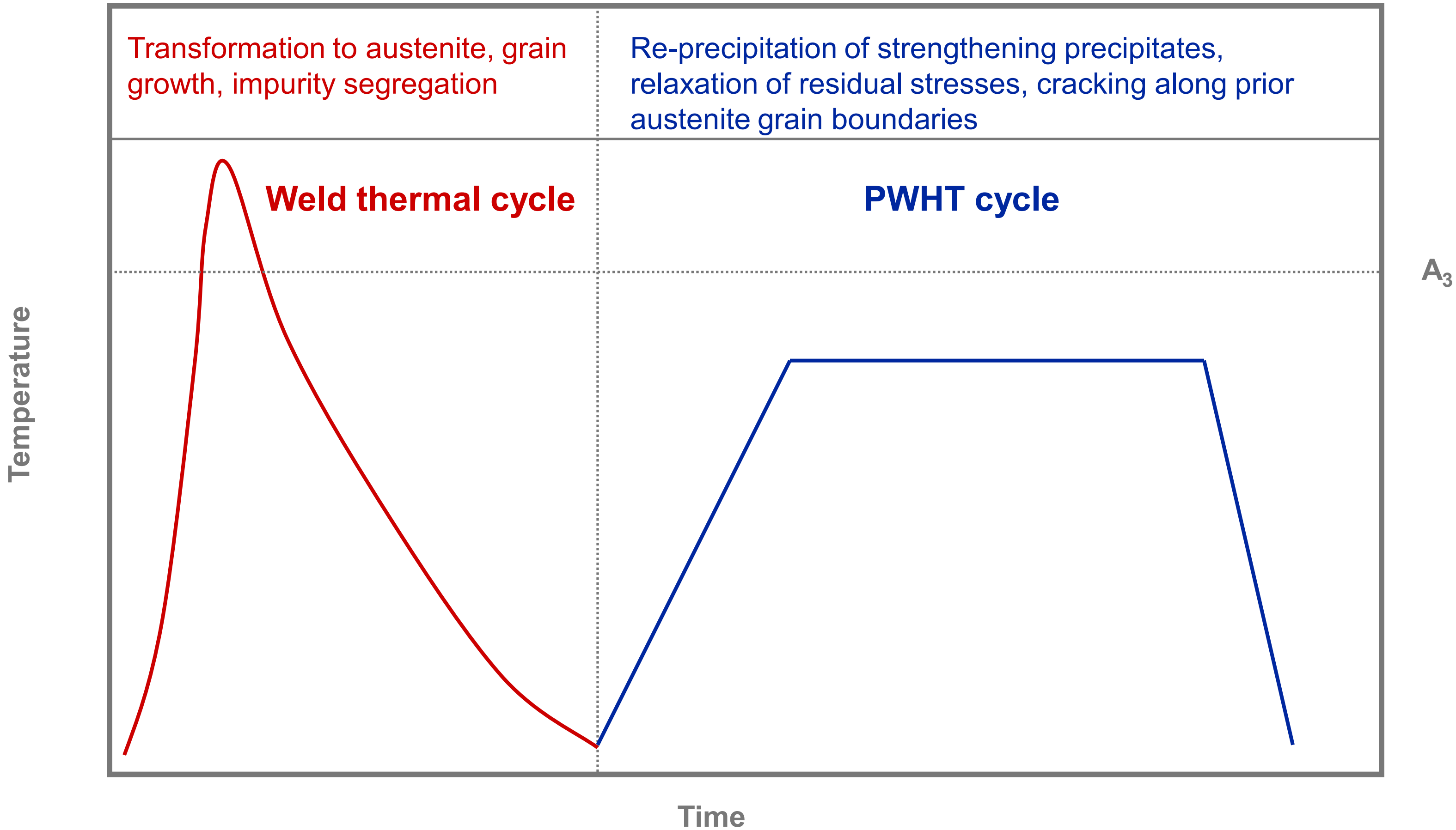

Identifying Reheat Cracking

- Metallography
  - Occurs in true HAZ in close proximity to the fusion boundary
    - Peak temperatures above A3
  - Intergranular along prior austenite grain boundaries
- Fractography
  - Smooth IG fracture at low PWHT temperatures or with high impurity levels
  - Ductile IG fracture at higher PWHT temperature (>500 ºC) or with low impurity levels

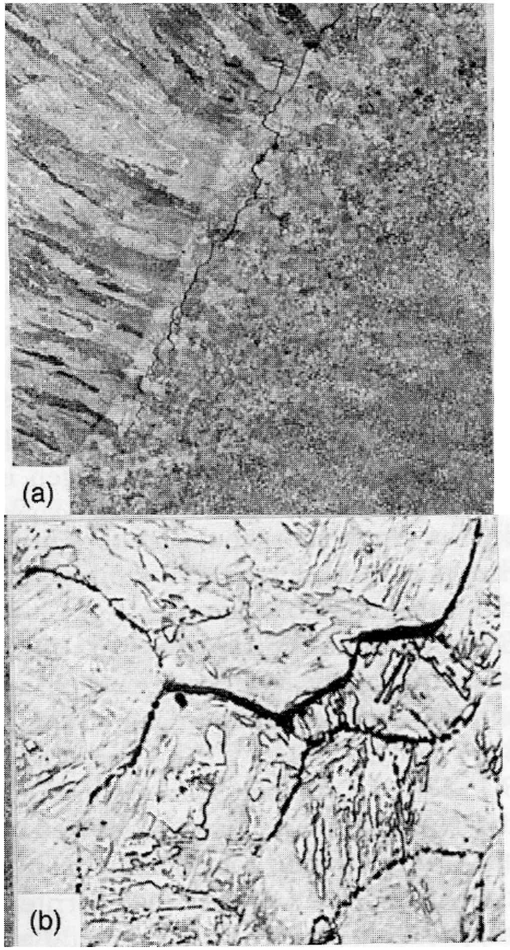

Courtesy: S. Kou, Welding Metallurgy

Preventing Reheat Cracking

- Select steels that do not contain secondary carbide formers (Cr, Mo, V)
- Reduce impurities, particularly S, P, Cu, As, Sb, Sn
- Reduce residual stress levels and subsequent stress relaxation during PWHT
- Eliminate stress concentrations near the fusion boundary (grinding, peening)
- Control weld heat input
- Use “buttering” technique

Reheat Cracking in Austenitic Stainless Steels

- Occurs in alloys containing secondary carbide formers (Nb, Ti)
- Observed in Type 347 WM and BM HAZ
- Associated with precipitation of NbC during heating to stress relief temperature or during service
- Ductile IG fracture mode
- Susceptibility reduced by “step” heat treatment

C-curve Cracking Susceptibility in Type 347

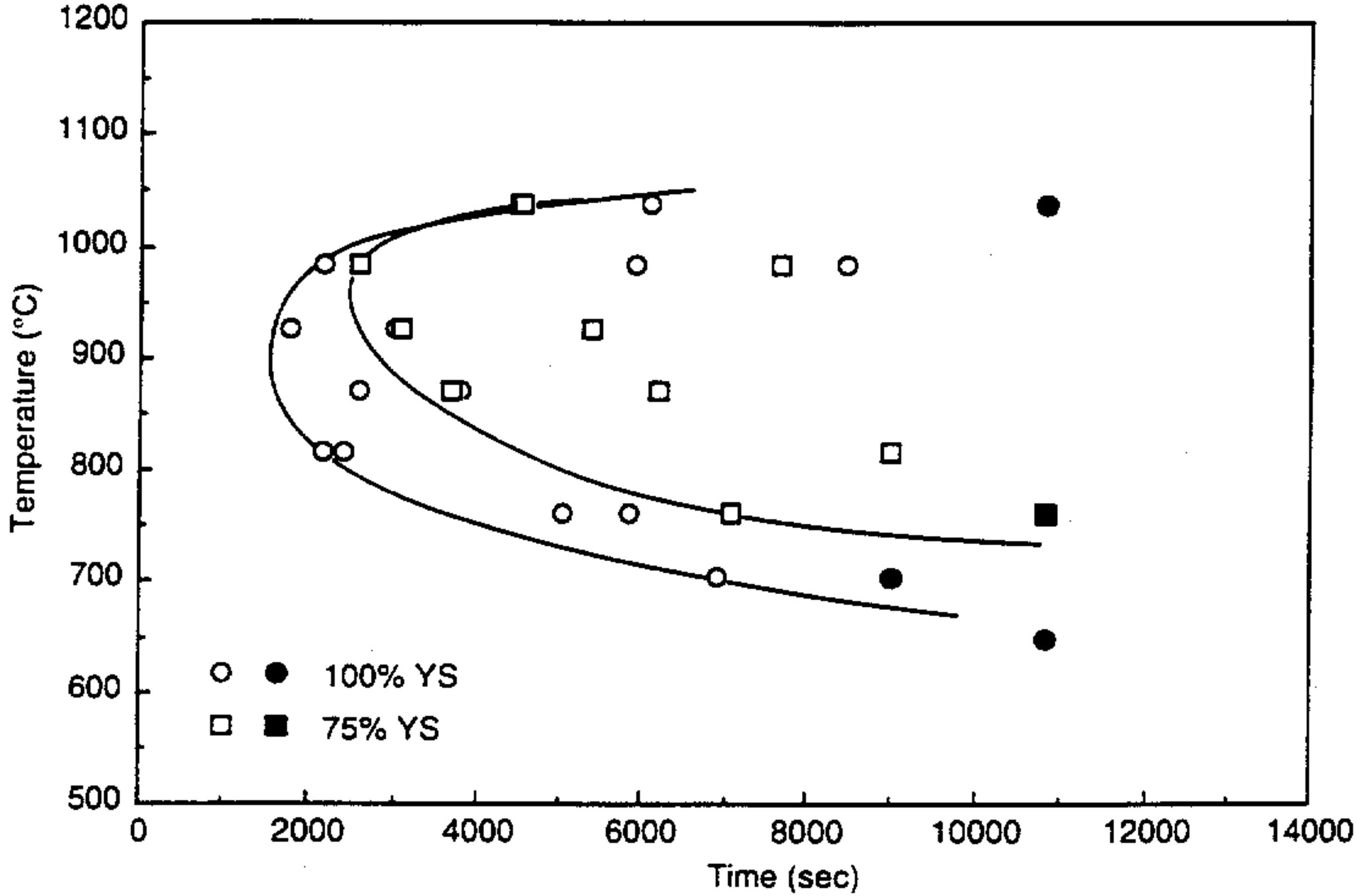

From W. Lin and J.C. Lippold

Strain-Age Cracking

- Associated with Ni-base superalloys (gamma-prime strengthened) and precipitation-strengthened steels
- Occurs during PWHT or during welding
- Cracking along austenite or prior austenite grain boundaries
- Three factors combine to promote cracking
  - Intragranular strengthening
  - Impurity segregation
  - Grain boundary embrittlement

Mechanism for Strain-Age Cracking

- Strengthening precipitates are solutionized in the HAZ during welding
- Liquation occurs along PMZ grain boundaries (optional)
- During PWHT, rapid reprecipitation of strengthening precipitates intragranularly
- Potential embrittlement of grain boundaries
- Strain accumulation at grain boundaries
  - Relaxation of residual stress
  - Thermal contraction stress
  - Local stress due to precipitation
- Intergranular fracture

Mechanism

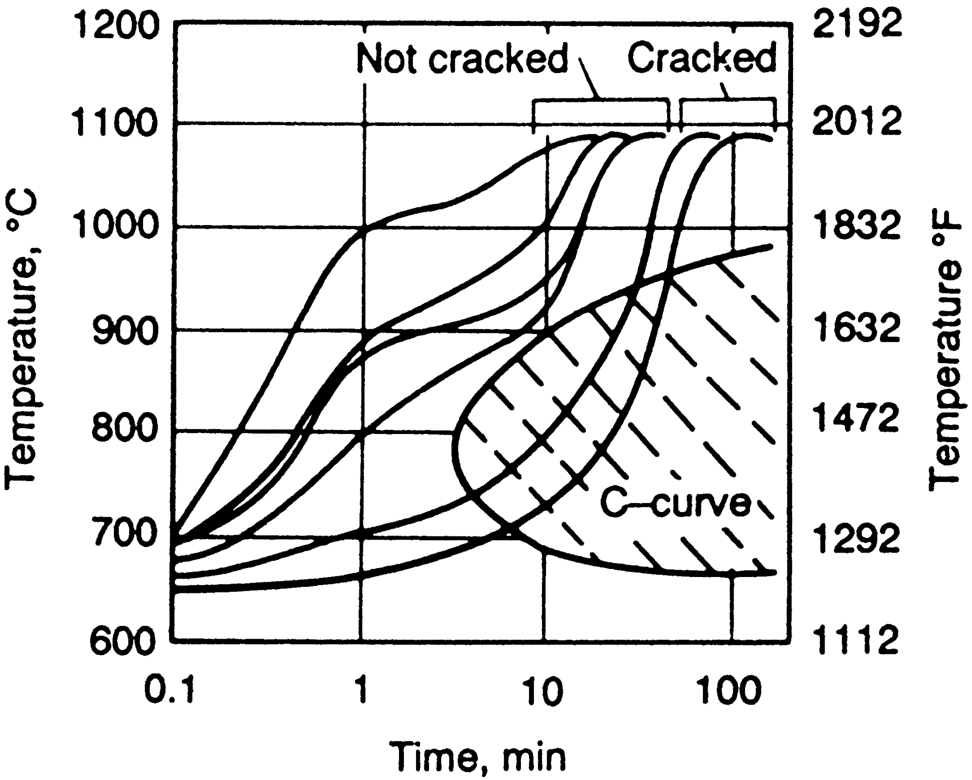

From ASM Handbook, Vol.6

- Precipitates are solutionized and grain growth occurs in the HAZ during welding
- During reheating
  - Intragranular precipitation
  - Relief of residual stresses
  - Localization of strain at the grain boundaries

Effect of Ti and Al

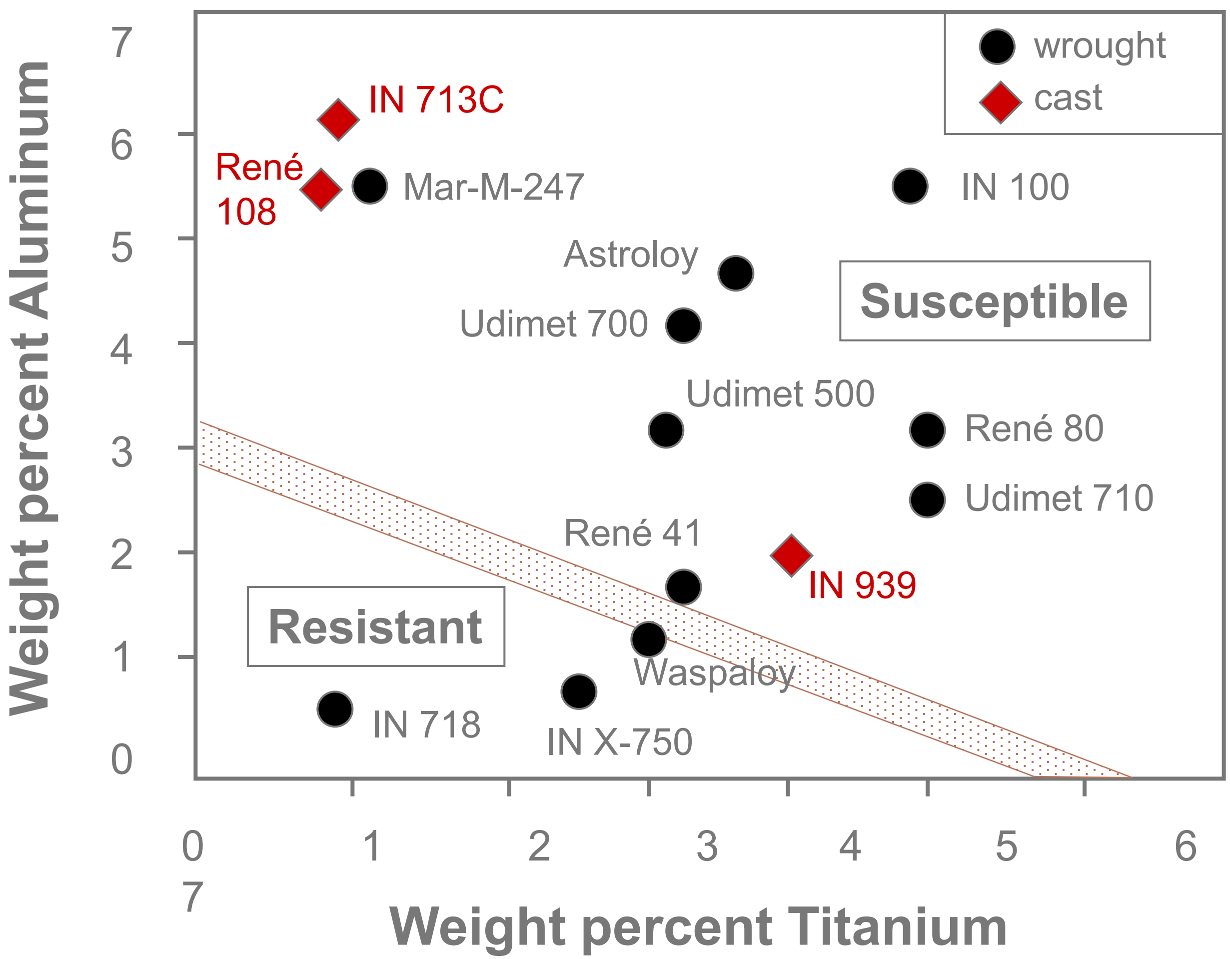

Effect of Precipitation

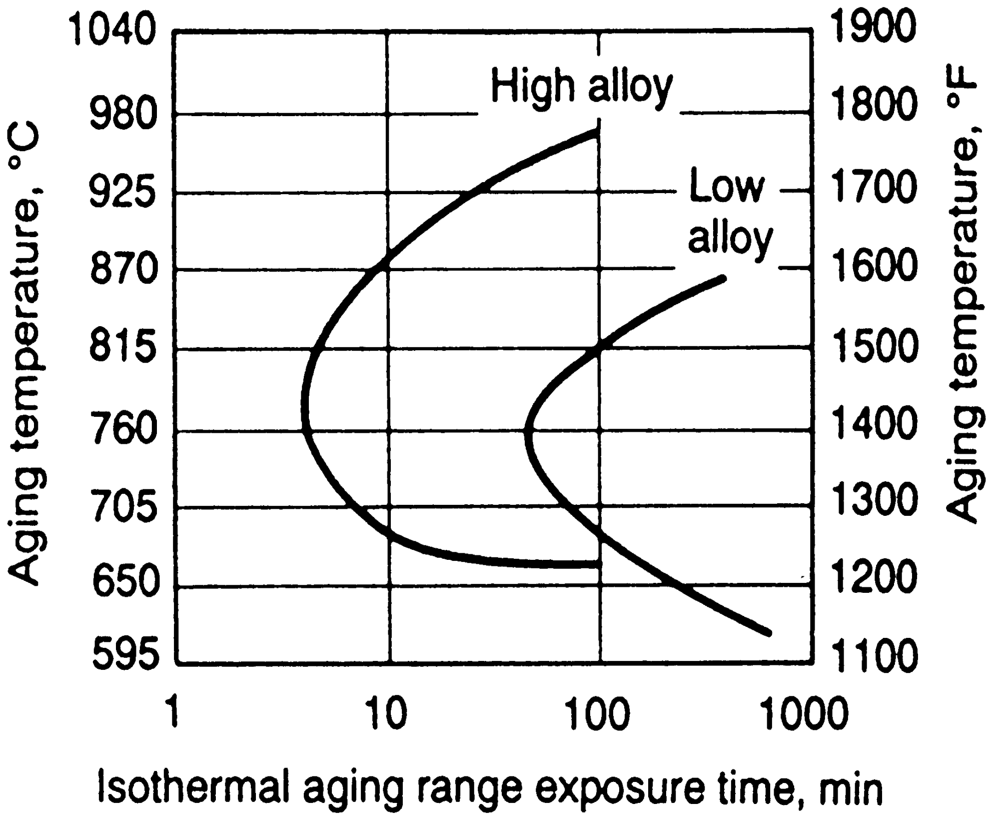

- Select resistant material (low Ti + Al)
- Heat rapidly during PWHT to avoid “nose” of precipitation curve
- Heat and hold below nose of curve to reduce residual stress
- Design issues

From ASM Handbook, Vol. 6

Identifying Strain-Age Cracking

- Metallography
  - Close proximity to the fusion boundary
  - Intergranular
- Fractography
  - Smooth or ductile intergranular
  - Possible presence of liquid films in PMZ

Preventing Strain-Age Cracking

- Select alloys with sluggish precipitation reactions
  - Alloy 718
- Minimize residual stresses
- Avoid/minimize PMZ formation
- Alter PWHT thermal cycle for heating to solutionizing temperature
  - Heat rapidly to avoid nose of precipitation curve
  - Use intermediate hold at temperature below the nose to relieve residual stress

Copper Contamination Cracking

- Austenitic steels or ferritic steels that are austenitic above 1000ºC
- Occurs in HAZ remote from fusion boundary
- Liquid Cu penetration along austenite grain boundaries
- No heat-to-heat variation in susceptibility

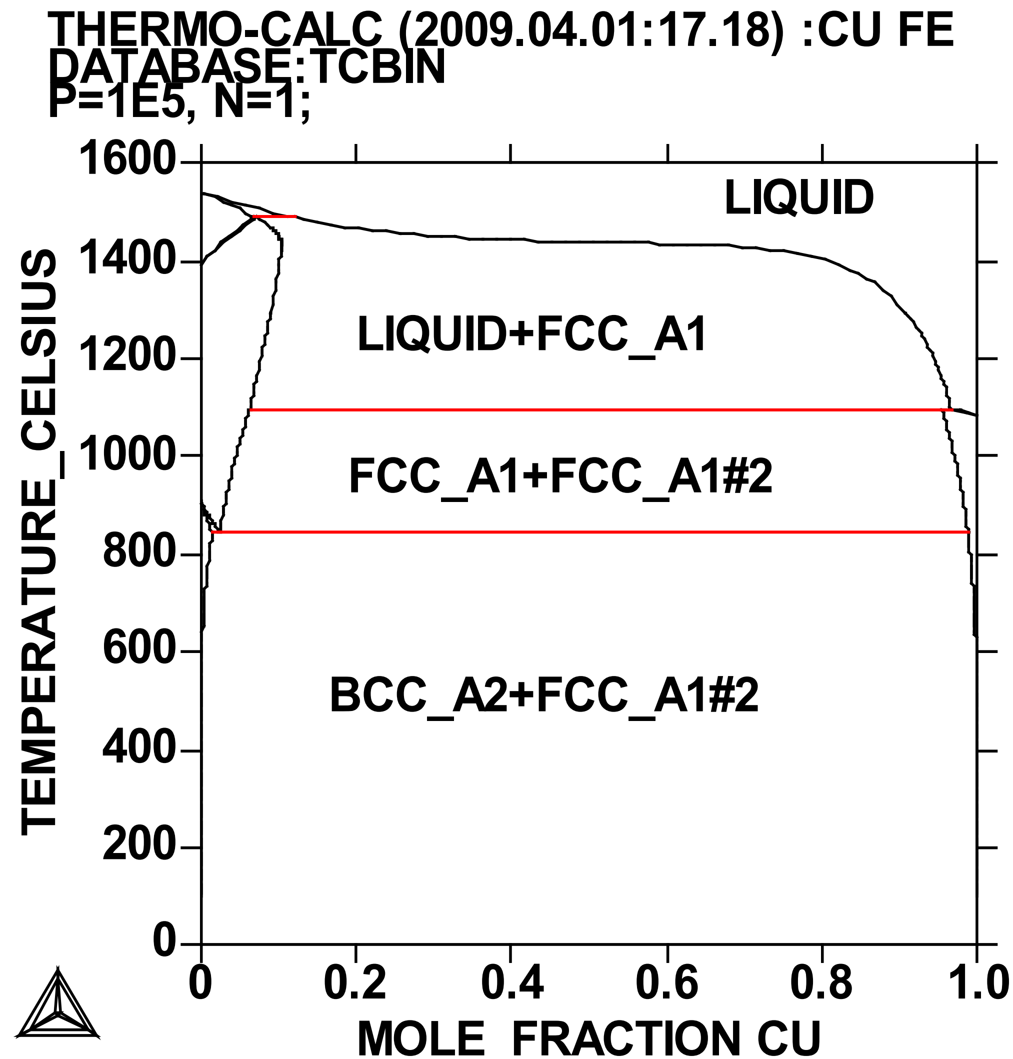

Mechanism for Copper Contamination Cracking

- Copper abraded onto surface of workpiece
- Heating above melting point of copper (1083ºC) or copper alloy
- Liquid copper penetrates the grain boundary via a liquid metal embrittlement (LME) mechanism
- Grain boundary embrittlement and cracking with threshold level of restraint

Identifying Copper Contamination Cracking

- Metallography
  - Intergranular failure in HAZ remote from the fusion boundary
  - Presence of copper along grain boundary in as-polished condition
- Fractography
  - Smooth intergranular fracture
  - Cu can be detected using SEM/EDS

Preventing Copper Contamination Cracking

- Eliminate source of copper
  - Fixturing, shielding gas delivery systems, or other sources that allow Cu to be abraded onto the material prior to welding
  - Cu added as an alloying element is not a potential source
- Alternate materials
  - Alloys that are ferritic at elevated temperatures (e.g., ferritic stainless steels)
  - Ni-base austenitic alloys

How Do We Test These Weldability in Controlled Conditions?

- Some laboratory tests for evaluating weldability
  - Varestraint Cracking Test (Linear and Spot)
  - SigmaJig®
  - Strain-to-Fracture Test
  - Gleeble Thermomechanical Simulation
- Due to the limited scope, we will see how we do the Gleeble thermomechanical simulation
- However, the general framework is same, temperature, stress and evaluate the material sensitivity

Thermomechanical Simulation

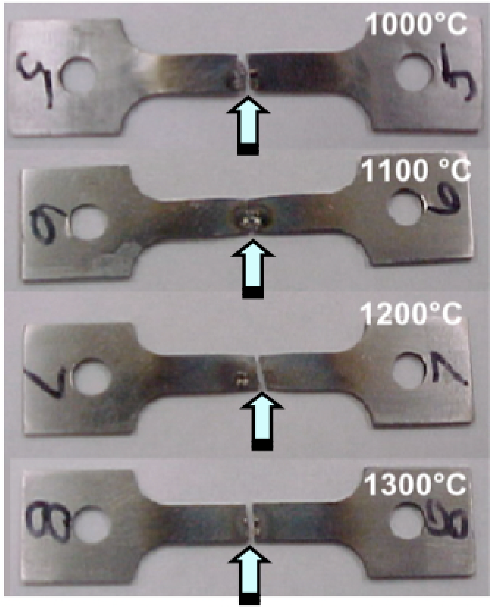

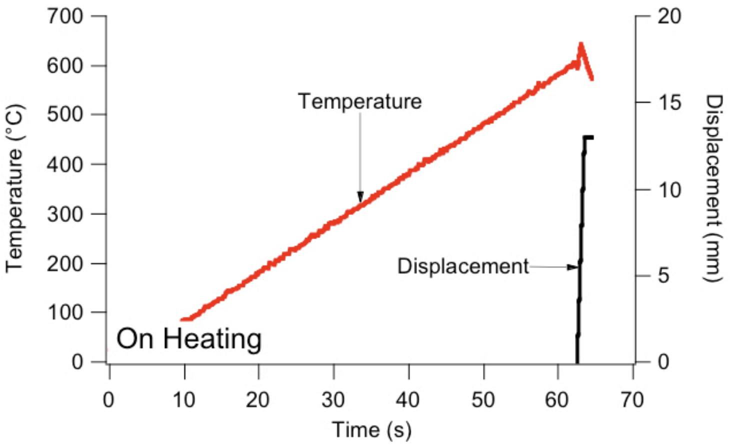

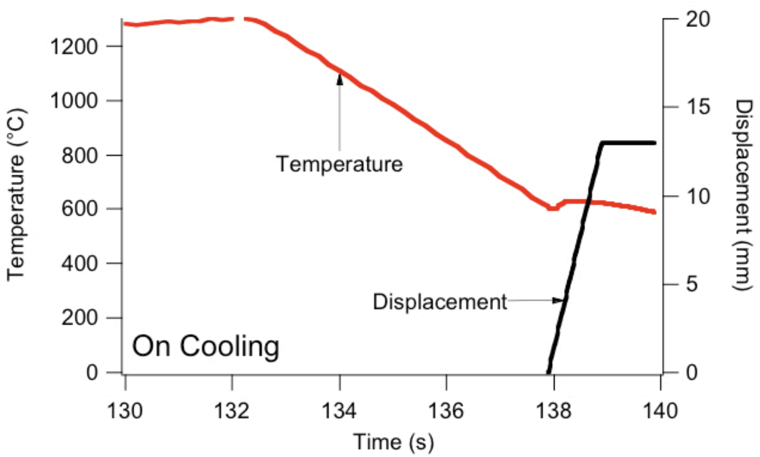

- On heating & on cooling tests are used to evaluate the solid-state cracking tendency
  - Ductility dip cracking

Typical Results

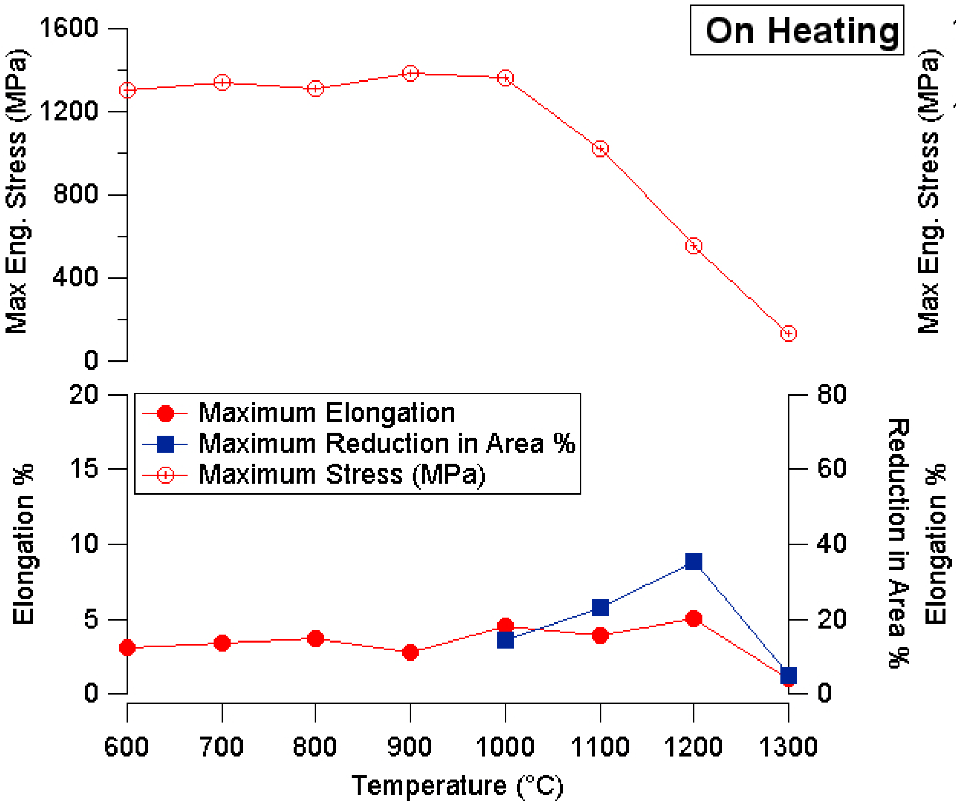

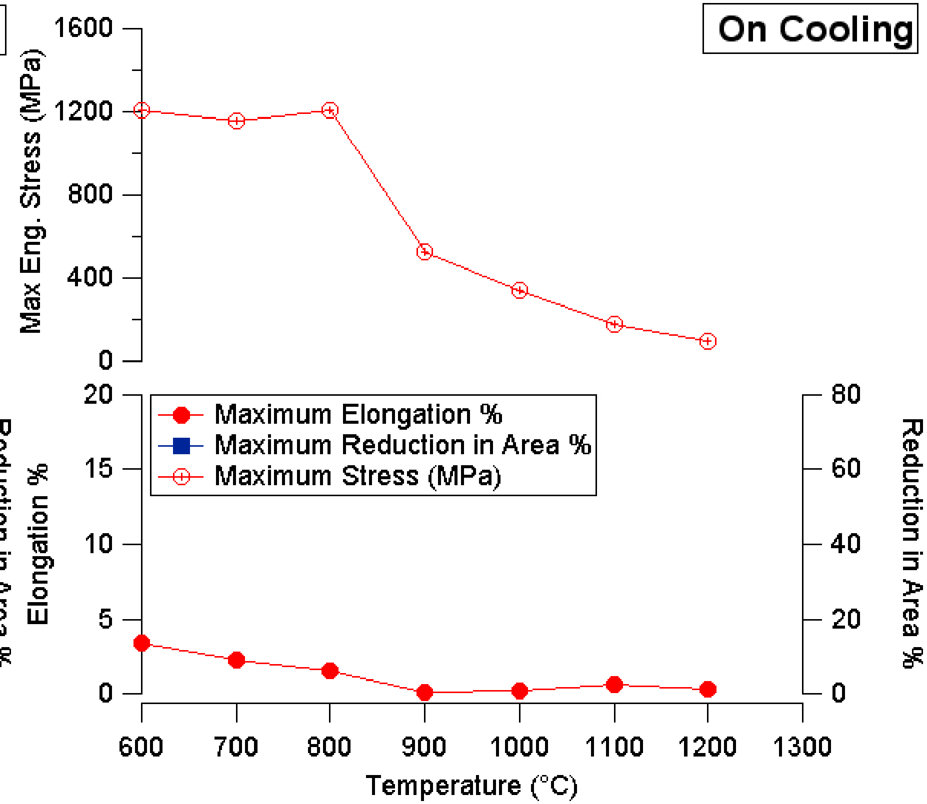

- This data is from CMSX4 nickel base superalloy

Hydrogen-Induced Cracking

Module 5A.3

Hydrogen-Induced Cracking

- Occurs in a wide range of materials if sufficient hydrogen is present
- Most common in structural steels and other alloys that are primarily ferritic at ambient temperature
- Associated with the diffusion and accumulation of hydrogen in the microstructure
- May occur immediately following welding or after an incubation, or delay, time
- A “unified” mechanism still does not exist

Conditions for Hydrogen-Induced Cracking

- Threshold level of hydrogen
- Susceptible microstructure
- Tensile restraint
- Ambient or near ambient temperature

- **If one of these conditions can be eliminated, hydrogen cracking in welds will be avoided**

Three Essential Elements for HIC

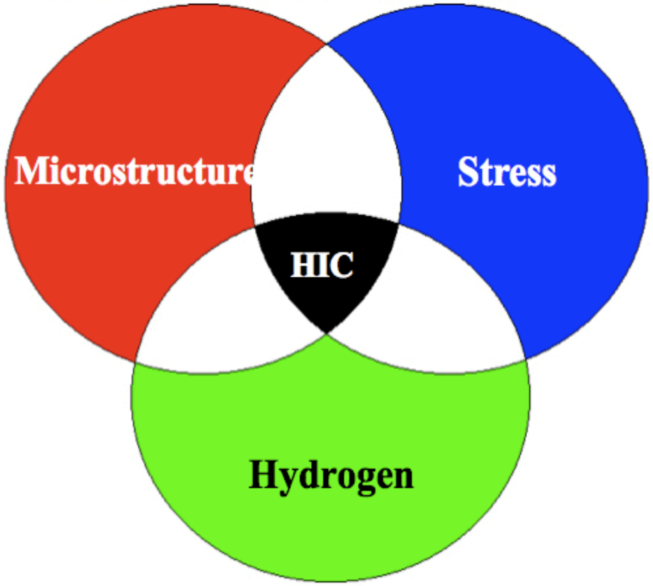

Hydrogen in Welds

- "Threshold" amount is difficult to define
- Sources of hydrogen
  - Base and/or filler metal
  - Moisture in fluxes and coatings (SMAW)
  - Organic contamination (oil, grease, paint, etc.)
  - Shielding gas
  - Condensation (dew point)
- Measurement
  - Diffusible
  - Total
- Hydrogen "trapping"

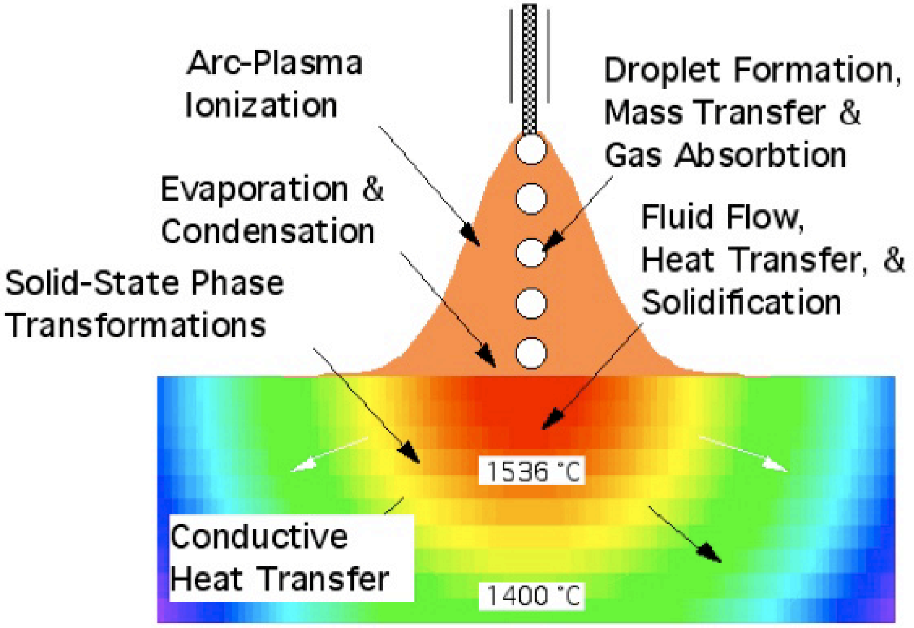

Effect of Microstructure

- Microstructure control very effective in eliminating HIC
- Wide range of microstructures possible as function of
  - Composition
  - Cooling rate from above A3
  - PWHT

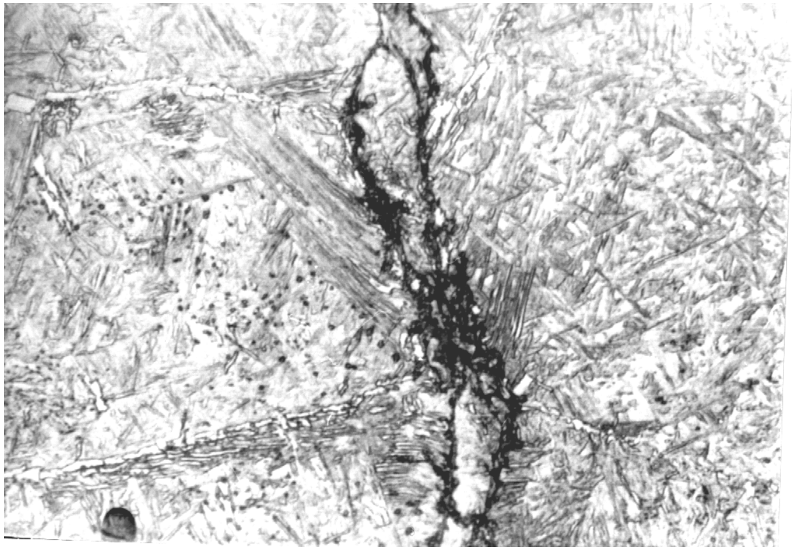

A hard martensitic microstructure in steel

Continuous Cooling Transformation (CCT) Diagram for a Plain Carbon Steel

- Softer microstructure

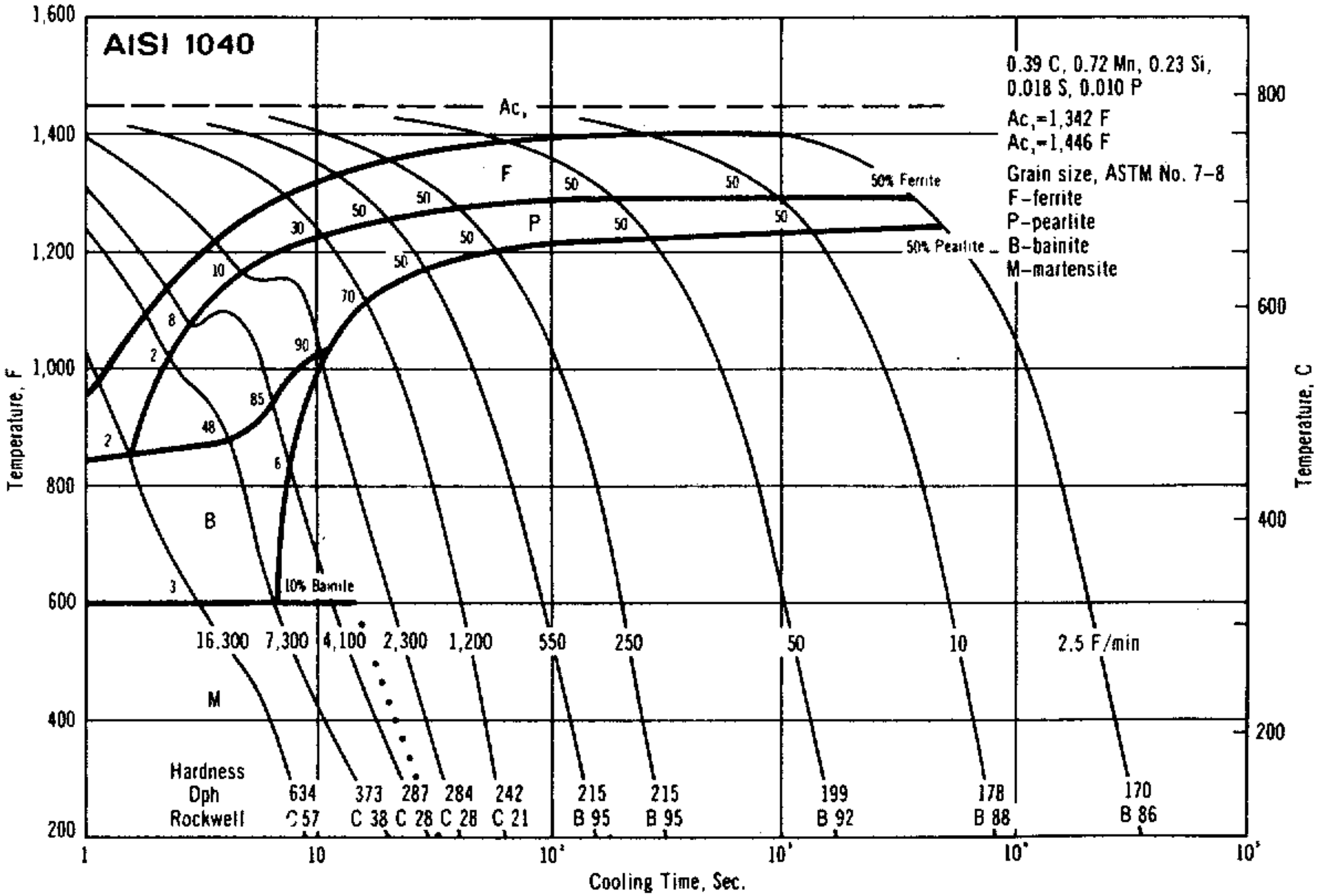

Continuous Cooling Transformation (CCT) Diagram for a Low Alloy Steel

- Harder microstructure

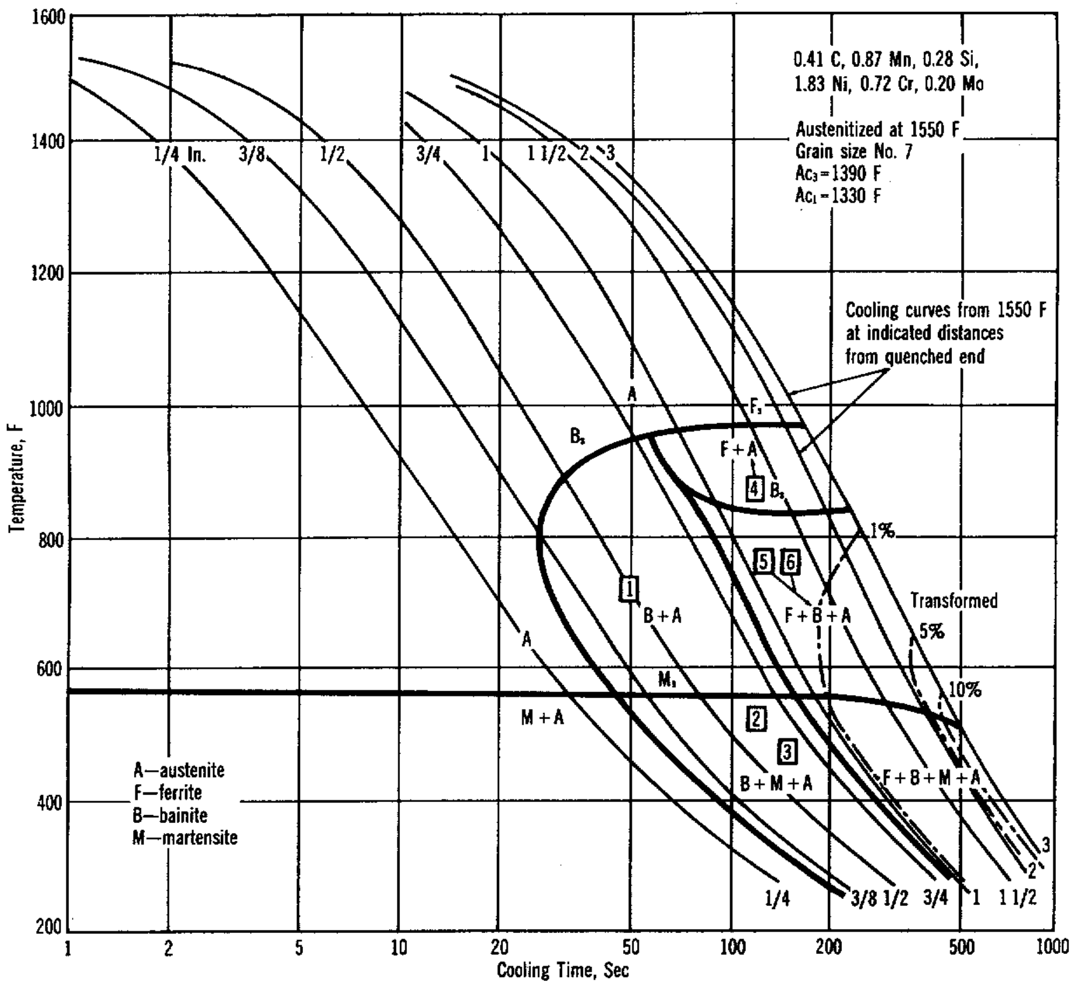

Relative Susceptibility of Microstructures to HIC

Microstructure	Susceptibility
Twinned martensite	***Highest***
Martensite	↓
Bainite + Martensite	↓
Bainite	↓
Tempered Martensite	↓
Pearlite	↓
Acicular ferrite	↓
Austenite	***Lowest***

Restraint

- Induces high tensile stress
- Difficult to quantify
- Combination of applied and residual
- Effect of stress concentrations
  - Cracks
  - Geometric
  - Slag inclusions

Temperature

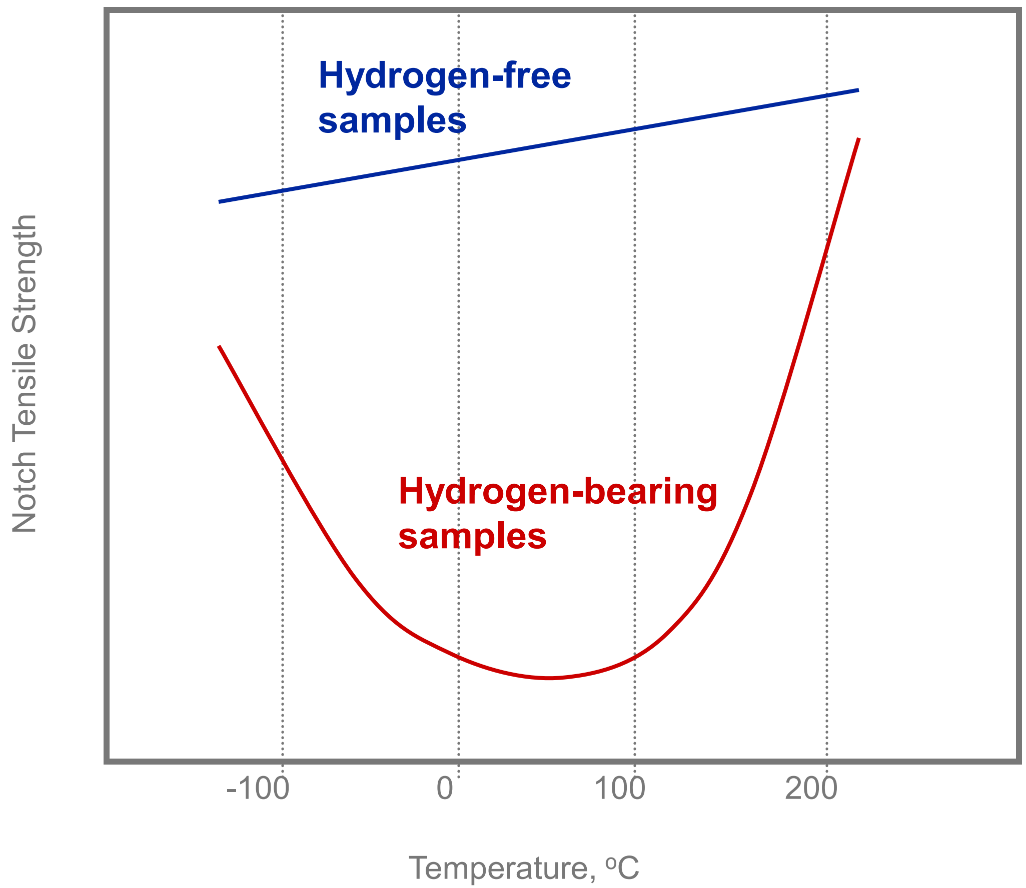

adapted from Threadgill

- Above 150ºC hydrogen is very mobile
- Below -100ºC mobility is low
- Hydrogen trapping effects

Identifying Hydrogen-Induced Cracking

- Metallography
  - Weld metal or HAZ
  - May be intergranular or transgranular
  - Initiation at stress concentration
  - Associated with transformed region of weldment
- Fractography
  - Intergranular fracture normally flat or micro-ductility
  - Transgranular
    - Cleavage or quasi-cleavage
    - Ductile dimples

Preventing Hydrogen-Induced Cracking

- Hydrogen
  - Low H practice
  - Cleaning prior to welding
  - Shielding gas
  - Preheat/interpass control
- Microstructure
  - Avoid martensitic structures
  - Acicular ferrite has best combination of strength and resistance to HIC
  - Minimize impurity segregation
- Restraint
  - Avoid stress concentrations
  - Reduce residual stress
  - Control weld contour
  - “Peening” of weld toes
- Temperature
  - Preheat/interpass control
  - Cooling rate control
  - Hydrogen diffusion
  - Microstructure

AWS Method

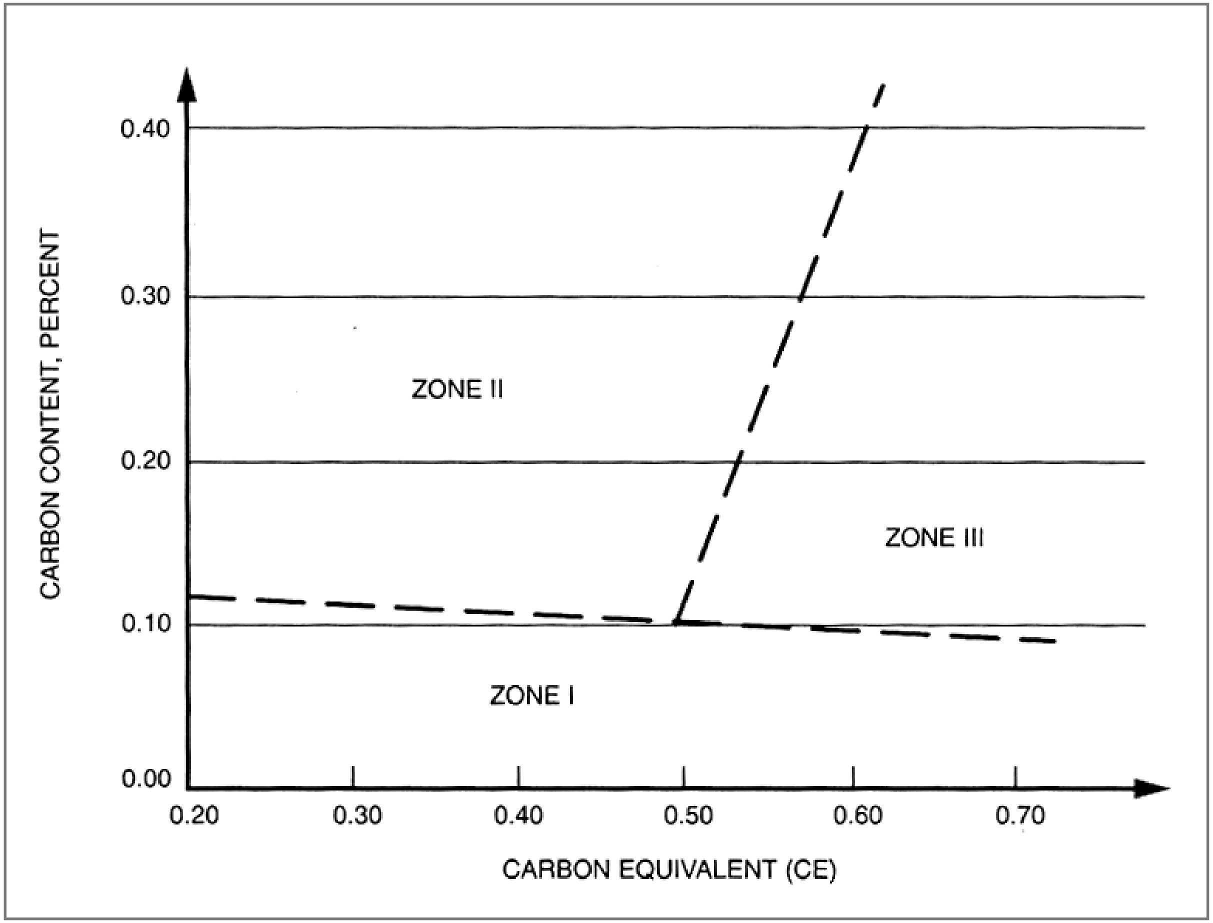

From AWS D1.1-2000, Appendix XI

$CE = C + (Mn + Si)/6 + (Cr + Mo + V)/5 + (Ni + Cu)/15$

AWS Hardness Control Method

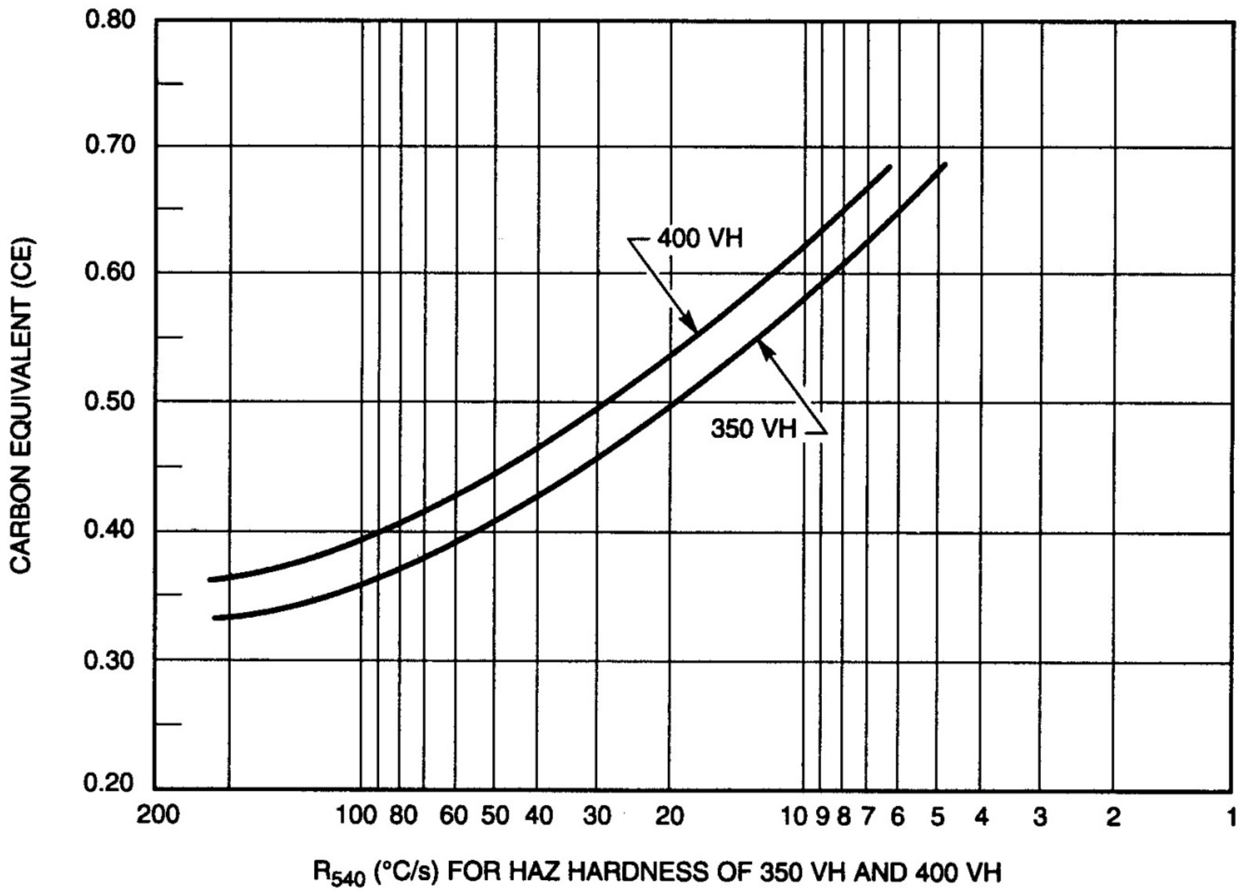

Note: CE = C + (Mn + Si)/6 + (Cr + Mo + V)/5 + (Ni + Cu)/15

AWS Hardness Control Method – Cooling Rate

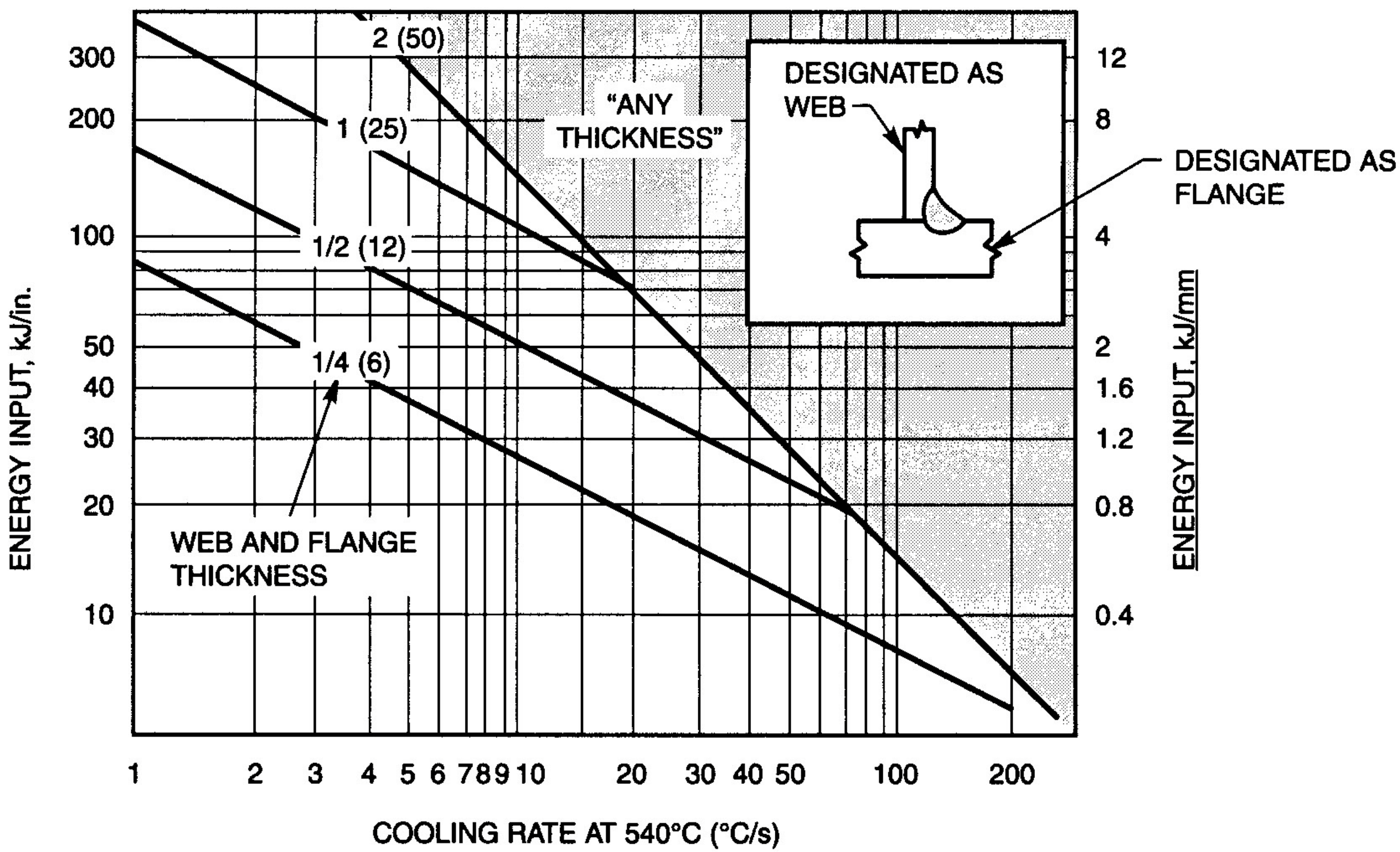

From AWS D1.1-2000, Annex XI

AWS Hardness Control Method – Cooling Rate

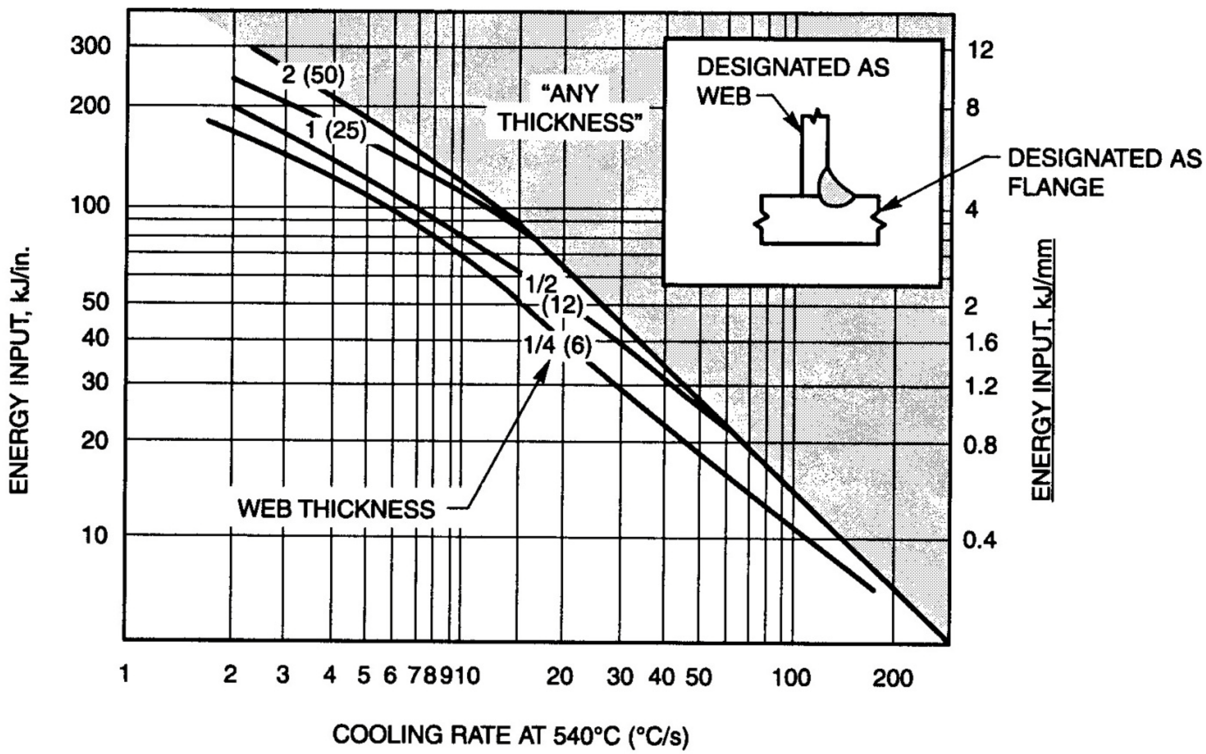

NOTE: ENERGY INPUT DETERMINED FROM CHART DOES NOT IMPLY SUITABILITY FOR PRACTICAL APPLICATIONS. FOR CERTAIN COMBINATION OF THICKNESSES MELTING MAY OCCUR THROUGH THE THICKNESS.

(D) SINGLE-PASS SAW FILLET WELDS WITH 1 in. (25 mm) FLANGES AND VARYING WEB THICKNESSES

From AWS D1.1-2000, Annex XI

AWS Method – Determining Susceptibility Index

Table XI-1
Susceptibility Index Grouping as Function of Hydrogen Level "H" and Composition Parameter P_{cm} (see XI6.2.3)

Hydrogen Level, H	Susceptibility Index[2] Grouping — Carbon Equivalent = P_{cm}^{1}				
	< 0.18	< 0.23	< 0.28	< 0.33	< 0.38
H1	A	B	C	D	E
H2	B	C	D	E	F
H3	C	D	E	F	G

Notes:

1. $P_{cm} = C + \frac{Si}{30} + \frac{Mn}{20} + \frac{Cu}{20} + \frac{Ni}{60} + \frac{Cr}{20} + \frac{Mo}{15} + \frac{V}{10} + 5B$
2. Susceptibility index—12 P_{cm} + $\log_{10}$ H.
3. Susceptibility Index Groupings, A through G, encompass the combined effect of the composition parameter, P_{cm}, and hydrogen level, H, in accordance with the formula shown in Note 2.

The exact numerical quantities are obtained from the Note 2 formula using the stated values of P_{cm} and the following values of H, given in ml/100g of weld metal (see XI6.2.2, a, b, c):

H1—5; H2—10; H3—30.

For greater convenience, Susceptibility Index Groupings have been expressed in the table by means of letters, A through G, to cover the following narrow ranges:

A = 3.0; B = 3.1–3.5; C = 3.6–4.0; D = 4.1–4.5; E = 4.6–5.0; F = 5.1–5.5; G = 5.6–7.0

These groupings are used in Table XI-2 in conjunction with restraint and thickness to determine the minimum preheat and interpass temperature.

AWS Method – Selection of Preheat Temperature

Table XI-2
Minimum Preheat and Interpass Temperatures for Three Levels of Restraint (see XI6.2.4)

Restraint Level	Thickness* in.	Minimum Preheat and Interpass Temperature (°F) — Susceptibility Index Grouping A	B	C	D	E	F	G
Low	< 3/8	< 65	< 65	< 65	< 65	140	280	300
	3/8–3/4	< 65	< 65	65	140	210	280	300
	3/4–1-1/2	< 65	< 65	65	175	230	280	300
	1-1/2–3	65	65	100	200	250	280	300
	> 3	65	65	100	200	250	280	300
Medium	< 3/8	< 65	< 65	< 65	< 65	160	280	320
	3/8–3/4	< 65	< 65	65	175	240	290	320
	3/4–1-1/2	< 65	65	165	230	280	300	320
	1-1/2–3	65	175	230	265	300	300	320
	> 3	200	250	280	300	320	320	320
High	< 3/8	< 65	< 65	< 65	100	230	300	320
	3/8–3/4	< 65	65	150	220	280	320	320
	3/4–1-1/2	65	185	240	280	300	320	320
	1-1/2–3	240	265	300	300	320	320	320
	> 3	240	265	300	300	320	320	320

*Thickness is that of the thicker part welded.

(continued)

By Controlling the Diffusible Hydrogen Concentration

- AWS Classification such as E7018-H4R
  - "H4" means electrode will deposit diffusible hydrogen average not to exceed 4 mL of hydrogen per 100g of deposited weld metal
  - "R" means electrode is resistant to hydrogen pick-up
    - Increased exposure limits
- Relevant: ASME Section II-Part C, SFA-5.1

Fatigue and Fracture

Module 5A.4

Fracture and Fatigue of Weldments

- Welds are often associated with structural failure
  - Catastrophic, brittle fracture
  - Overload
  - Fatigue
- Presence of brittle microstructures
  - Low toughness
  - Low ductility
- Stress concentration
  - Defects
  - Stress risers
- Residual stress effects

What Causes Brittle Fracture?

- Three factors contribute to brittle fracture
  - Material toughness
  - Crack, or flaw, size
  - Stress level

Material Toughness

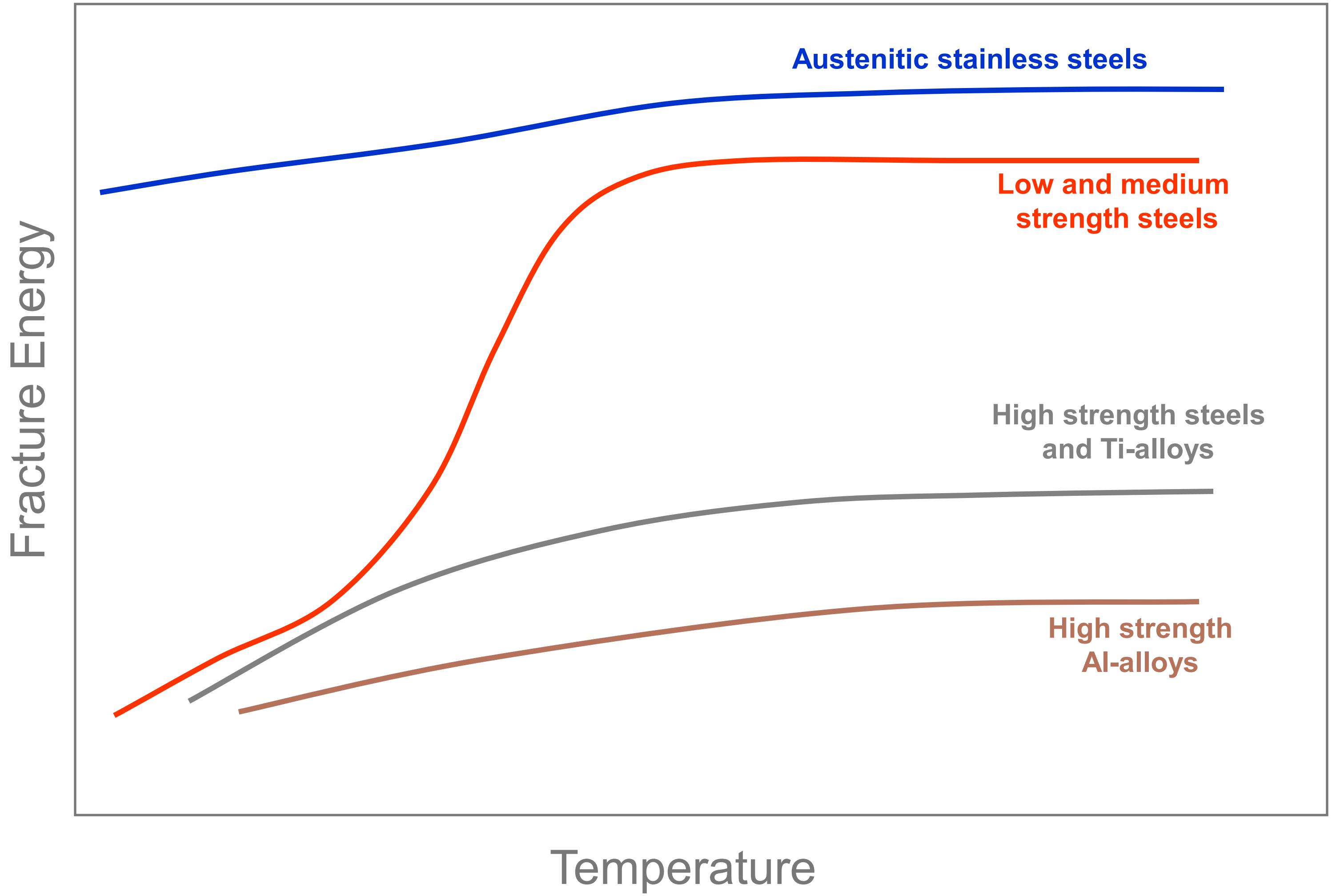

Fracture Toughness

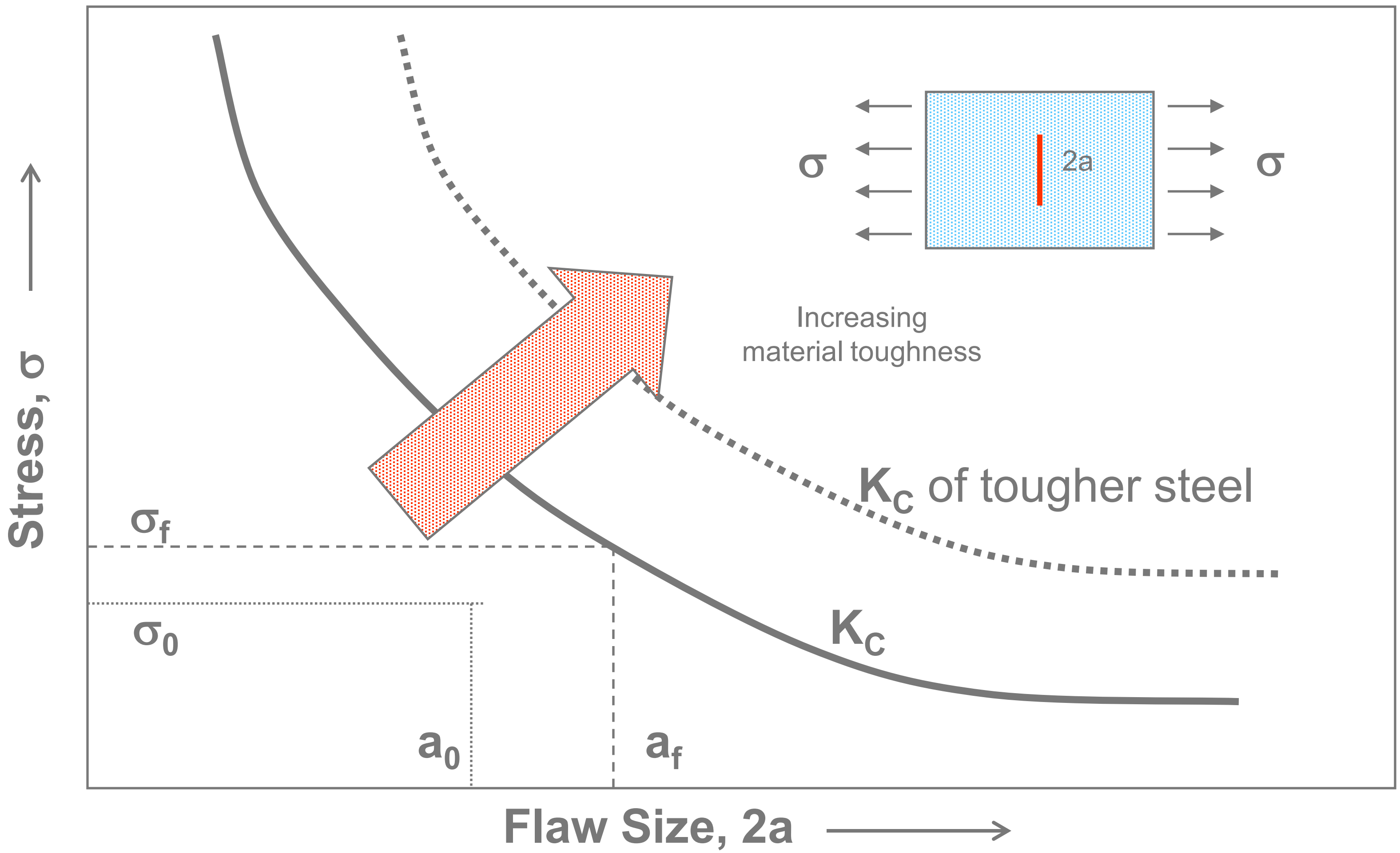

Adapted from Barsom and Rolfe

Application of Fracture Mechanics to Engineering Materials

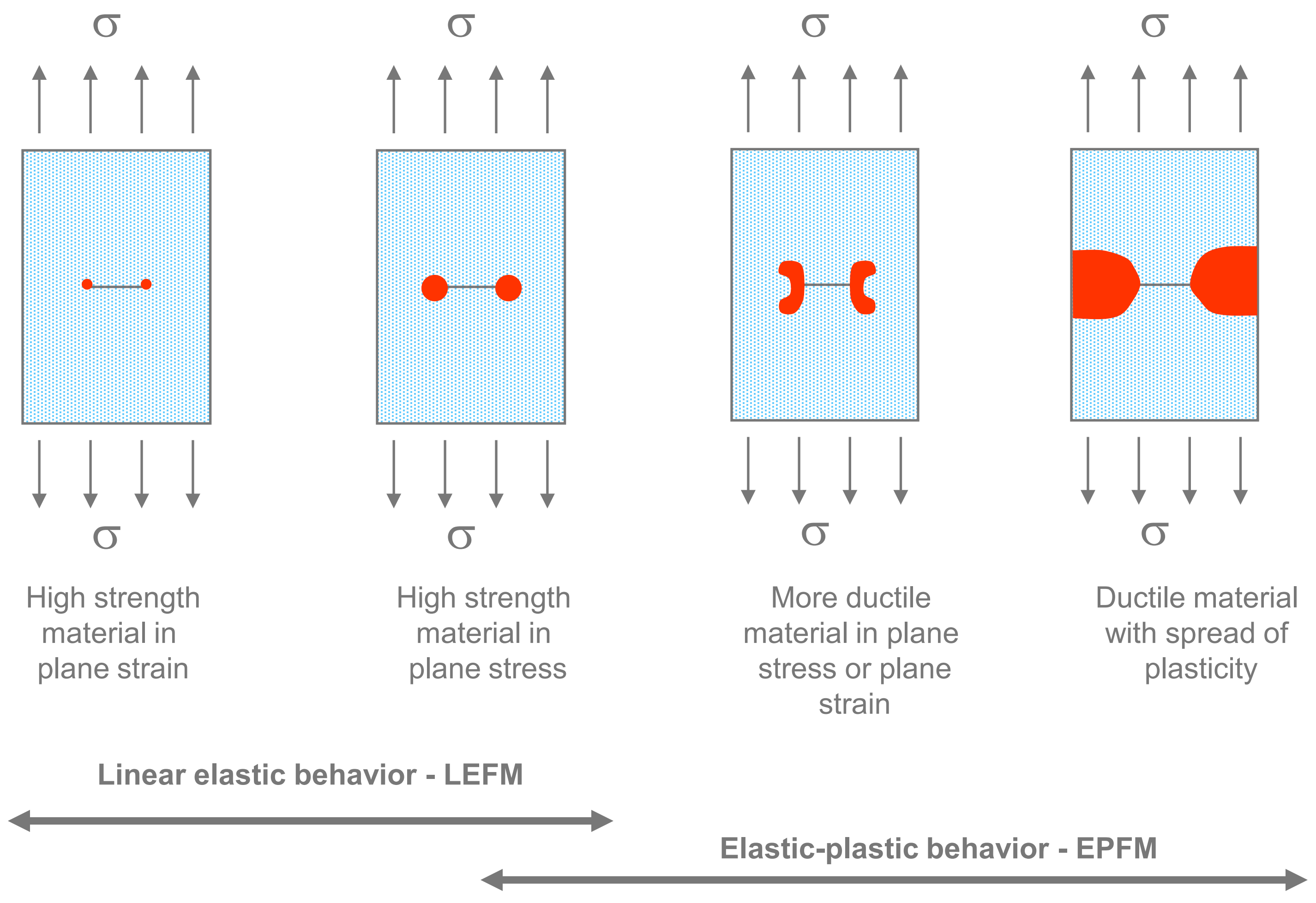

Sketch adapted from Barsom and Rolfe

Fatigue Cracking

- Repetitive, or cyclic, application of load
- Three stages
  - Initiation
  - Propagation
  - Failure
- Effect of stress intensity

S-N Curve

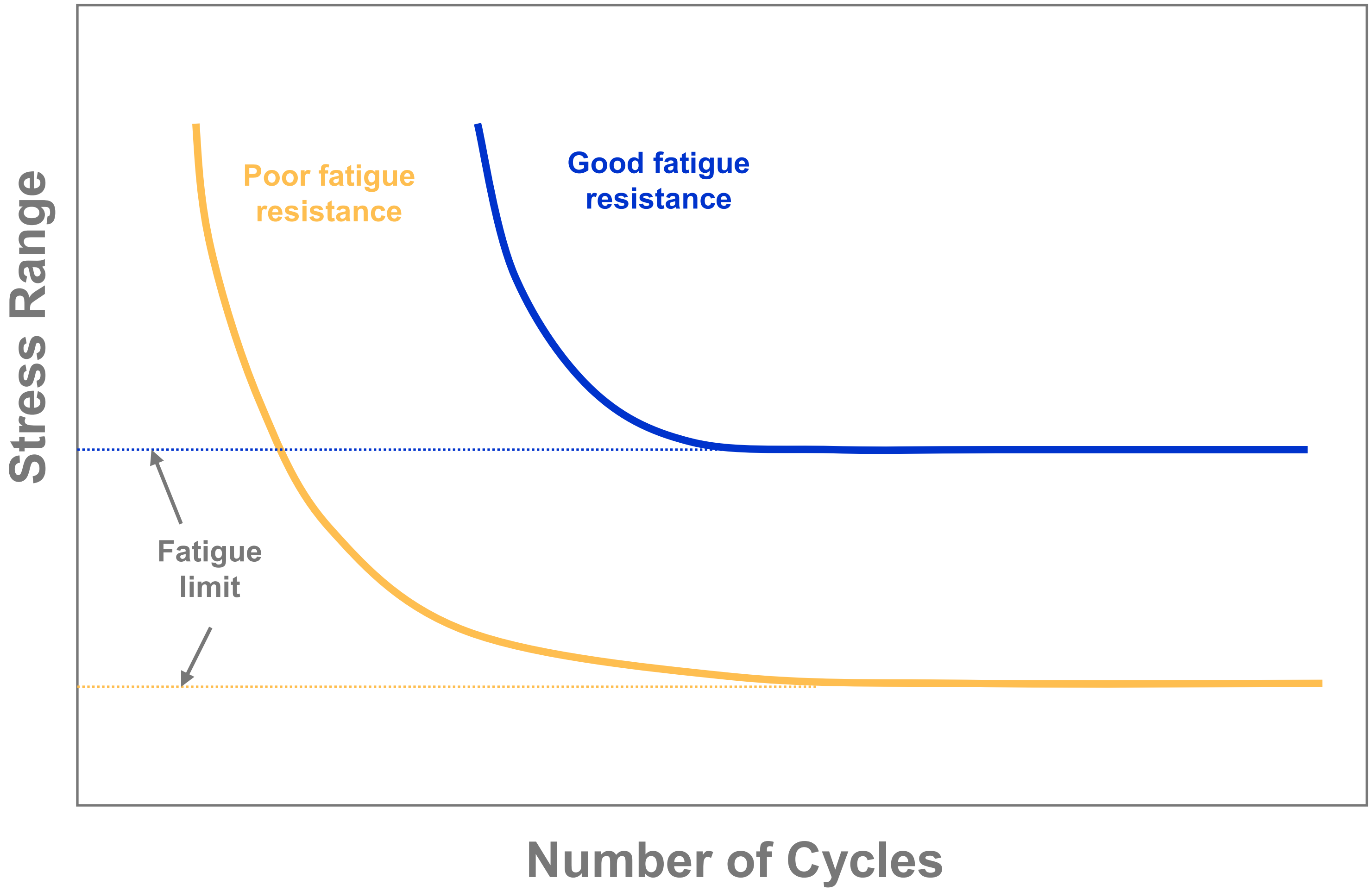
Poor fatigue resistance
Good fatigue resistance
Stress Range
Fatigue limit
Number of Cycles

Initiation versus Propagation

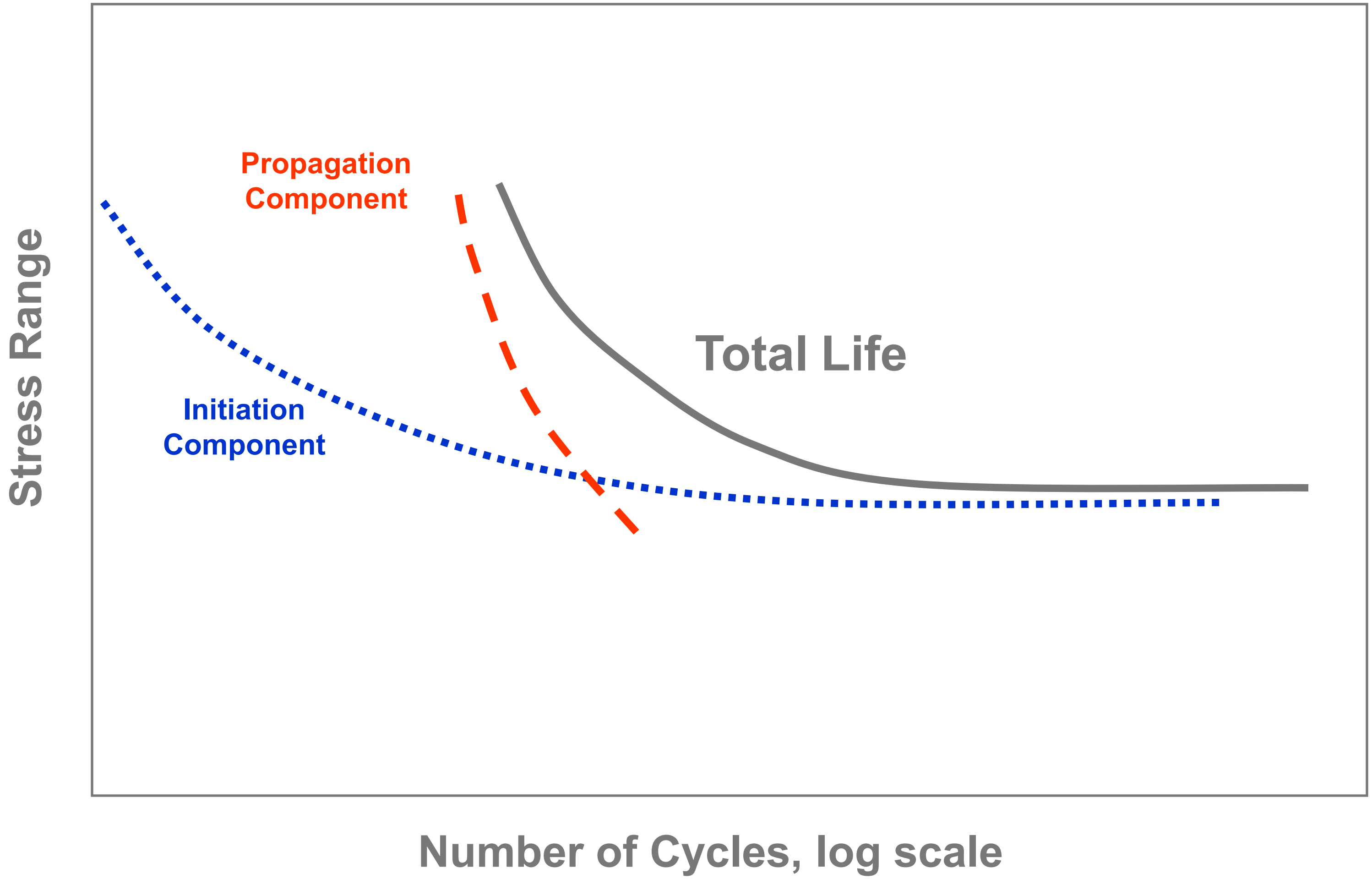

S-N Curve for Welded Joint

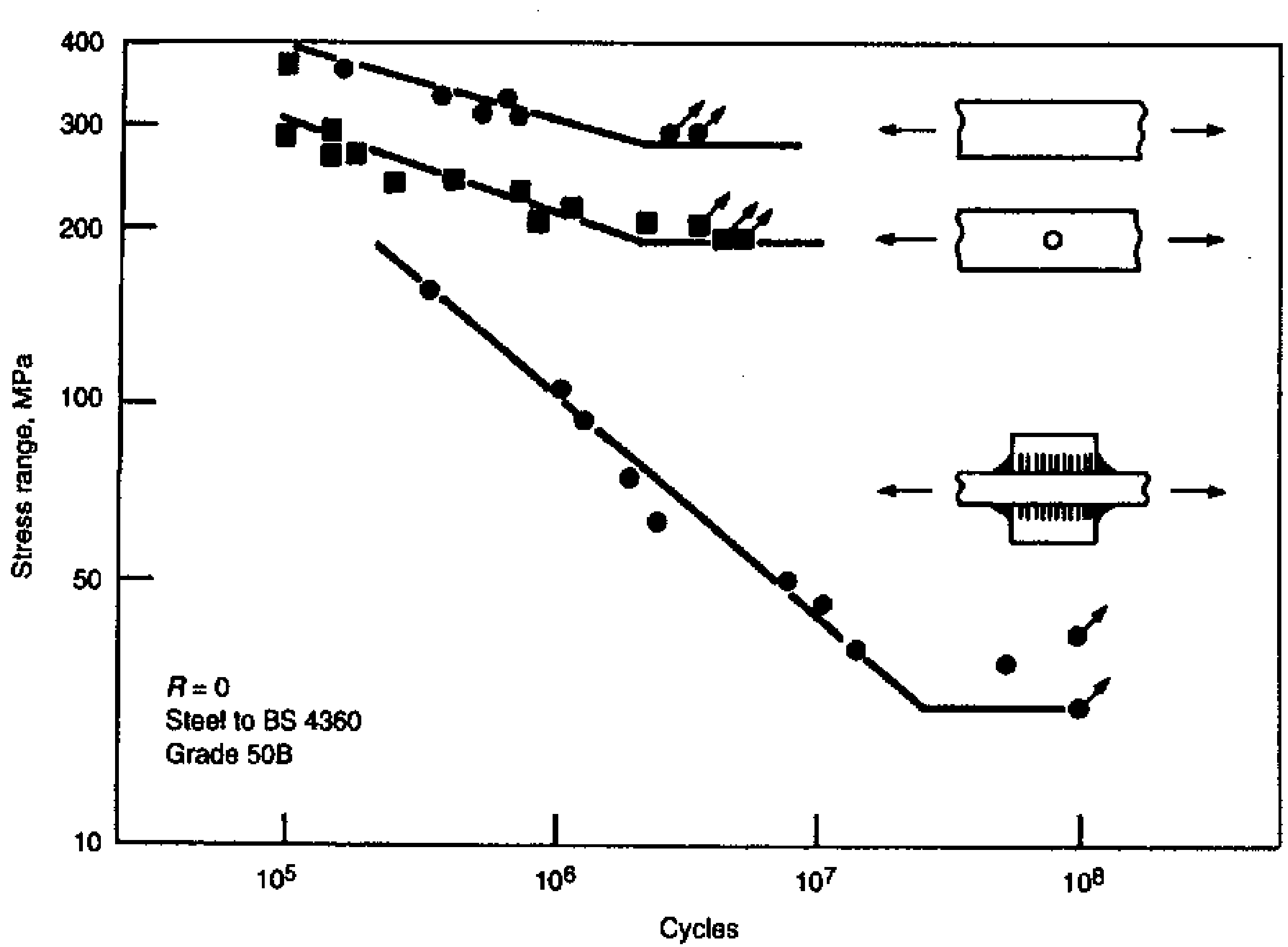

Effect of Fluctuating Stress on Crack Growth

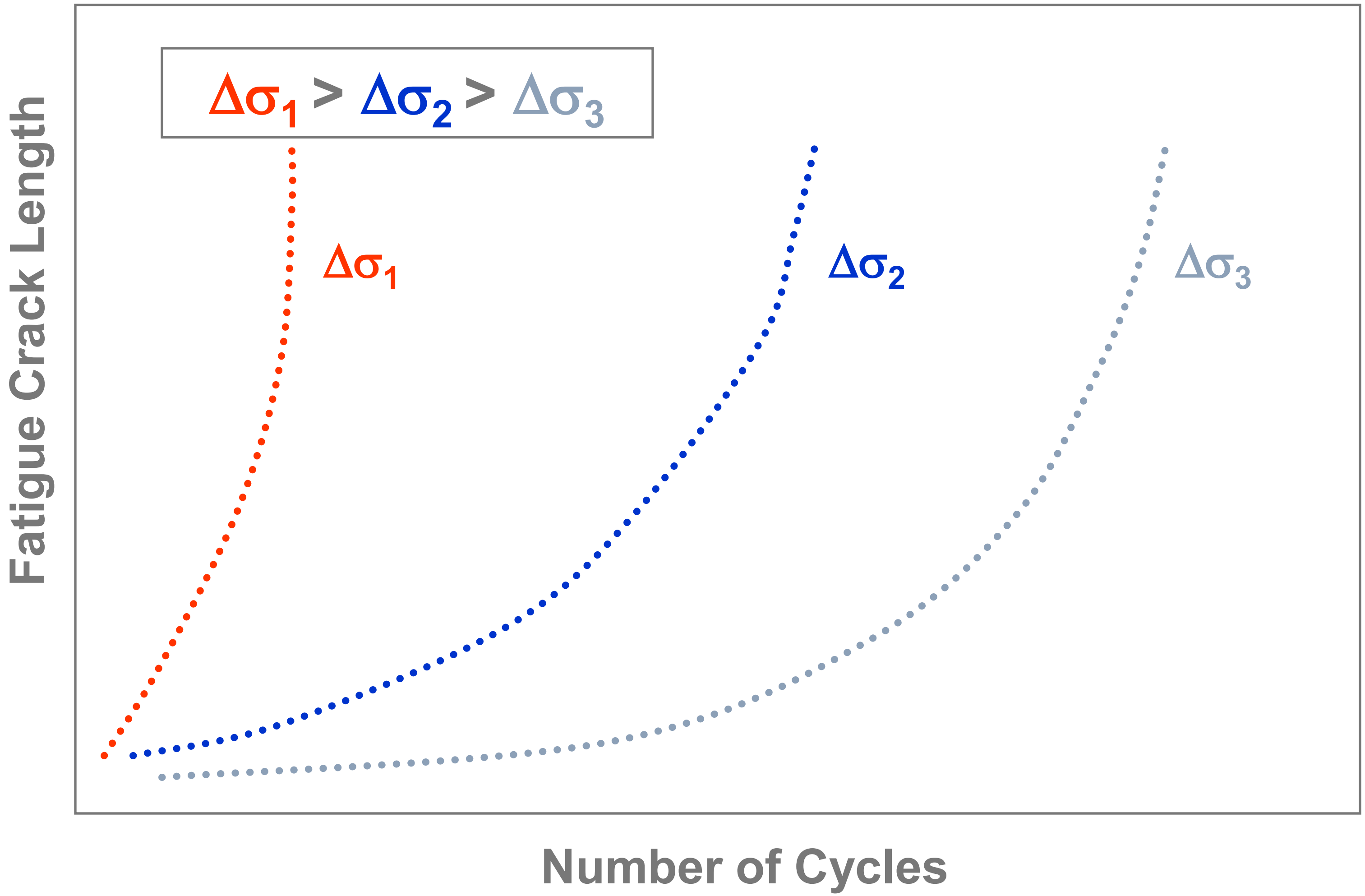

Effect of Material on Crack Growth Rate

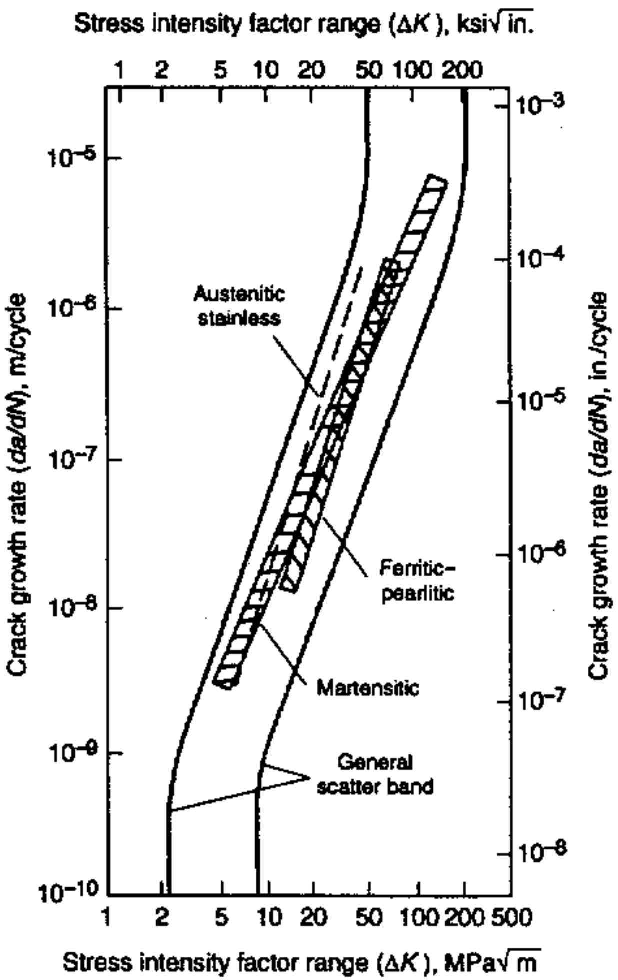

- Three regions
- Steady state crack growth rate defined by Paris Law

$$da/dN = C(\Delta K)m$$

- Increasing crack growth rate with stress intensity
- Little effect of material type in steady state crack growth region
- Initiation and final failure regions more influenced by material type, strength, and environment

From ASM Handbook, Volume 19

Effect of Microstructure on Crack Growth Rate

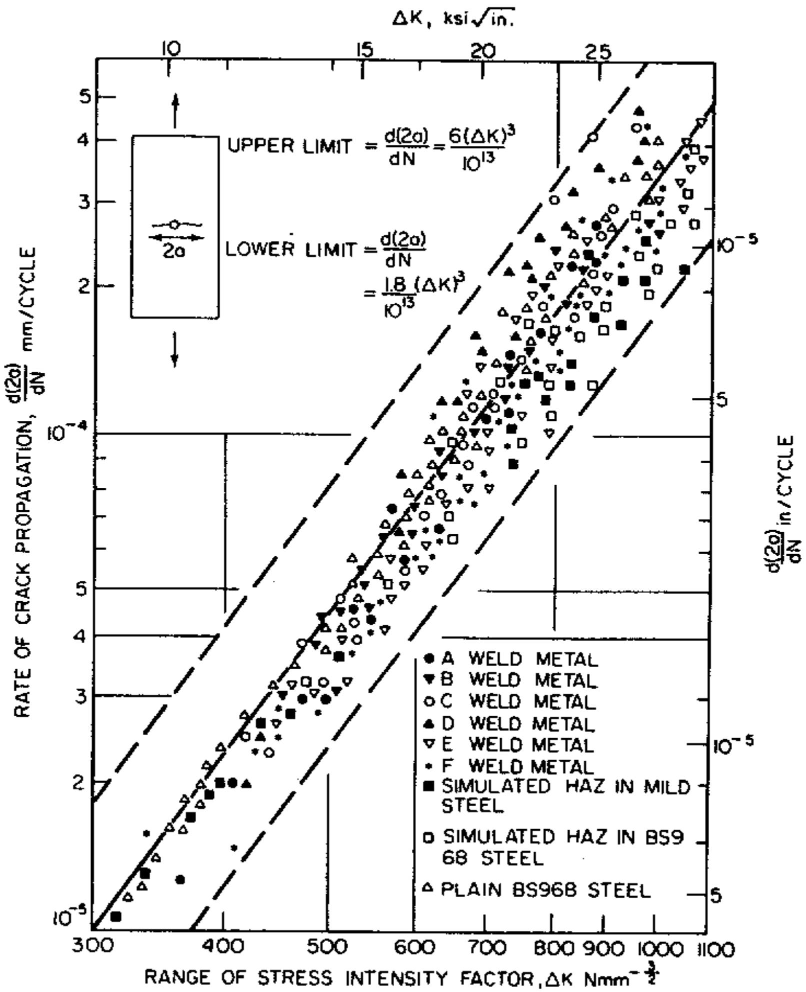

- Little effect of microstructure on steady state crack growth
- Base metal, weld metal, and HAZ fall within scatter band for mild steels and matching weld metals
- Similar behavior observed in other alloy systems

From Barsom and Rolfe

Identifying Fatigue Cracks

- Initiation at flaws or stress concentration points
  - Weld toe (slag intrusions, undercut, etc.)
  - Lack of penetration
  - Fabrication cracks (weld metal or HAZ)
- Visual and metallography
  - Little macroscopic deformation
  - Cracks tend to be straight
  - Usually transgranular
- Fractography
  - Macroscopically flat
  - Beach marks and river lines
  - Finely spaced striations related to da/dN

Fatigue Fracture Surface Features

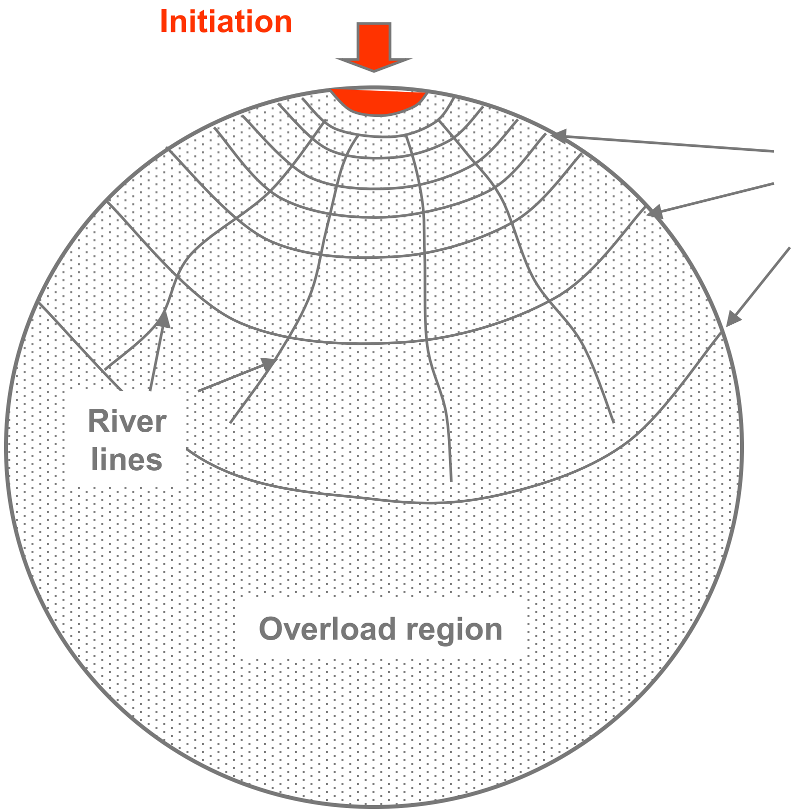

Failure in rotating shaft

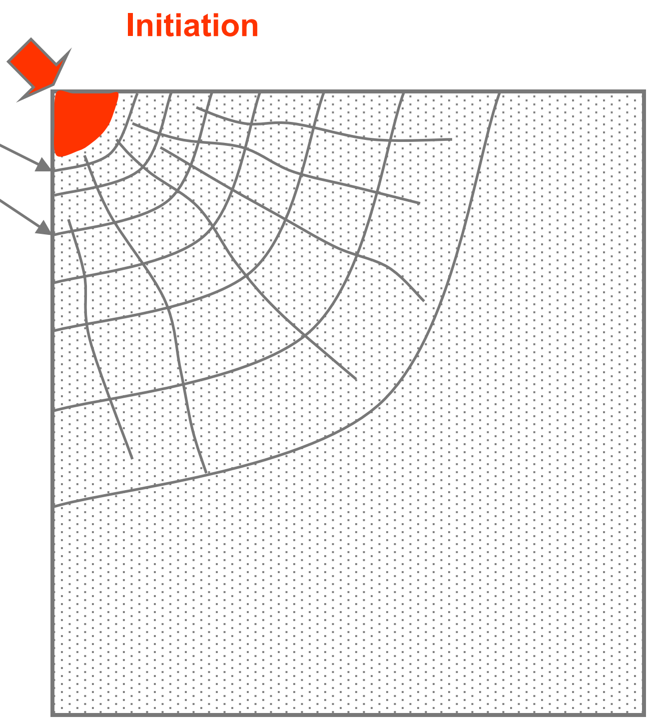

Failure initiating at corner

Corrosion

Module 5B

Eight Forms of Corrosion

- General
- Galvanic
- Crevice
- Pitting
- Intergranular
- Selective leaching
- Erosion corrosion
- Stress-assisted

General Corrosion

- General, or uniform, surface attack
- Function of composition
- Nature of oxide
  - Continuous or porous
  - Adherence
  - Stability
- Influence of welding
  - Thermal “damage”
  - Local changes in composition
  - Residual stress

Galvanic Corrosion

- Chemical potential difference between dissimilar metals
- Galvanic “couple” between dissimilar metals
  - Anode - active metal has lower potential
  - Cathode - noble metal has higher potential
- Net current flow from anode to cathode
- Effect of dissimilar base and/or weld metals

Galvanic Series for Commercial Metals in Seawater

- Platinum
- Gold
- Titanium
- Silver
- Hastelloy C
- 18-8 stainless steel (passivated)
- Copper, monel, and cupronickels
- Nickel and Inconels (active)
- Tin Lead
- 18-8 stainless steel (active)
- Steel and iron
- Aluminum alloy 2024
- Aluminum alloy 1100
- Zinc
- Magnesium and Mg-alloys

↑ **Cathodic (noble)**

Anodic (active) ↓

Adapted from Fontana and Greene

Solution Potential versus Location

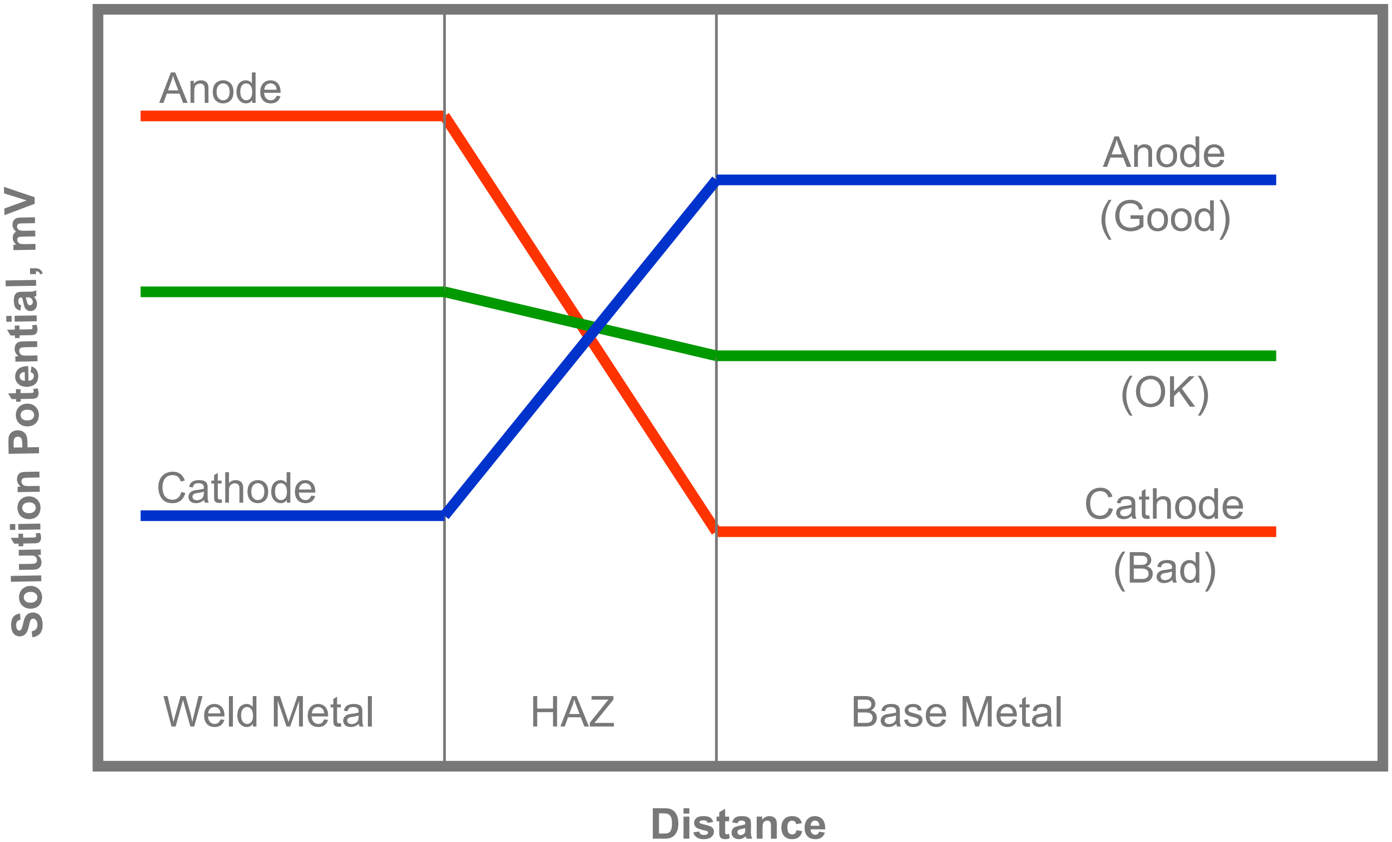

Crevice Corrosion

- Localized corrosion at mechanical discontinuity or crevice
- Weld-induced crevices
  - Slag intrusions or entrapment
  - Lack-of-fusion or penetration defects
  - Cracks

Pitting Corrosion

- Localized attack
- Small “pit” or pinhole at surface
- Grows in direction of gravity
- Strong effect of composition
- Microstructure effects

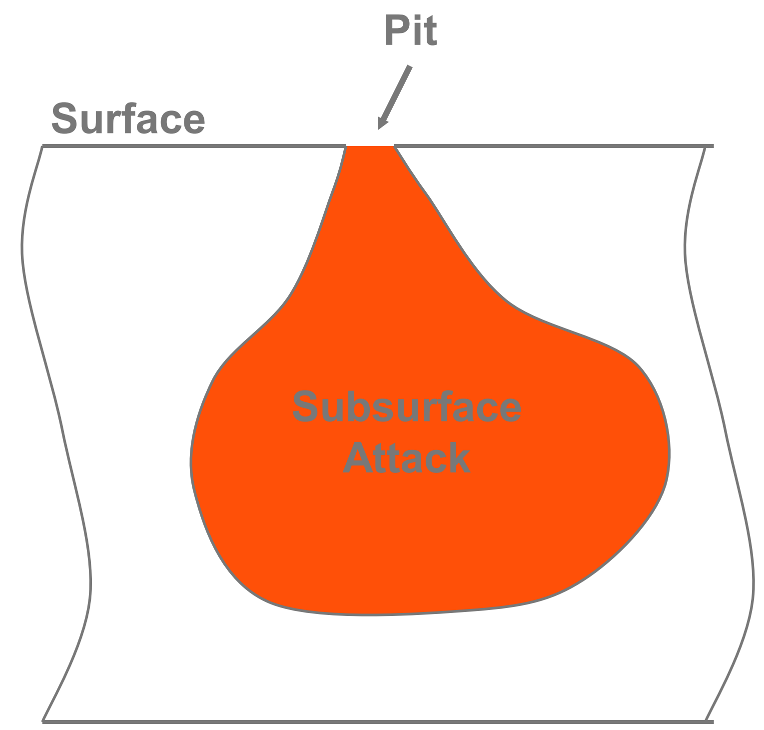

Pitting Resistance

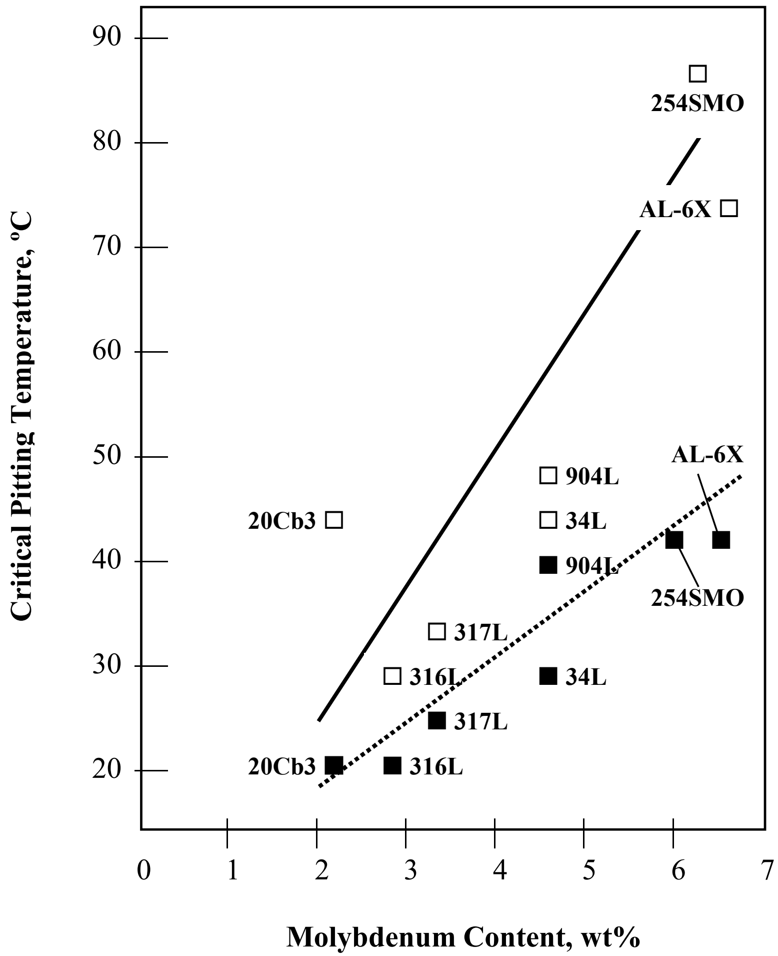

- Strong function of Mo content
- Measured in terms of critical pitting temperature (CPT)
  - Minimum temperature at which pits form
- Welds have lower CPT than base metal

Pitting Corrosion - Effect of Alloying Elements

Element	Effect on Pitting Resistance
Chromium	Increases
Nickel	Increases
Molybdenum	Increases
Tungsten	Increases
Silicon	Decreases, except with Mo
Titanium and Niobium	Decreases resistance in $FeCl_3$
Sulfur	Decreases
Carbon	Decreases, especially when sensitized
Nitrogen	Increase

Pitting Resistance Equivalent (PRE) = Cr + 3.3(Mo + 0.5W) + 16N

Selective Leaching

- Referred to as “de-alloying”
  - Loss of an alloying element
  - “Dezincification” in brass alloys

Erosion Corrosion

- Similar to general corrosion
- Accelerated by relative motion and impingement of the corrosive medium
- Softer metals most susceptible
- Welds may be more susceptible than base metals due to softened regions

Intergranular Corrosion

- Localized attack at, or adjacent to, grain boundaries
- Associated with
  - Impurity segregation
  - Enrichment/depletion of alloying elements
  - Formation of intermetallics
  - Second phases
- Galvanic contribution
- Attack may be quite rapid

"Sensitization" Mechanism

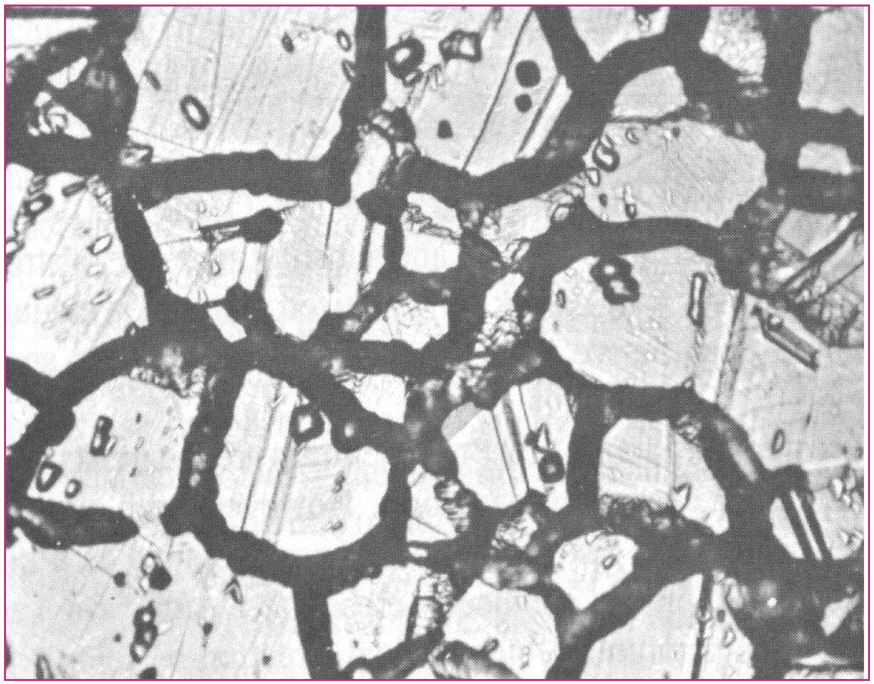

Grain boundary attack in Type 304

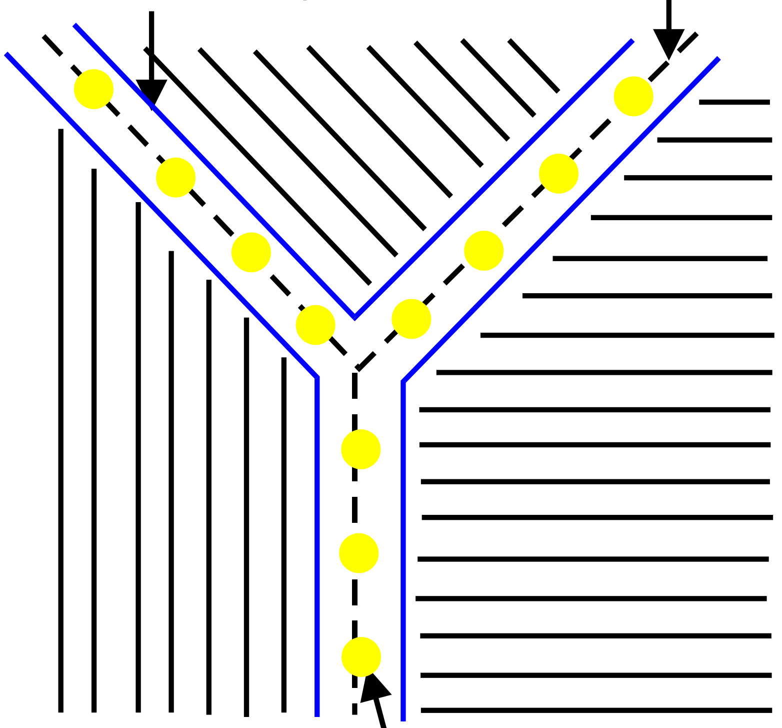

Carbide Precipitation

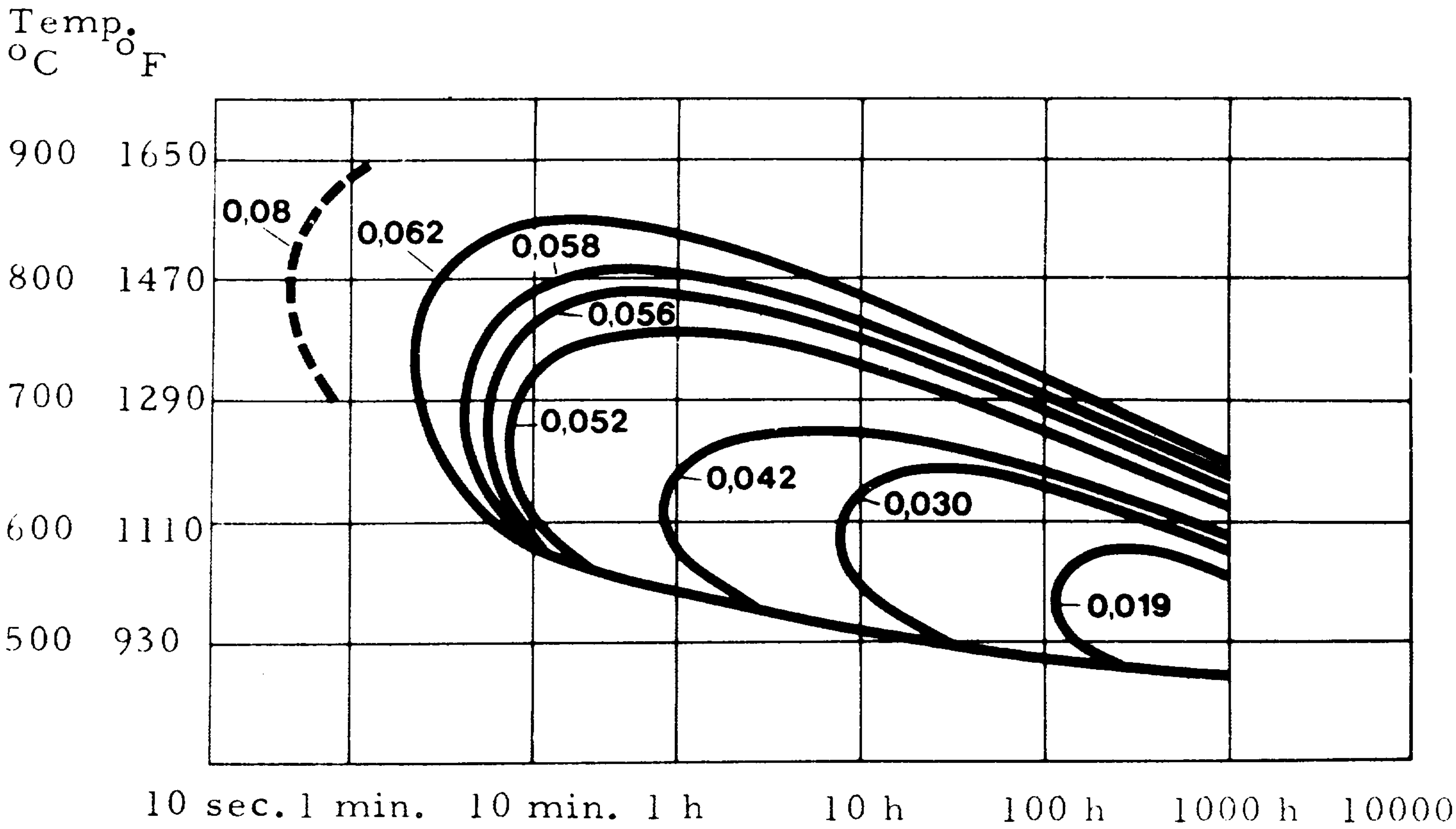

"Knifeline" Attack

- Associated with stabilized grades of stainless steel (321 and 347)
- Dissolution of NbC or TiC adjacent to fusion boundary
- Formation of Cr-rich carbide during cooling
- Sensitization of boundary in very narrow region

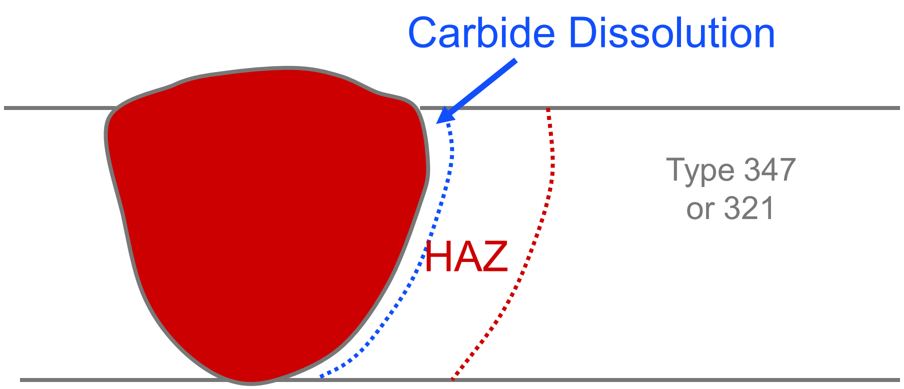

Low Temperature Sensitization

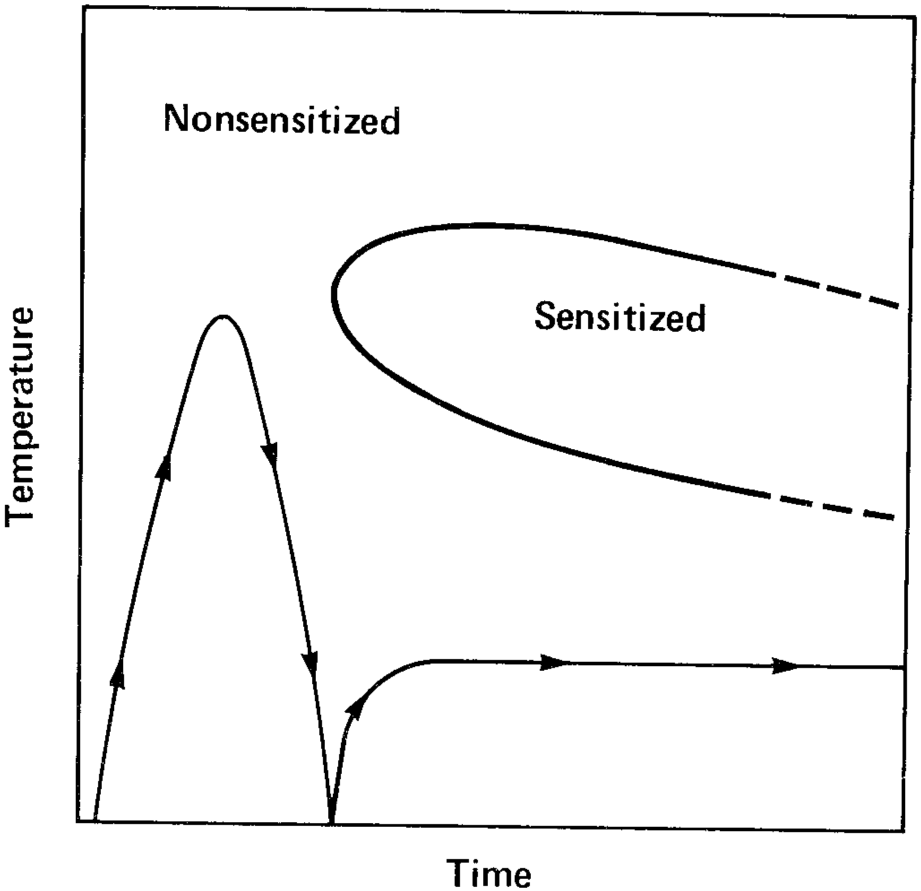

- Cr-carbide formation in service
  - 10-20 years
  - Service temperature below 300° C (572° F)
- Results in IGA or IGSCC

Avoiding Intergranular Attack in Stainless Steels

- Composition control
  - Low-carbon (L-grade) alloys
  - Stabilized alloys (additions of Nb and Ti)
- Microstructure control
  - Use annealed base metals (cold work accelerates precipitation)
  - Solution heat treat after welding and cool rapidly
- Welding process/procedure
  - Low heat input
  - Low or no preheat and interpass
  - Accelerated cooling

Stress-Corrosion Cracking

- Localized cracking resulting from combination of
  - Tensile stress
  - Corrosive environment
- Variables
  - Environment (concentration)
  - Temperature
  - Material composition
  - Stress level
  - Microstructure
- Transgranular or intergranular

Systems Susceptible to SCC

Alloy or Alloy System	*Environment*
Aluminum alloys	NaCl solutions, seawater
Copper alloys	Ammonia vapors and solutions
Gold alloys	$FeCl_3$ solutions, acetic acid-salt solutions
Inconel	Caustic soda solutions
Lead	Lead acetate solutions
Magnesium alloys	Distilled water
Monel	Fused caustic soda, hydrofluoric acid
Nickel	Fused caustic soda
Carbon and Low Alloy Steels	Multiple
Stainless Steel	Multiple, including seawater and H_2S
Titanium alloys	Fuming nitric acid, seawater, N_2O_4

SCC in Stainless Steels and Nickel Alloys

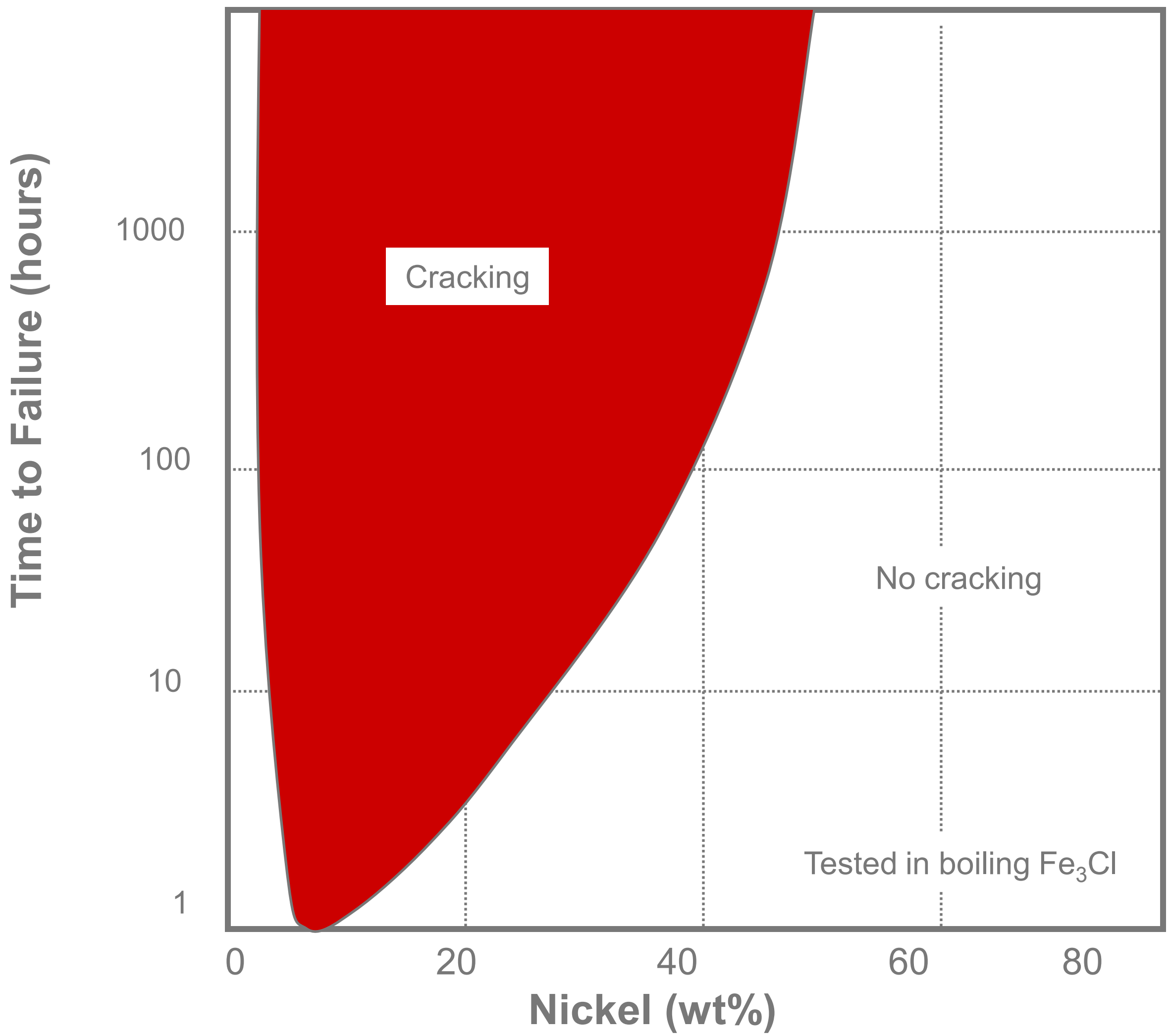

Transgranular SCC in Type 316 Tubesheet

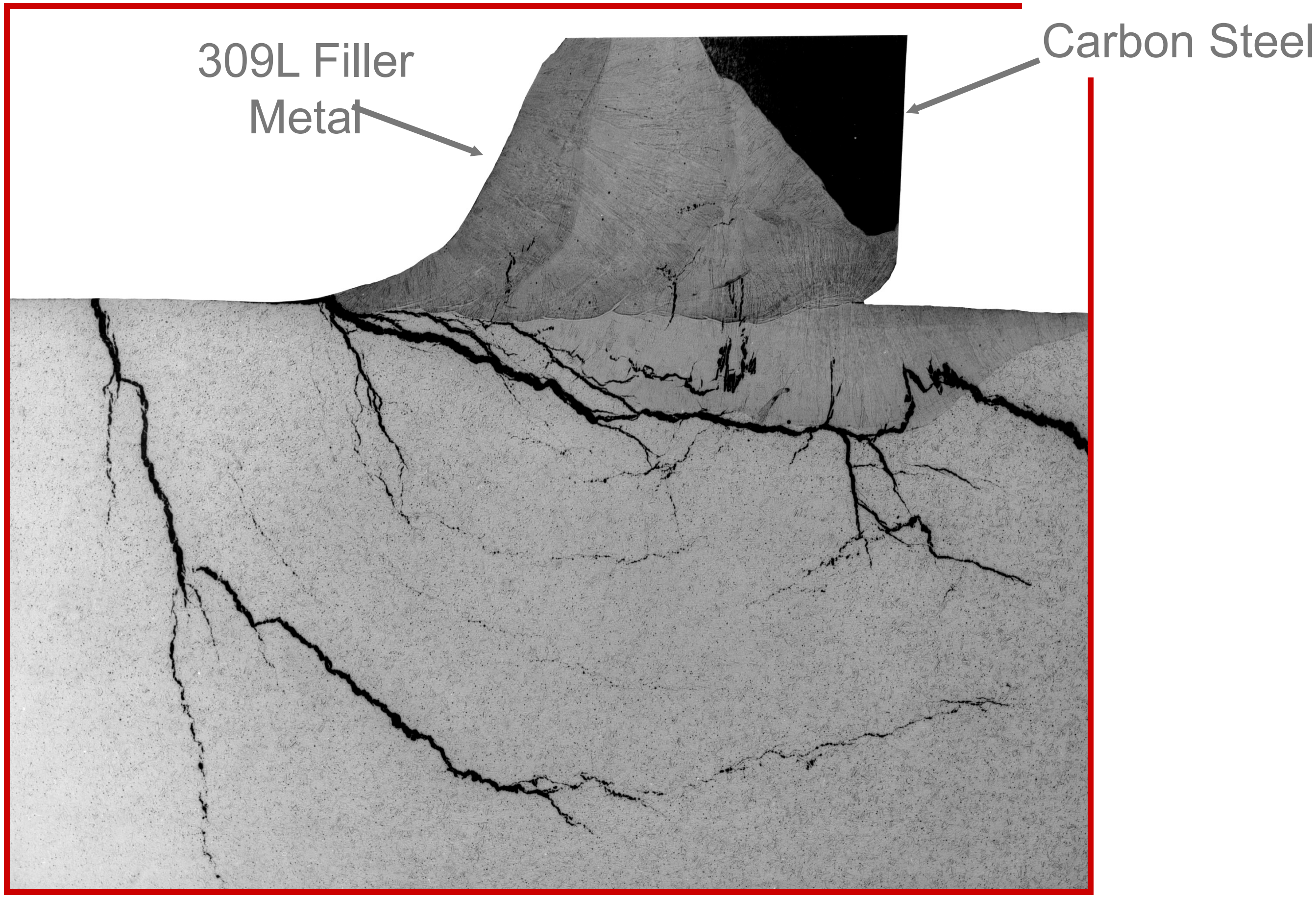

Avoiding SCC in Welded Structures

- Alloy selection
  - Substitute ferritic or duplex alloy for austenitic stainless steels
  - Use high-Ni alloys
- Avoid sensitization
- Eliminate stress concentrations
- Reduce residual stresses
- Environmental control or isolation

Heat Tint and Sugaring

- If stainless steel surfaces are heated to moderately high temperatures in air during welding or grinding, a chromium oxide heat tint develops
  - Heat tints are thicker than Chromium oxides films and are very visible
  - Color depends on thickness, with the thickest oxides appearing black
  - Chromium content of the metal is reduced
    - Lower corrosion resistance
- Heat tints should be removed as well as the underlying layer with reduced carbon content

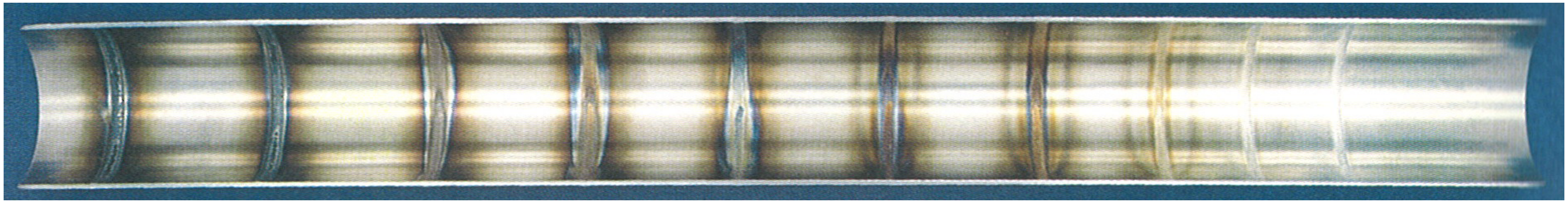

Figure showing decrease in heat tint as a function of oxygen exposure. AWS D18.1 1999

Primary Water Stress Corrosion Cracking (PWSCC)

- PWSCC is a form of stress corrosion cracking unique to primary cooling water containment in nuclear power plants
- Operating experience has shown that Ni-base Alloy 600 and Filler Metal 82 are susceptible to PWSCC
- Minimum Cr content of 25 wt% required to avoid PWSCC
- Use of Structural Weld Overlay (SWOL) and Pre-emptive Weld Overlay (PWOL) approaches to avoid PWSCC

Structural Weld Overlay (SWOL) and Pre-emptive Weld Overlay (PWOL)

- "Safe-end" welds used to attach stainless steel piping to steel nozzle
- FM82 dissimilar weld between nozzle and SS casting or forging
- IN52/52M overlay contains ~30 wt% Cr
- Structural support and corrosion resistance against PWSCC
- SS buffer layer required in some cases to prevent cracking during welding

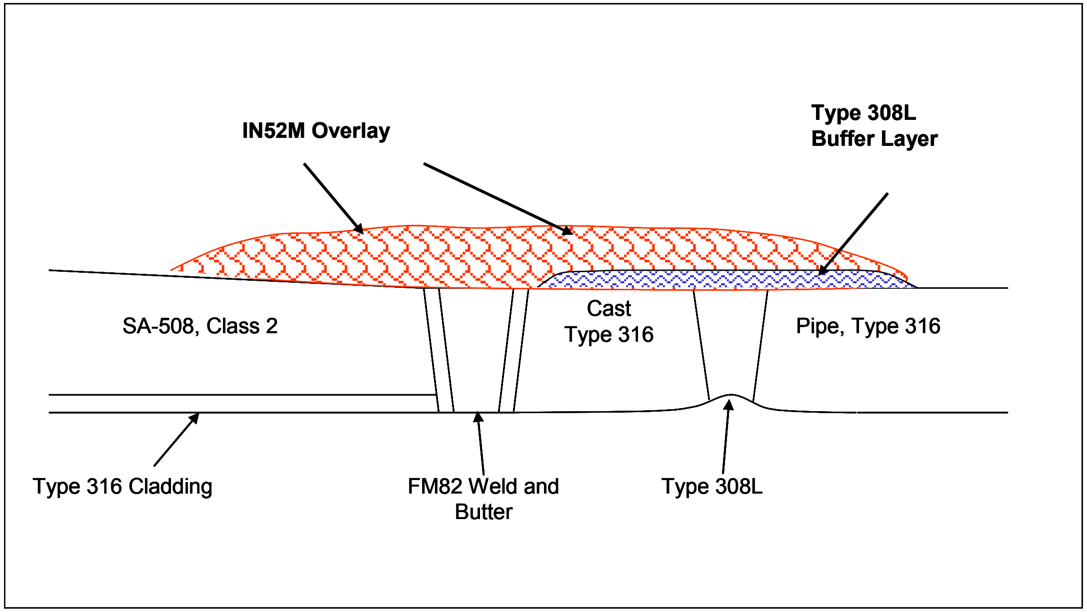

Courtesy J.C. Lippold

Microbiologically-Induced Corrosion (MIC)

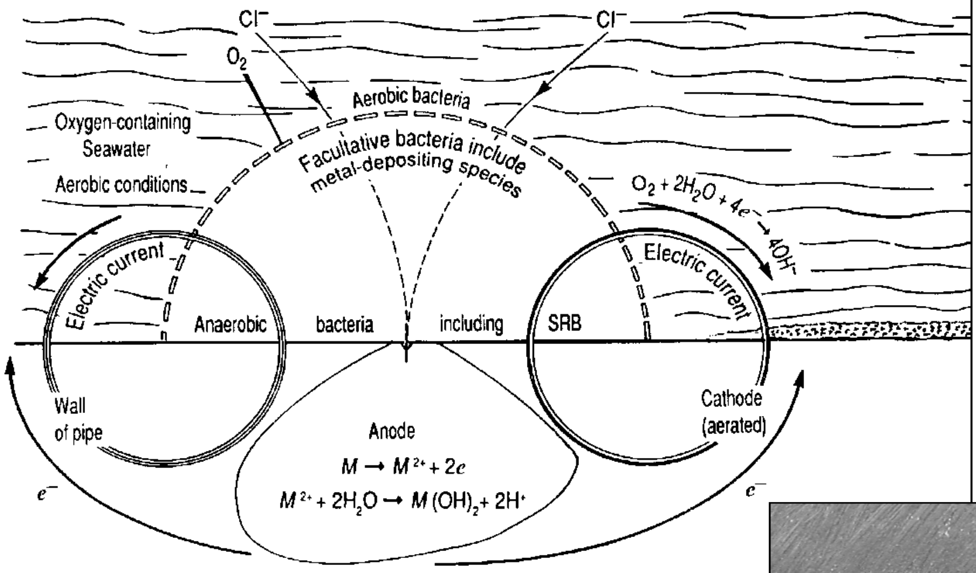

Reactions possible under tubercules created by metal depositing bacteria

MIC attack in Type 308 SMA weld

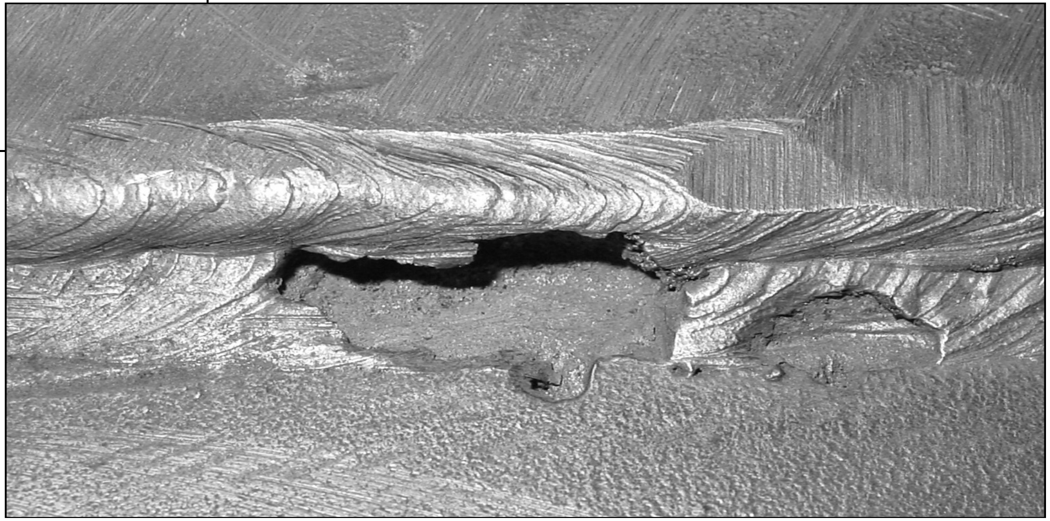

Fractography

Module 5C

Fractography Outline

- Introduction – description of fractography and its development
- Scanning Electron Microscope – overview of SEM components and operating principles
- Fracture morphologies – fracture paths and principal fracture modes
- Fractography of defects in welds – hot cracking, warm cracking, cold cracking

Fractography

- Term coined in 1944 by Carl A. Zapffe
- Definition: The study of fracture surfaces for the purpose of relating the topographical features to the causes and/or basic mechanisms of fracture.
- An important tool for fracture or failure analysis and understanding of material properties.

History of Fractography

- Fracture surfaces analyzed since the Bronze Age
- First written description of fracture surface to estimate metal quality in 1540’s
- In 1722 de Re’aumur used engravings to reproduce fracture morphologies and classified 7 fracture types

History of Fractography

- In 1800's metallography caused decline in fractography
- In 1940's fractography experienced a rebirth with the development of light fractography
- The electron microscope began to be used in the 1950's to look at fracture surfaces ushering in modern fractography
  - SEM – bulk sample analysis
  - TEM – fracture surface replicas

Fracture Morphologies

- Fracture Paths
  - Transgranular
  - Intergranular
  - Interphase
- Fracture Modes
  - Dimple rupture
  - Cleavage
  - Fatigue
  - Decohesive rupture

Fracture Paths

- Transgranular
  - Fracture passes through the grain
  - Intragranular
- Intergranular
  - Fracture follows path along grain boundaries

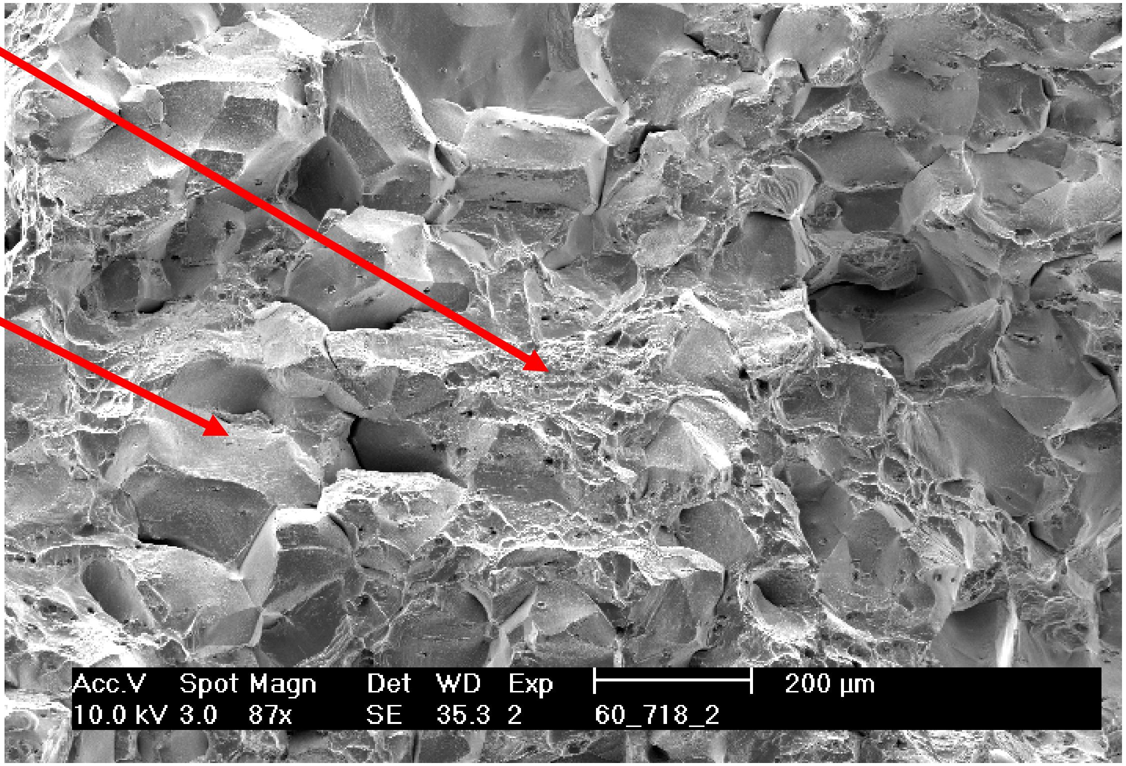

Alloy 718

Courtesy Seth Norton

Dimple Rupture Mode

- Occurs when overload is the primary cause of failure
- Microvoid Coalescence
  - Nucleation
    - Local strain concentrations
    - Second phase particles
    - Inclusions
    - Grain boundaries
    - Dislocation pileups
  - Coalesce to form a continuous network of “cuplike” dimples

Ductile Rupture: Microvoid Coalescence

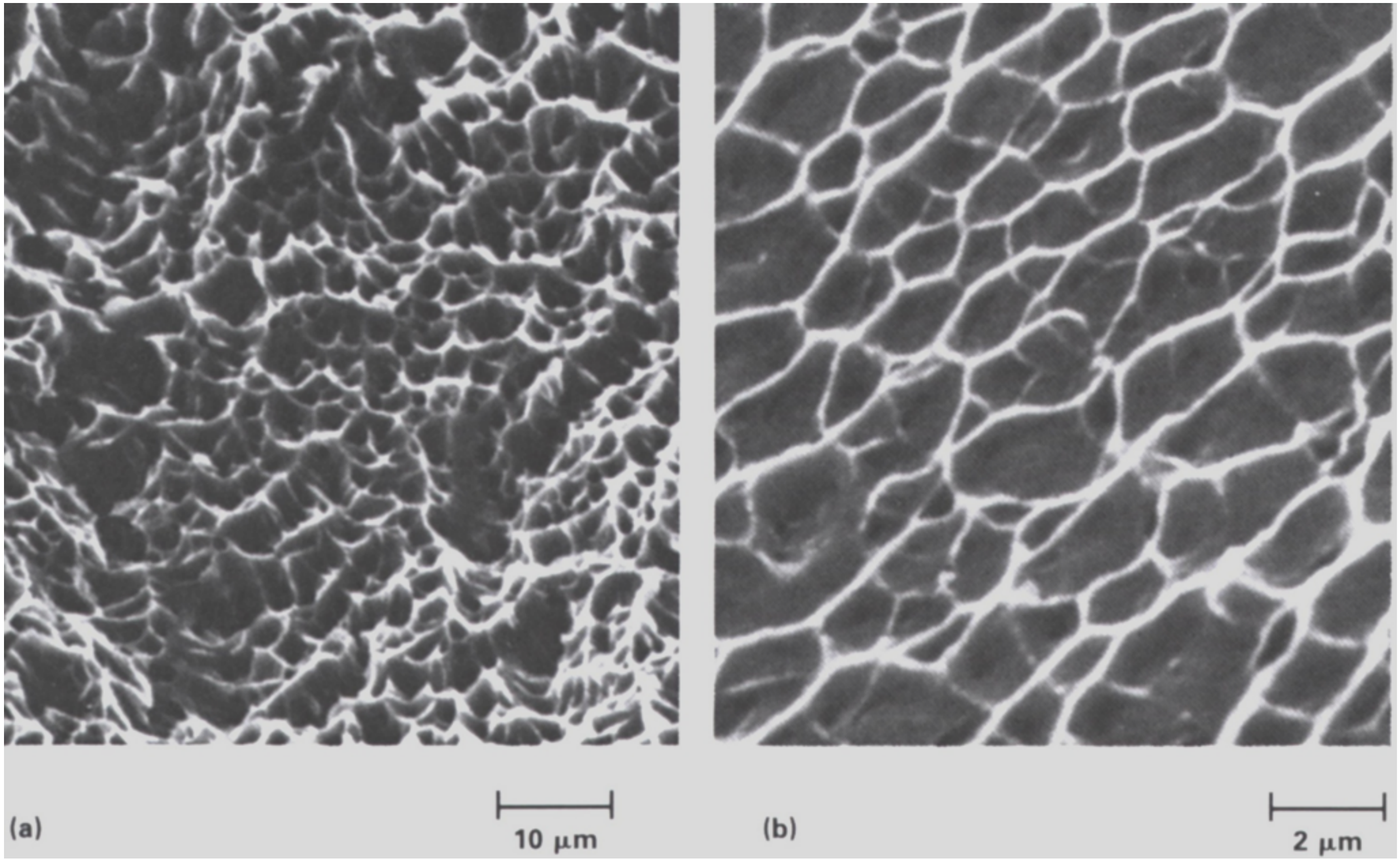

From ASM Handbook, Fractography, 1992

State of Stress

- Mode I
  - Tension
- Mode II and Mode III
  - Shear

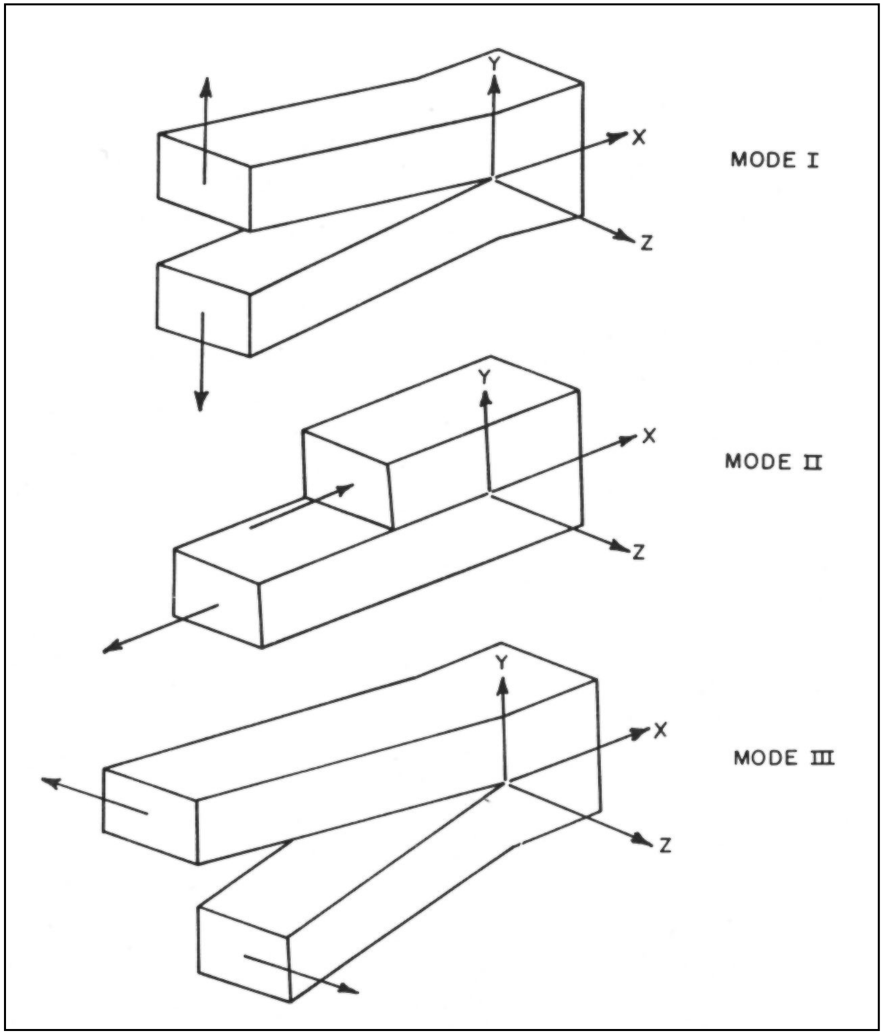

From Barsom, et al, Fracture & Fatigue Control in Structures, 1987

Effect of State of Stress on Dimple Direction

- Mode I - tear
  - Dimples oriented in the same direction
- Mode II and III - shear
  - Dimples oriented in opposing directions

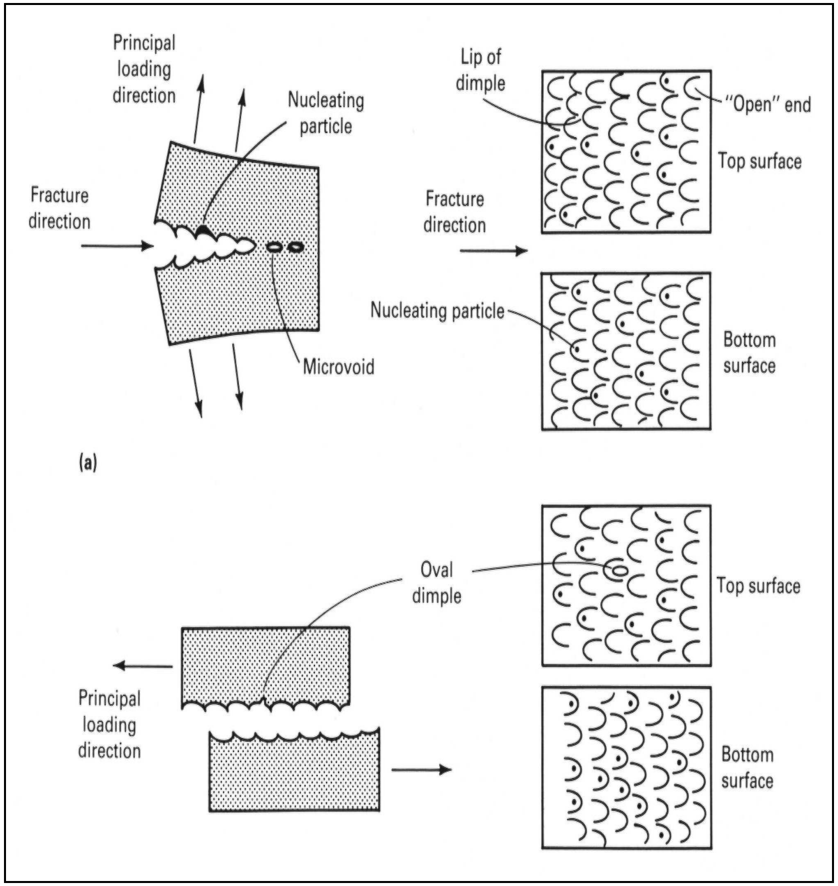

Cleavage Fracture Mode

- Low energy fracture along crystallographic planes called “cleavage planes”
- Fracture is typically smooth and featureless
- Associated with brittle failure
- Failure often initiates at flaw with loads below design levels

Cleavage Initiation and Propagation

- Initiate on many parallel planes
- Continue uninterrupted through tilt boundaries
- Re-initiate at twist boundaries

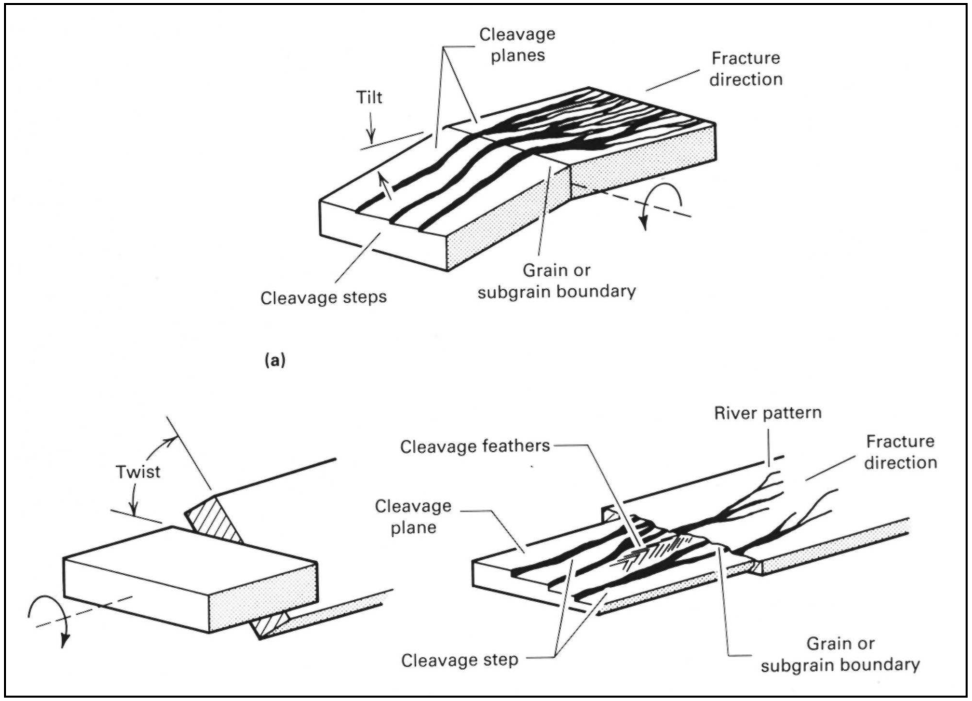

From ASM Handbook, Fractography, 1992

Cleavage Fracture

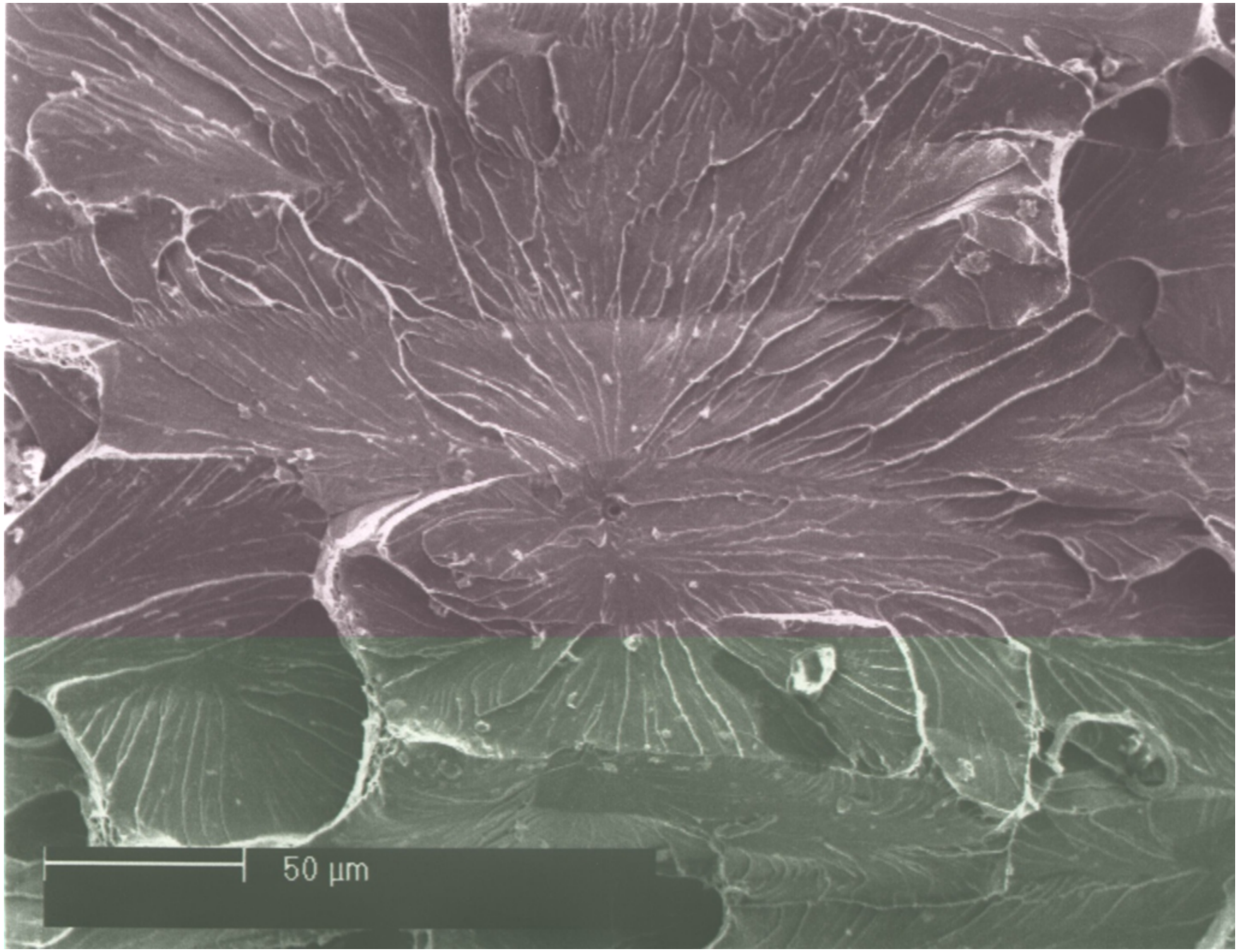

Ferritic Stainless Steel Weld Metal

Courtesy John Lippold

Fatigue Fracture Mode

- Fracture that is a result of repetitive or cyclic loading
- Three stages
  - Stage I : Initiation
    - Follows crystallographic planes
    - Faceted, resembles cleavage
    - High cycle, low stress
  - Stage II
    - Generally transgranular
    - Fatigue striations related to da/dN
  - Stage III
    - Static fracture: dimple rupture or cleavage takes over

Fatigue Cracks

Aluminum Alloy 7050-T7651

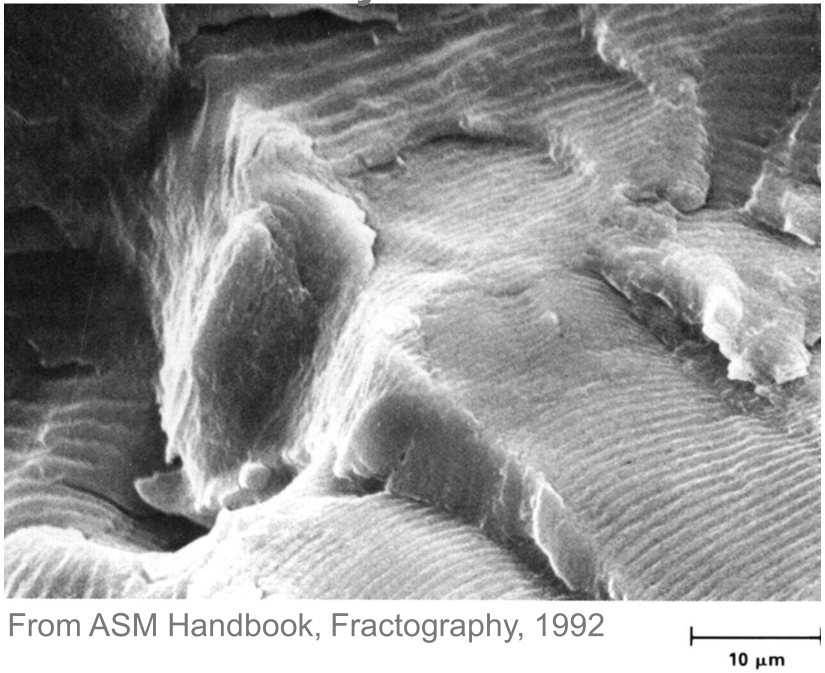

From ASM Handbook, Fractography, 1992

Commercially Pure Titanium

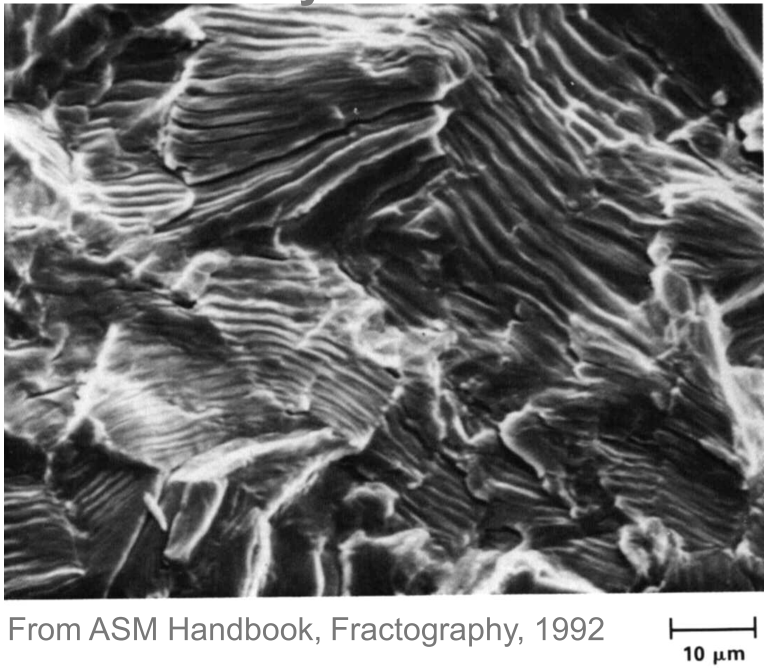

From ASM Handbook, Fractography, 1992

Fractography Weld Defects

- Hot Cracking
  - Solidification cracking
  - Liquation cracking
- Warm Cracking
  - Ductility dip cracking
  - Strain age cracking
  - Reheat cracking
- Cold Cracking
  - Hydrogen embrittlement

Solidification Cracking

- Along solidification grain boundaries
- Evidence of liquid films – smooth surfaces
- Two morphologies
  - Type D : Deep dendritic
    - Cracking near the liquidus and bulk solidus
    - “Egg crate” appearance
  - Type F : Shallow dendritic or Flat
    - Cracking between the bulk solidus and true solidus

Solidification Cracking of a Nickel Base Superalloy

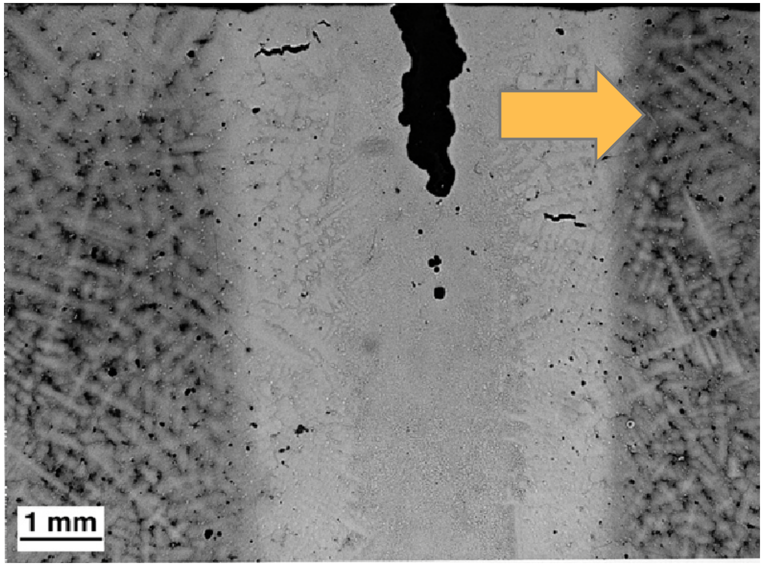

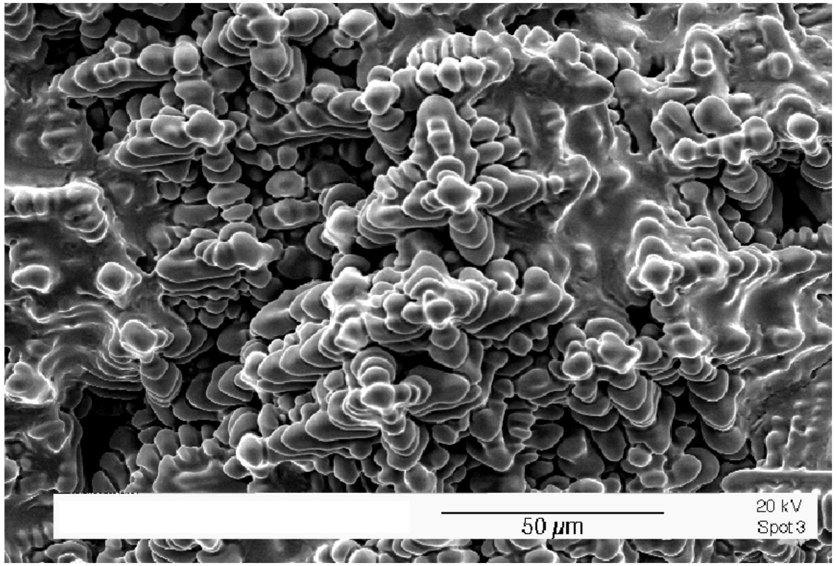

IN939 Alloy

Courtesy E. P. George et al

Solid-Solid Bridging During Solidification

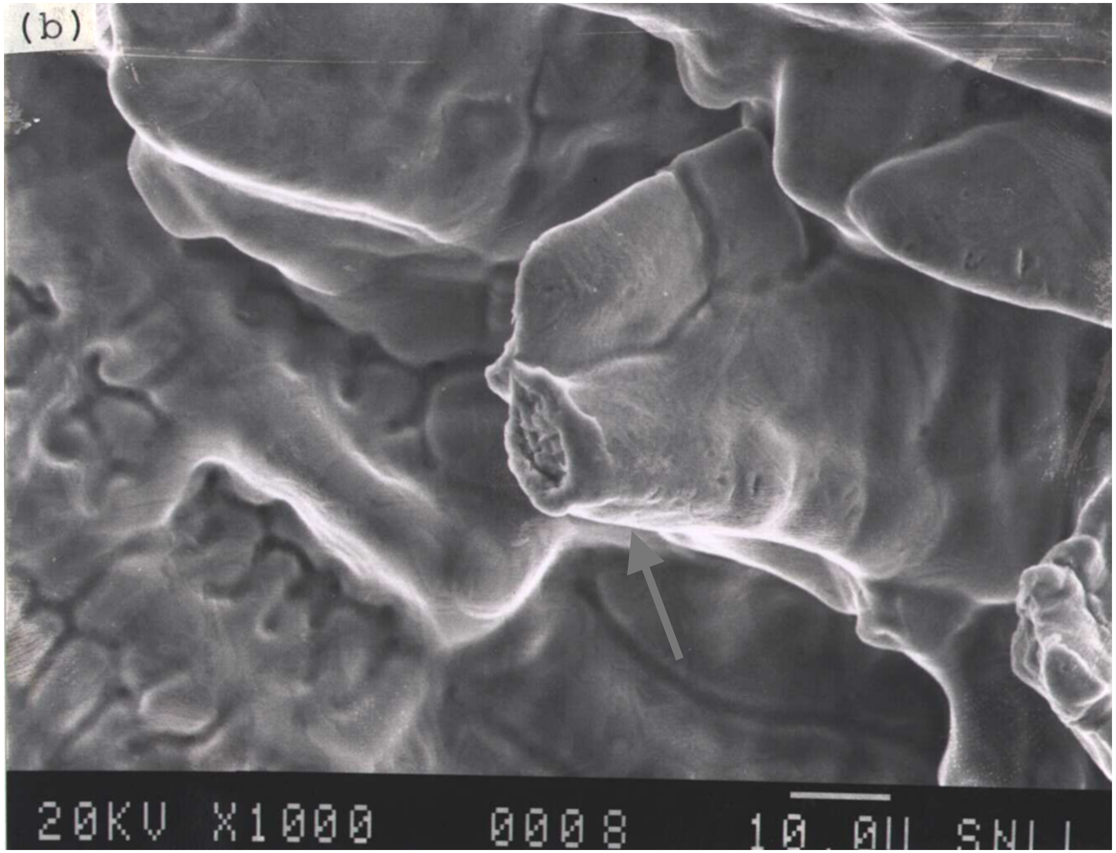

Uddeholm NU744LN

Courtesy David Nelson

Liquation Cracking

- HAZ and Weld Metal Liquation
- Intergranular
- Evidence of liquid films
  - Thin liquid layer: clearly intergranular
  - Thicker liquid layer: more irregular and dendritic appearance

HAZ Liquation Cracking of Duplex Stainless Steel

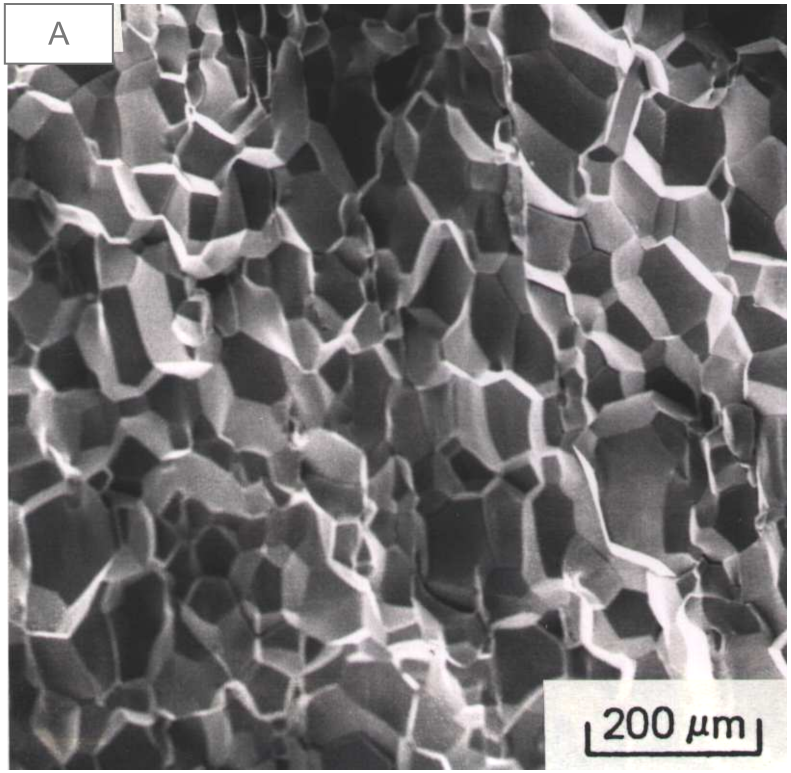

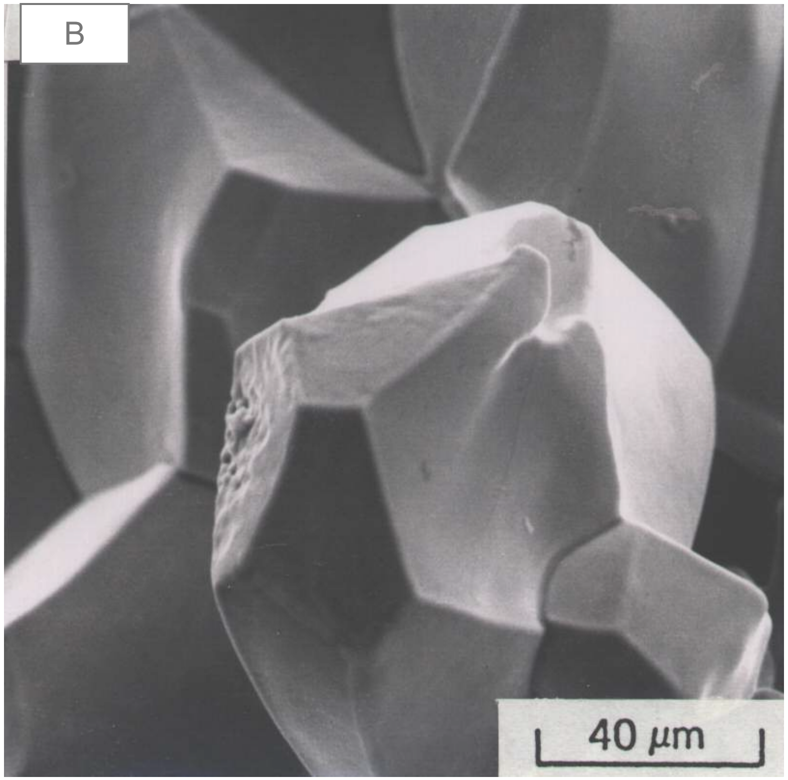

Ferralium Alloy 255

Courtesy David Nelson

Constitutional Liquation

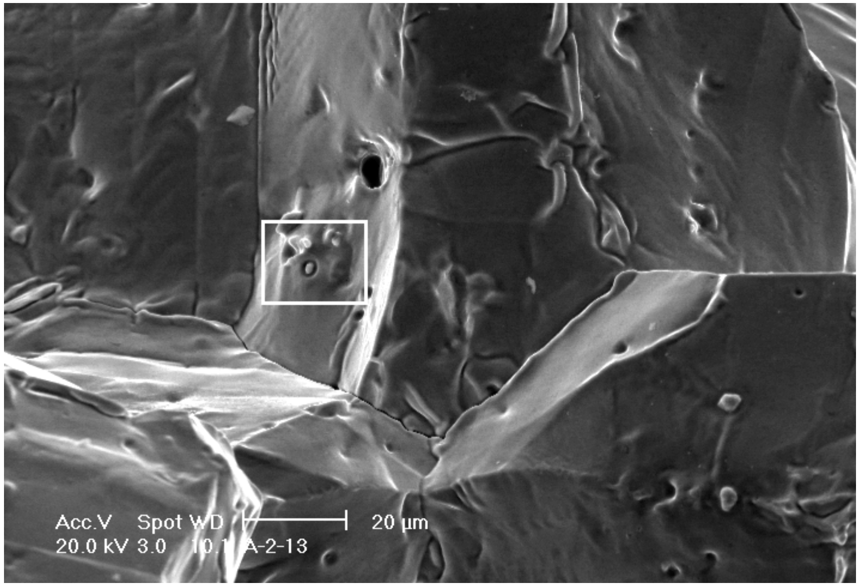

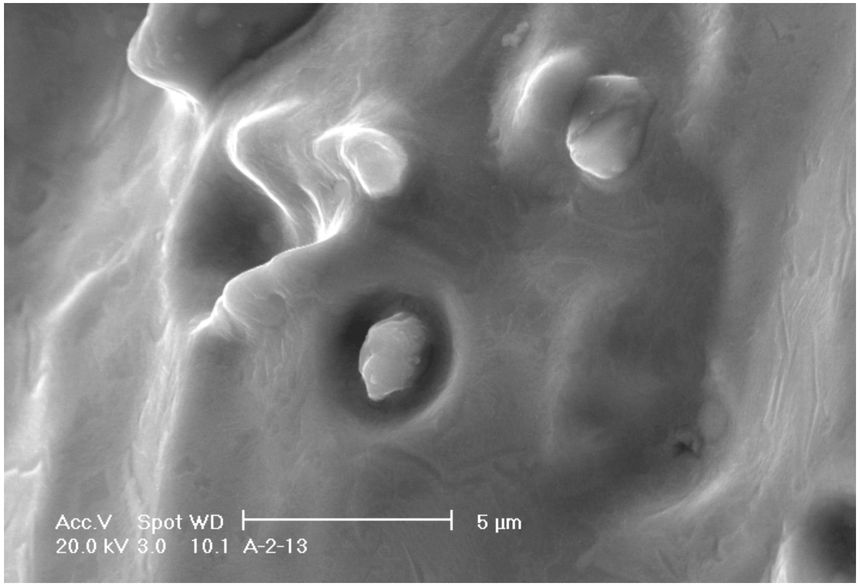

Waspaloy

Courtesy Ming Qian

Grain Boundary Liquation

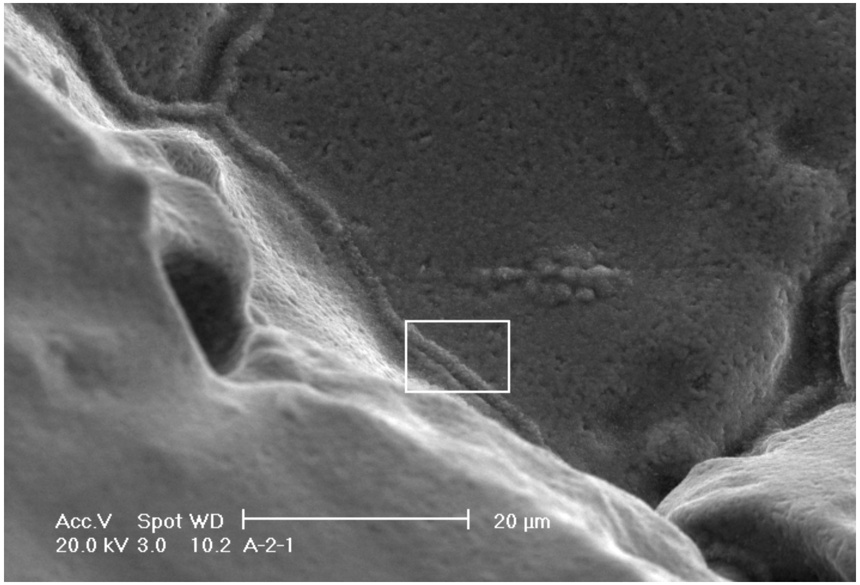

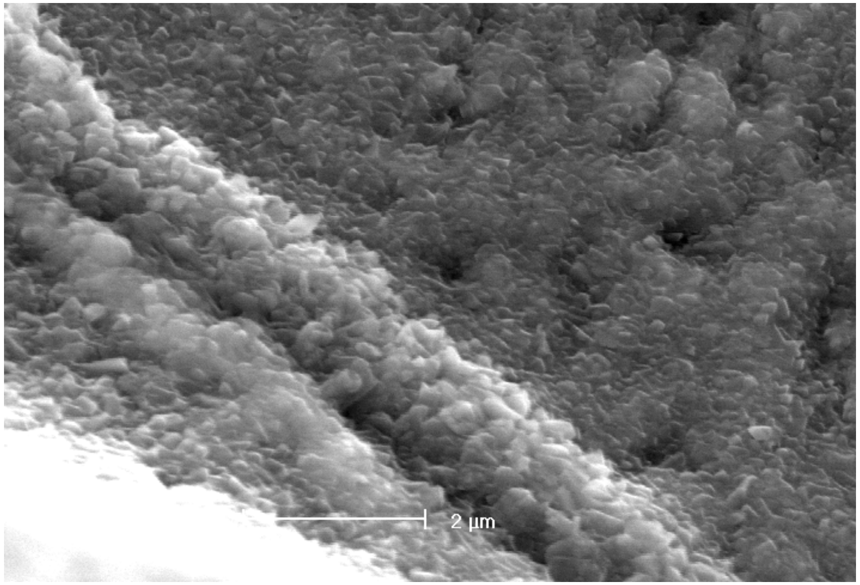

Waspaloy

Courtesy Ming Qian

Ductility Dip Cracking

- Macroscopic crack appearance
  - Short and relatively straight
  - Flat crack surfaces
- Intergranular along migrated grain boundaries in weld metal
- Transition of surface as temperature increases
  - Low temperature: flat with ductile dimples
  - Mid and high temperatures : wavy with fine ruggedness and minor ductile dimples
  - Extreme high temperatures: reverts back to flat or smooth with ductile dimples

DDC Fracture Appearance

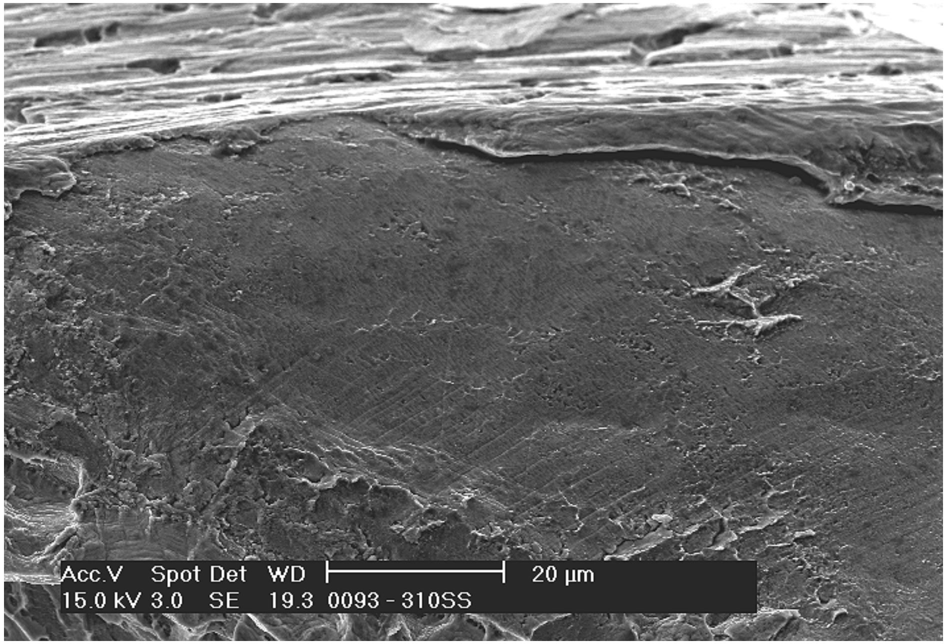

Macroscopically Flat (700° C)

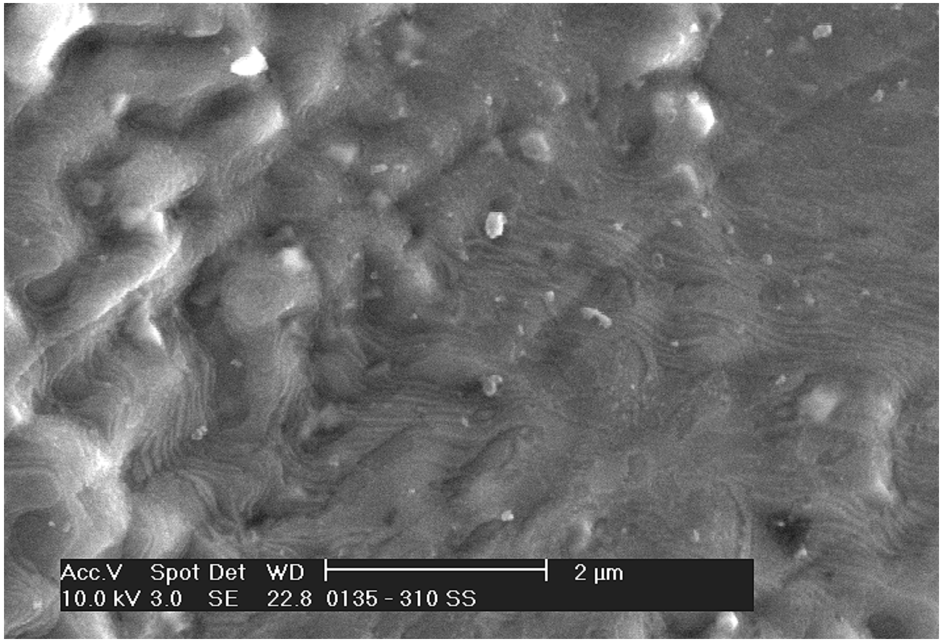

Microscopic Wavy features (950° C)

310 stainless steel

Courtesy Nathan Nissley

DDC Fracture Appearance

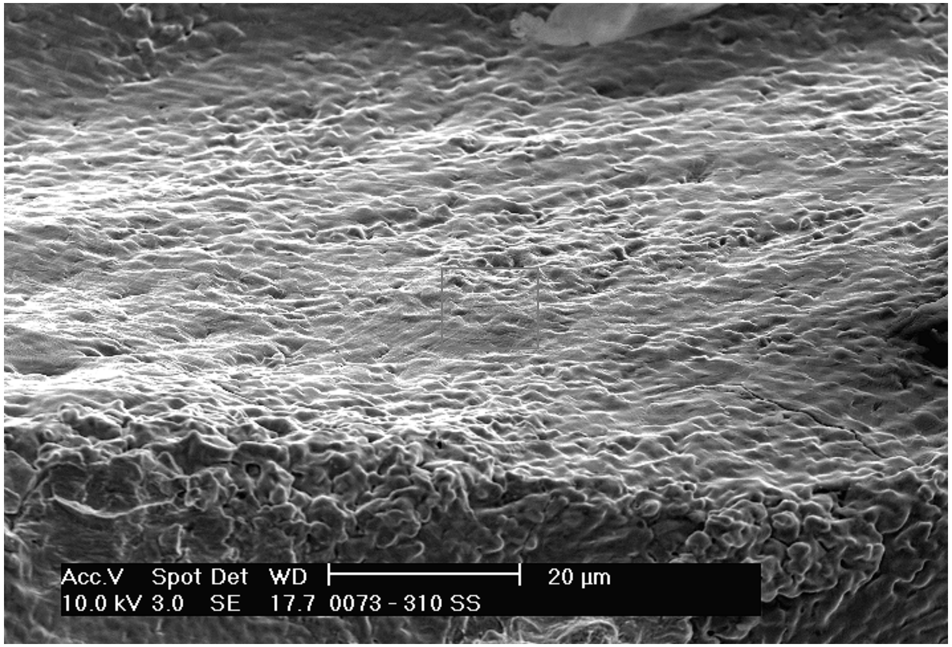

Macroscopic Flat Appearance (1100° C)

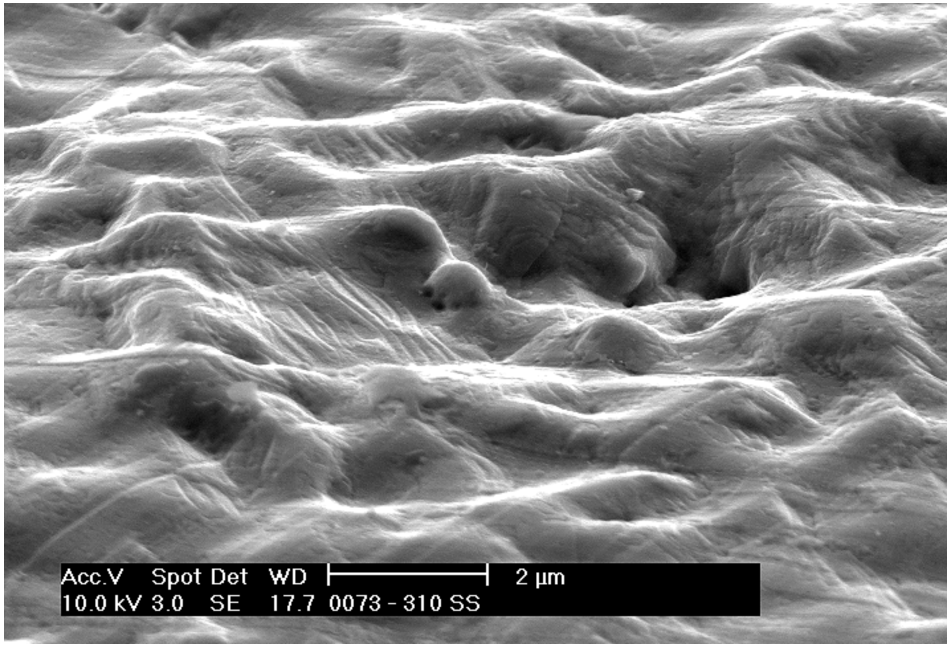

Increased Waviness at high temperatures (1100° C)

310 Stainless Steel

Courtesy Nathan Nissley

Strain Age Cracking

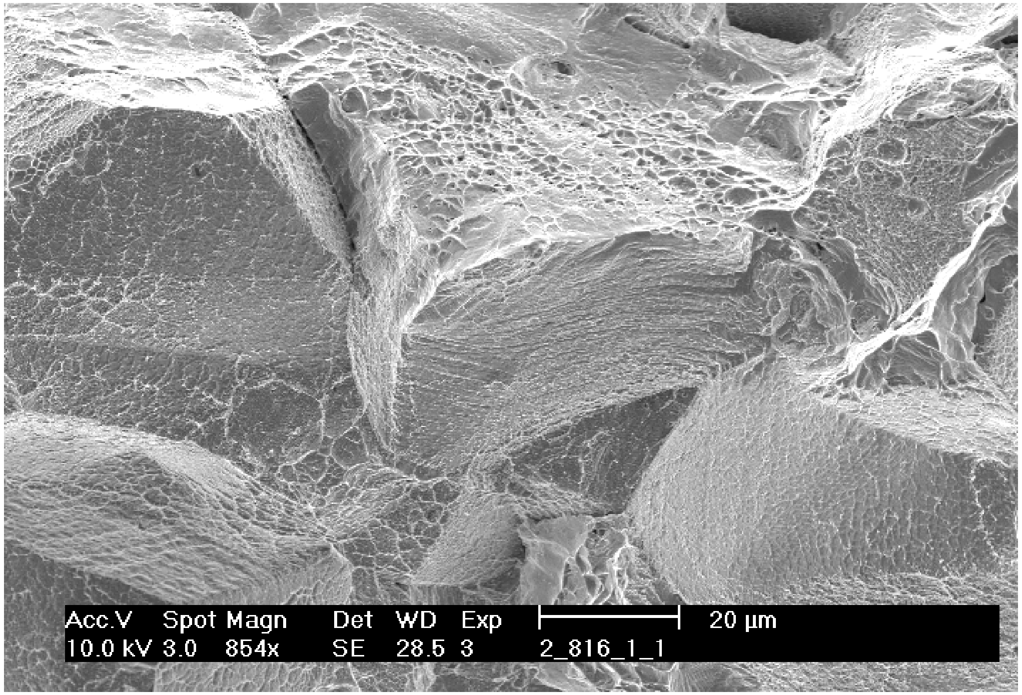

Alloy 718

Courtesy Seth Norton

- Precipitation-strengthened, Ni-base alloys
- Intergranular
- Fracture surface varies with grain boundary orientation
  - Microductility
  - Flat

Strain Age Cracking: Grain Orientation Effect

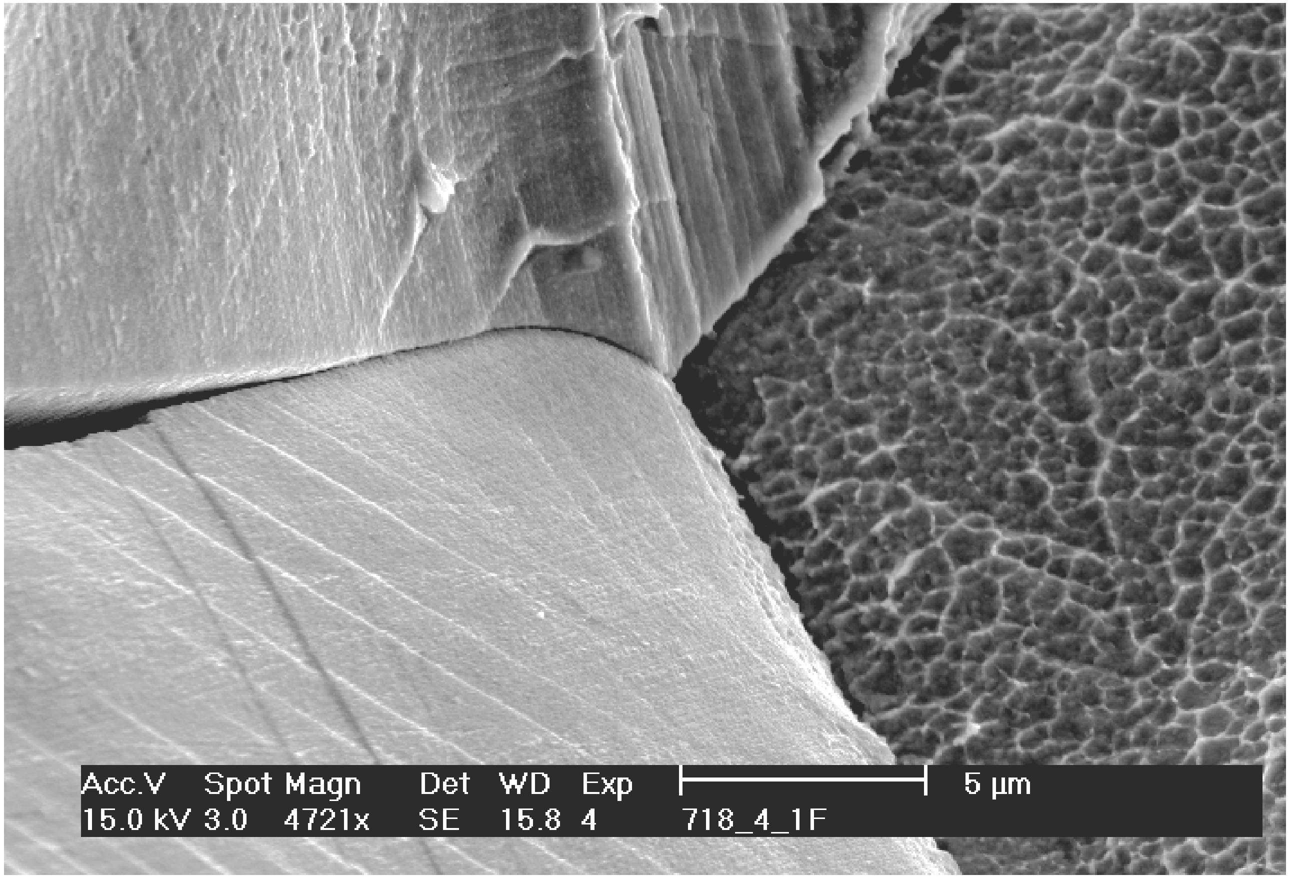

Alloy 718

Courtesy Seth Norton

Reheat Cracking

- Low alloy steels and stabilized stainless steels
- Reheat cracking mechanism
  - On heating
    - Carbide dissolution
    - Impurity segregation to grain boundaries
  - On reheating
    - Intragranular precipitation of carbides
    - Simultaneous stress relaxation
- Intergranular failure
- Fracture surface varies with grain boundary orientation
  - Microductility
  - Flat

Reheat Cracking

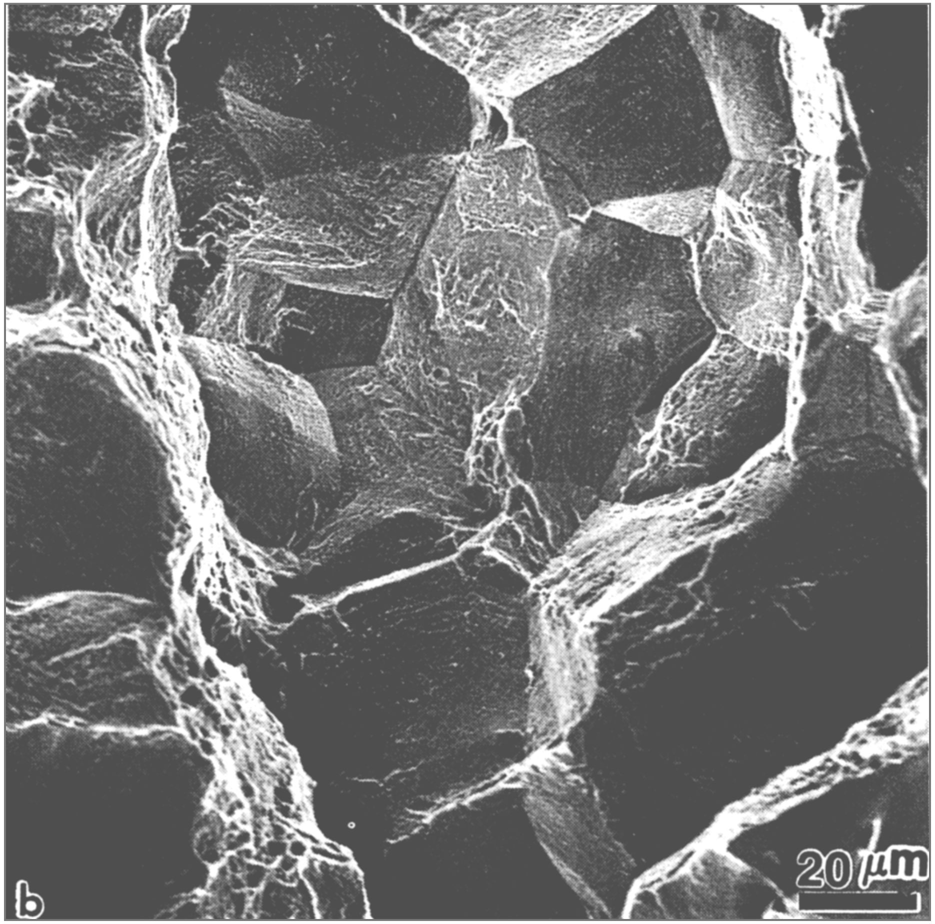

From Nawrocki, et al, The Weldability of a Modified 2.25 Cr-Mo Steel (HCM2S), 1998

Hydrogen Assisted Cracking

- No single characteristic fracture surface for Hydrogen Assisted Cracking (HAC)
- Three fracture morphologies
  - Microvoid Coalescence (MVC)
  - Quasi-cleavage (QC)
  - Intergranular Fracture (IG)
- Crack morphology is a function of
  - Stress intensity factor at crack tip
  - Concentration of hydrogen at the crack tip
  - Material characteristics

HAC Fracture Morphologies

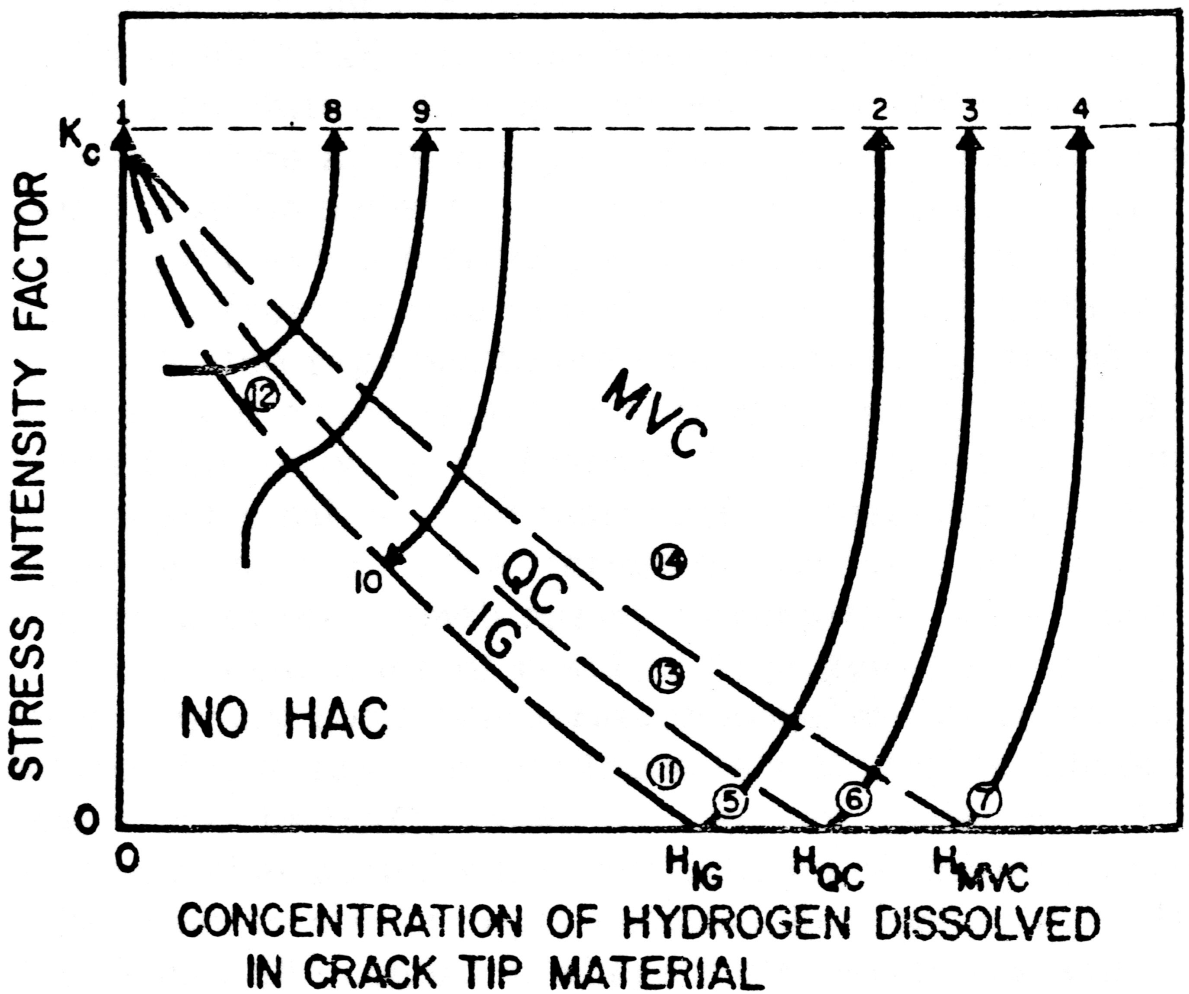

From C.D. Beachem, A New Model for Hydrogen-Assisted Cracking (Hydrogen "Embrittlement"), 1972

HAC Microvoid Coalescence

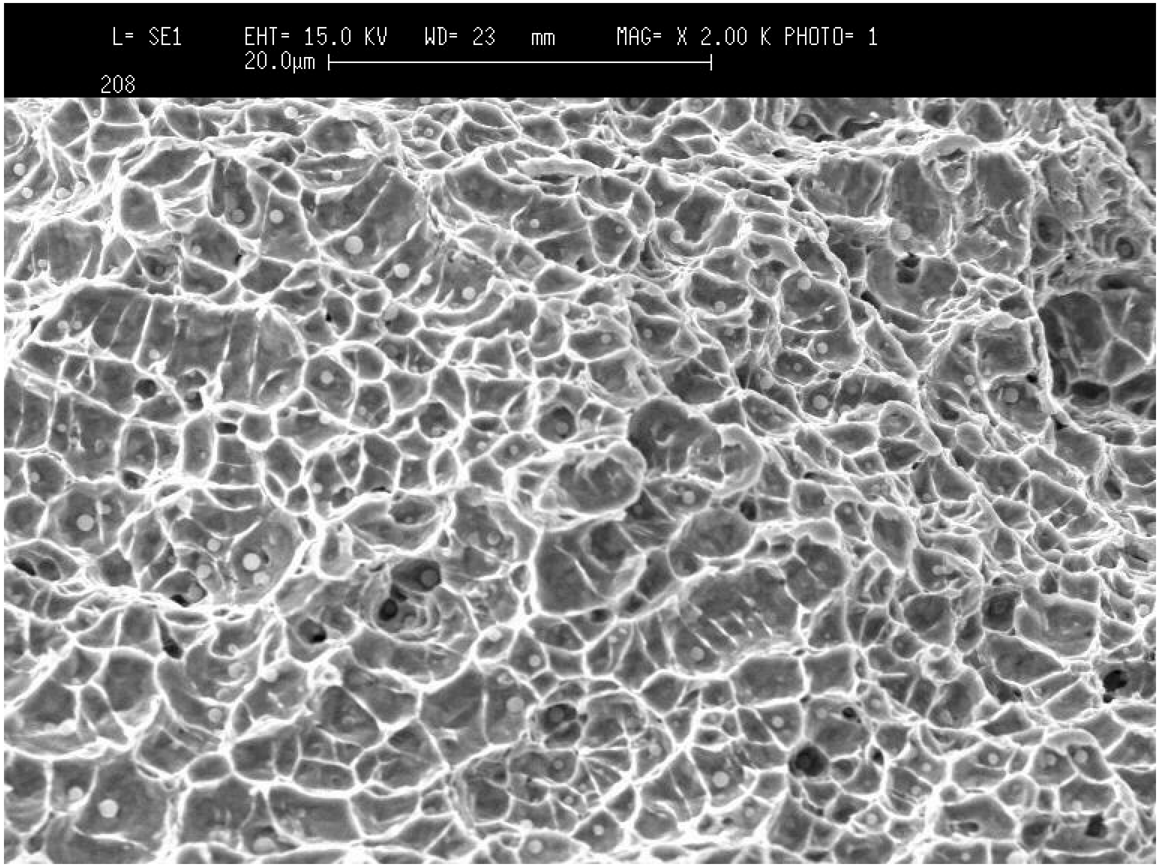

Weld Metal

Courtesy Matt Johnson

HAC Quasi-Cleavage

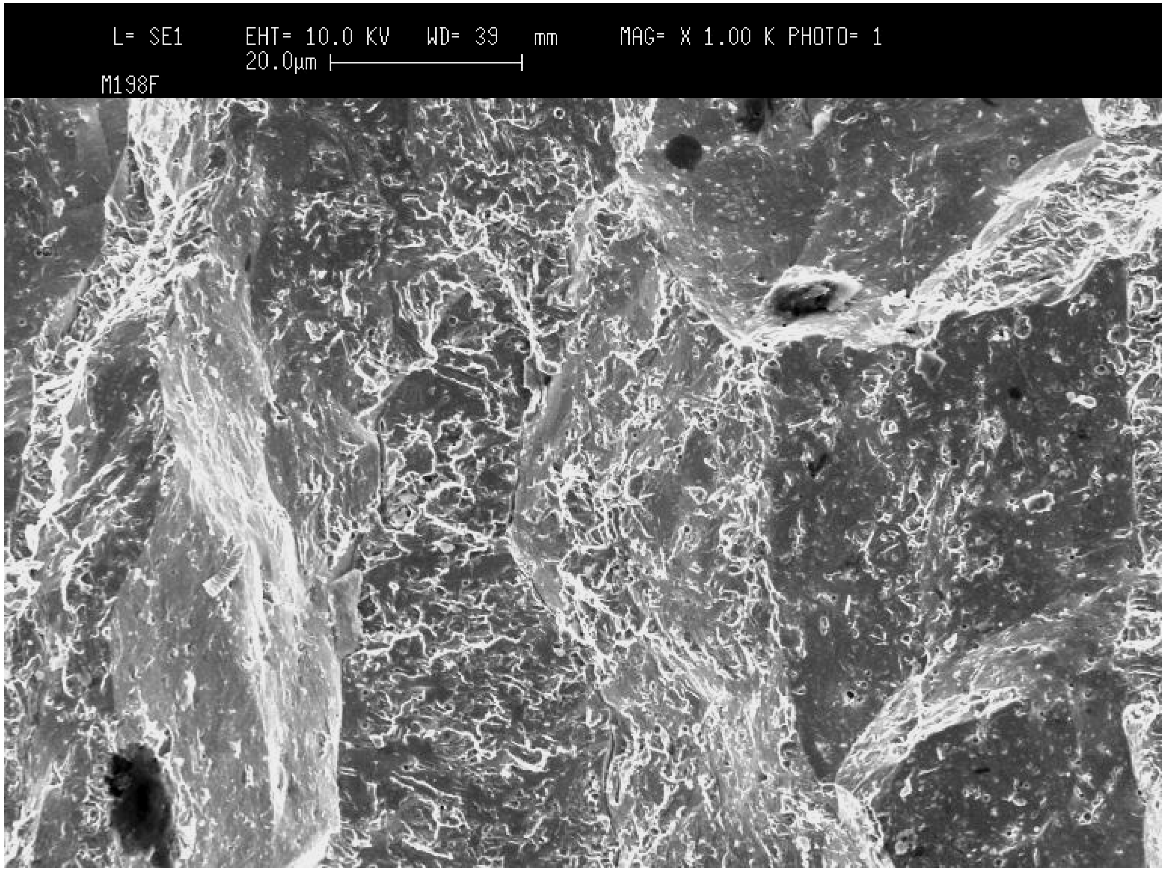

E9010-G Weld Metal

Courtesy Matt Johnson

HAC Quasi-Cleavage

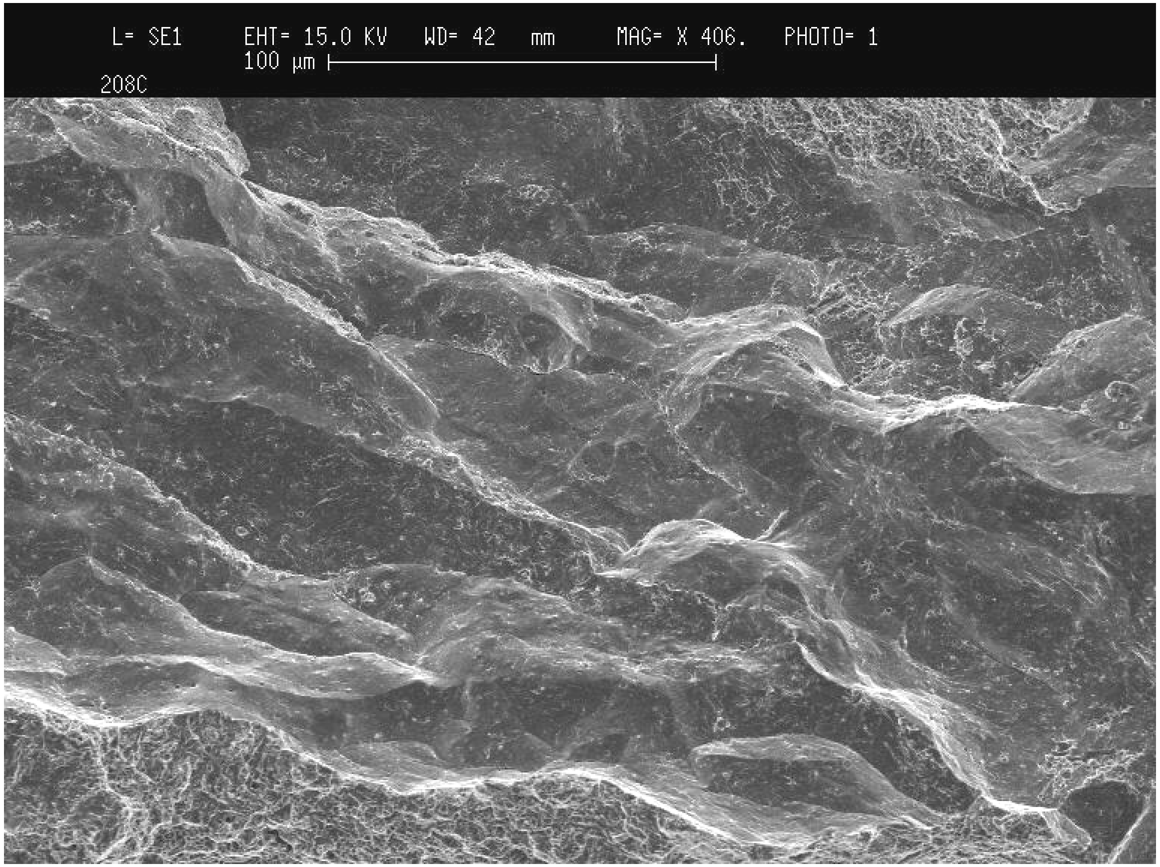

E71T-1 Weld Metal

Courtesy Matt Johnson

HAC Intergranular

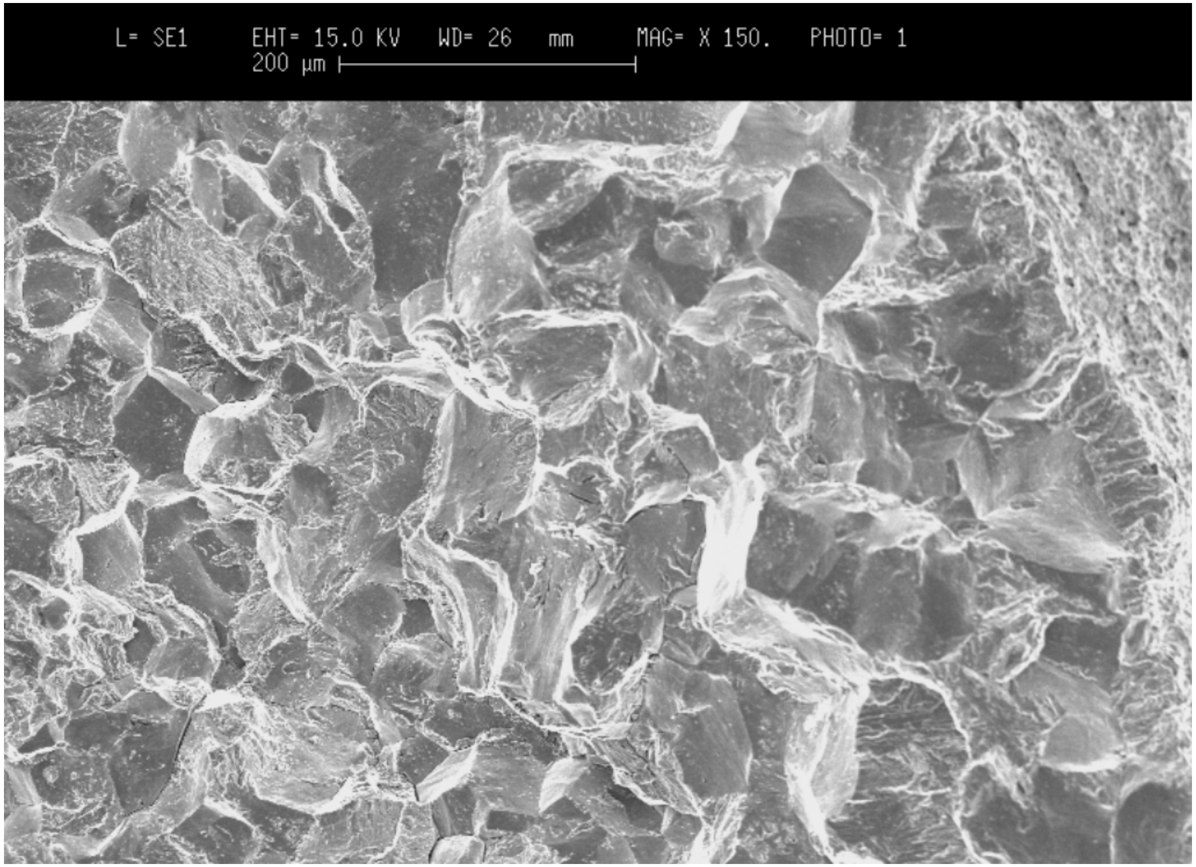

HSLA-100 Steel Base Metal HAZ

Courtesy Matt Johnson

Weldability Case Studies

Module 5D

Case Study 1: Hydrogen Assisted Cracking

- Alexander Kielland Disaster
- Background
  - Nb - microalloyed fine ferrite grain steel
  - 6 mm fillet weld on a non-load bearing flange initiated the failure
  - Sea temperature was 6° C
  - Some of the findings reported in the book by Easterling
  - This is available on the Carmen web site
  - Please study the notes carefully
- Web Pages
  - http://www.exponent.com/kielland_platform/
  - http://en.wikipedia.org/wiki/Alexander_Kielland_(Platform)

One of the braces fractured suddenly!

Figure 4.44 The *Alexander Kielland* photographed a few weeks before the disaster. From ref. 37

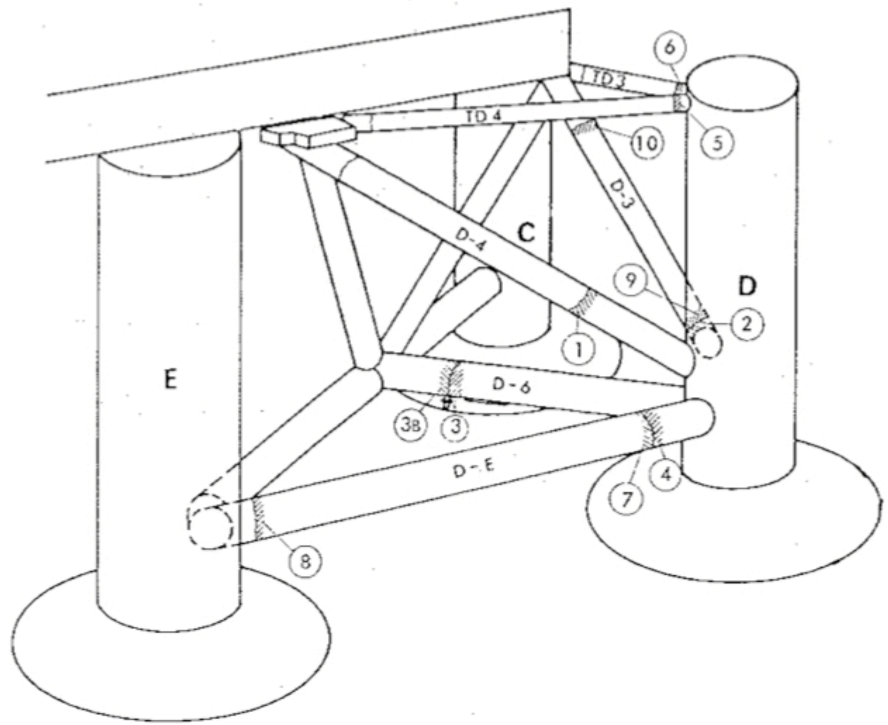

Failure Analyses was done

What do we learn from the failed part?

(a)

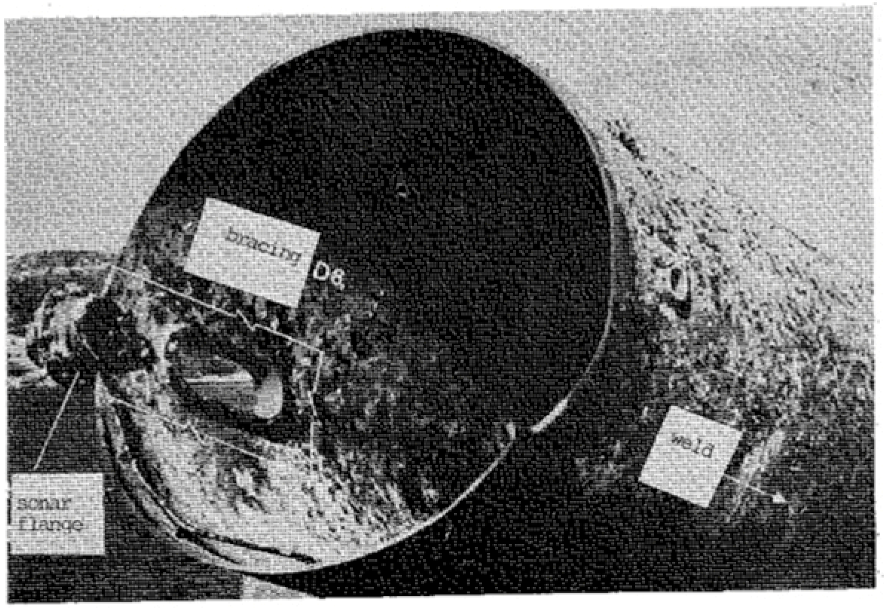

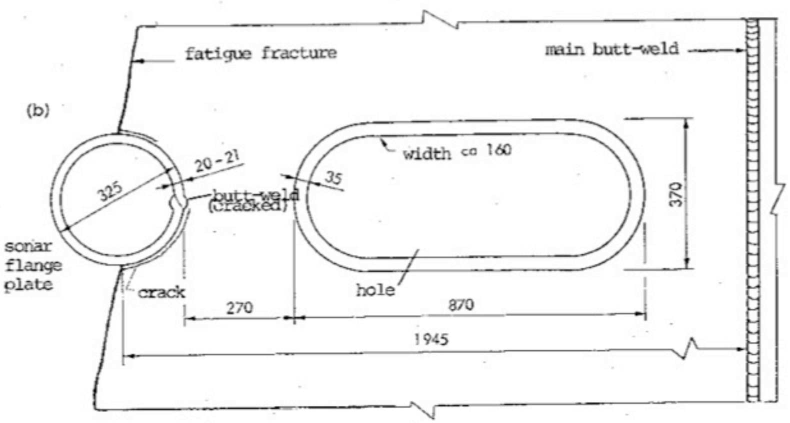

Figure 4.46 (a) The recovered bracing D-6. (b) A detail of the fracture position relative to the sonar flange plate. After ref. 37

Unzipping cracks were NOT associated with girth welds!

Fracture analyses showed interesting features

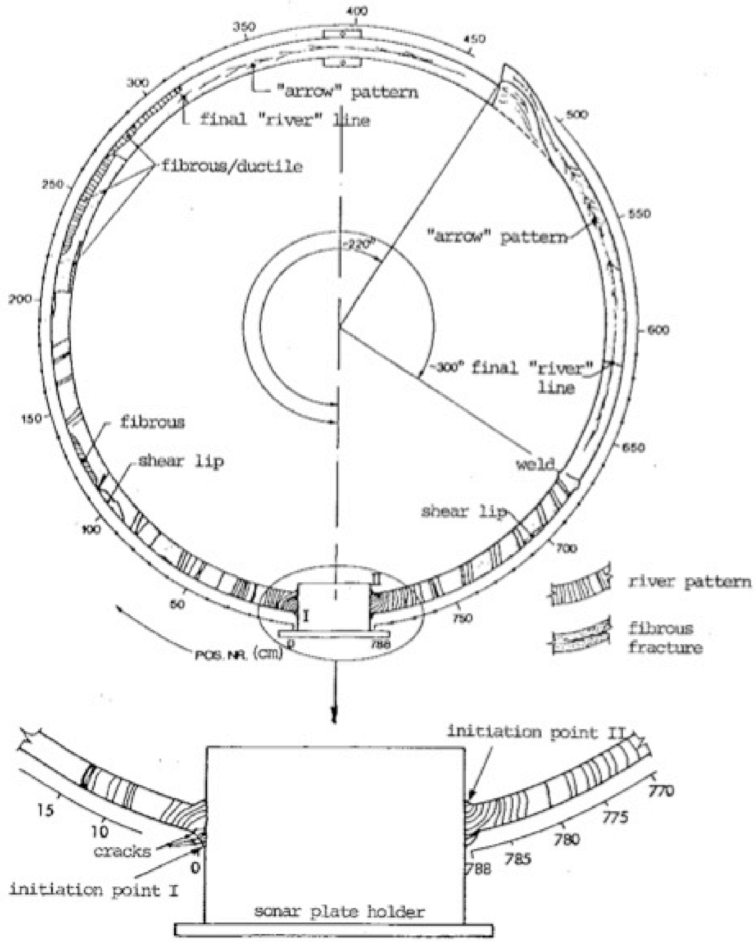

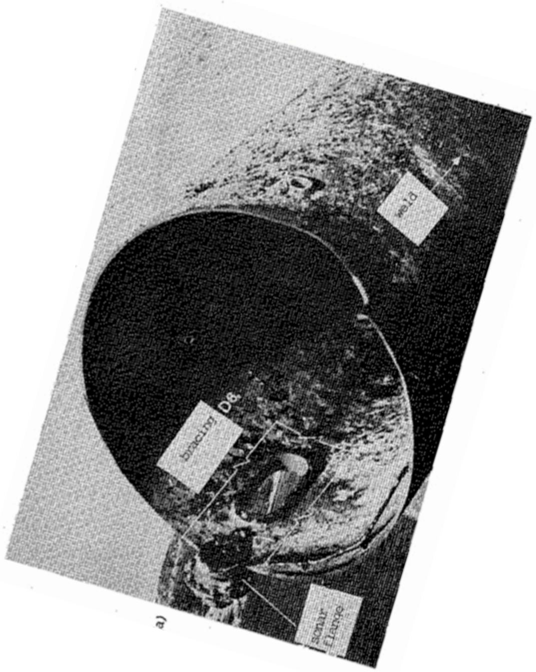

Fatigue cracks were present already!

Flange welds: Lack of penetration!

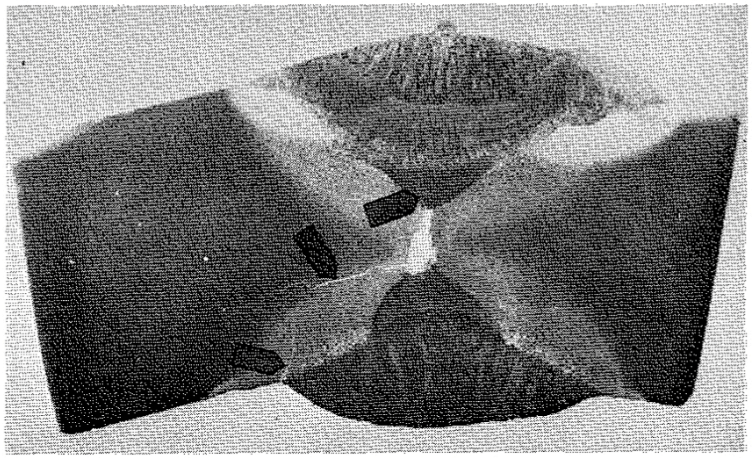

Figure 4.48 Butt weld of the sonar flange plate. Root and toe cracks, as well as lamellar tearing are indicated by markers. After ref. 37

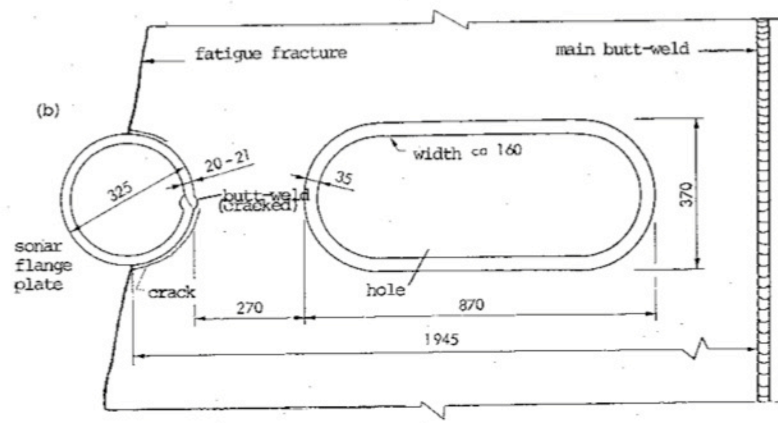

Figure 4.46 (a) The recovered bracing D-6. (b) A detail of the fracture position relative to the sonar flange plate. After ref. 37

How about the fillet welds?

Fillet welds: Showed many problems!

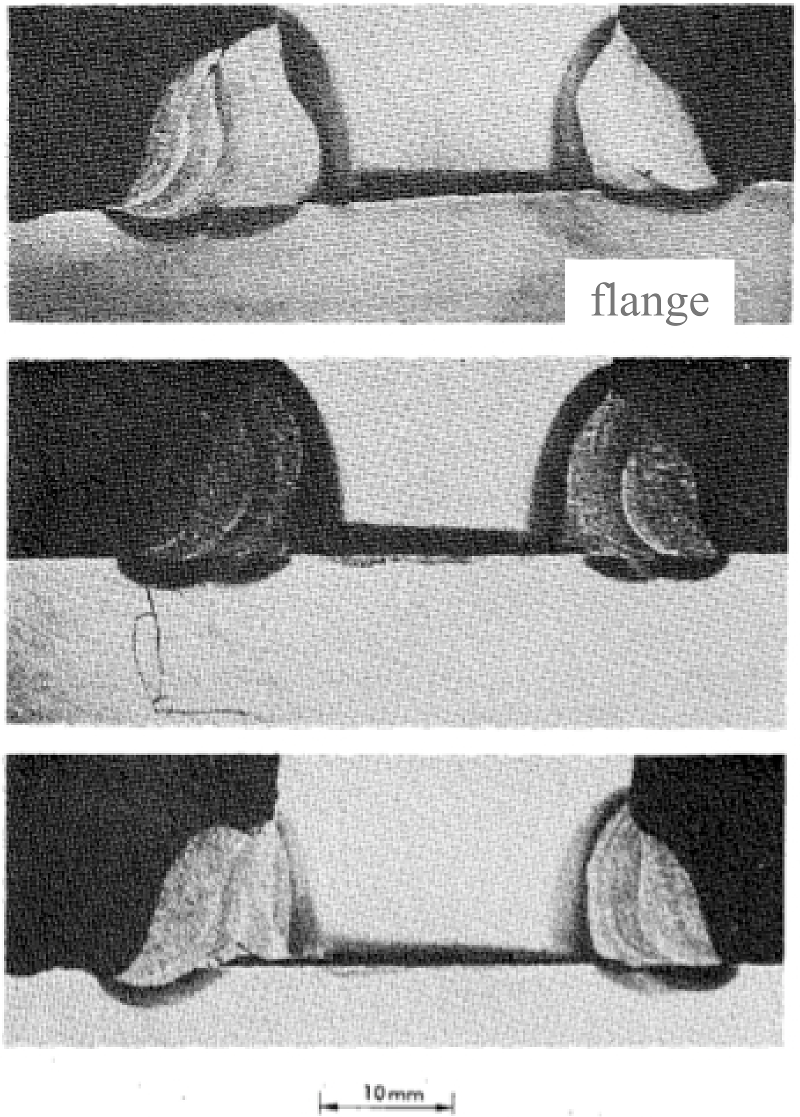

- Bead shape concave
- Lamellar tearing!
- Undercuts!
- Where did the fatigue crack start?

Micro-cracks near the fillet welds initiated the crack!

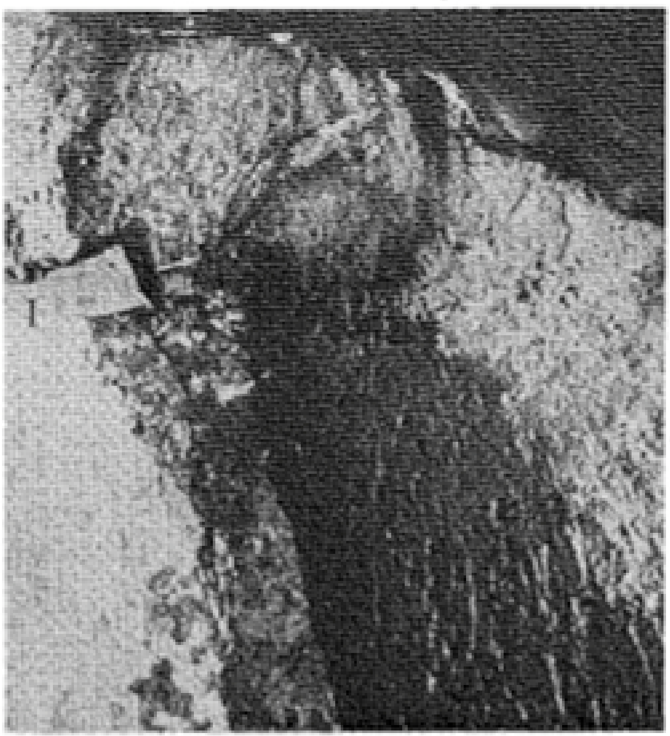

- Paint was observed inside the crack
  - Means the cracking started as soon as the welds were done!
- What are the specifications of these steels?

Microstructural and Mechanical Property Requirements

TABLE 4.4 Summary of microstructural and mechanical properties

Property	*Main bracing*	*Flange plate*
Composition (approx.)	0.17wt%C; 0.32 Si; 1.37 Mn; 0.044 Al; 0.029 Nb	Not specified
C_{equiv}	0.41	Not specified
Grain size (normalized)	ASTM 11.5 (*ca.* 8 μm)	ASTM 10.7 (*ca.* 7 μm)
Microstructural features	1. Banded, ferritic–pearlitic 2. Slag content low; mainly MnS, finely distributed	1. Banded, ferritic–pearlitic 2. Slag content fairly high; mainly MnS in extreme rolled-out form
σ_y (rolling direction)	345–353 N mm^{-2}	Not specified
σ_t (rolling direction)	506–518 N mm^{-2}	Not specified
σ_t (transverse direction)	419–474 N mm^{-2}	215–437 N mm^{-2}
Area reduction (rolling direction)	30–34%	Not specified
Area reduction (transverse)	6–13%	1–7%
Impact strength (Charpy)		
0 °C	83 J	Not specified
−40 °C	36 J	16 J

Failure Analysis – Hardness Testing Results

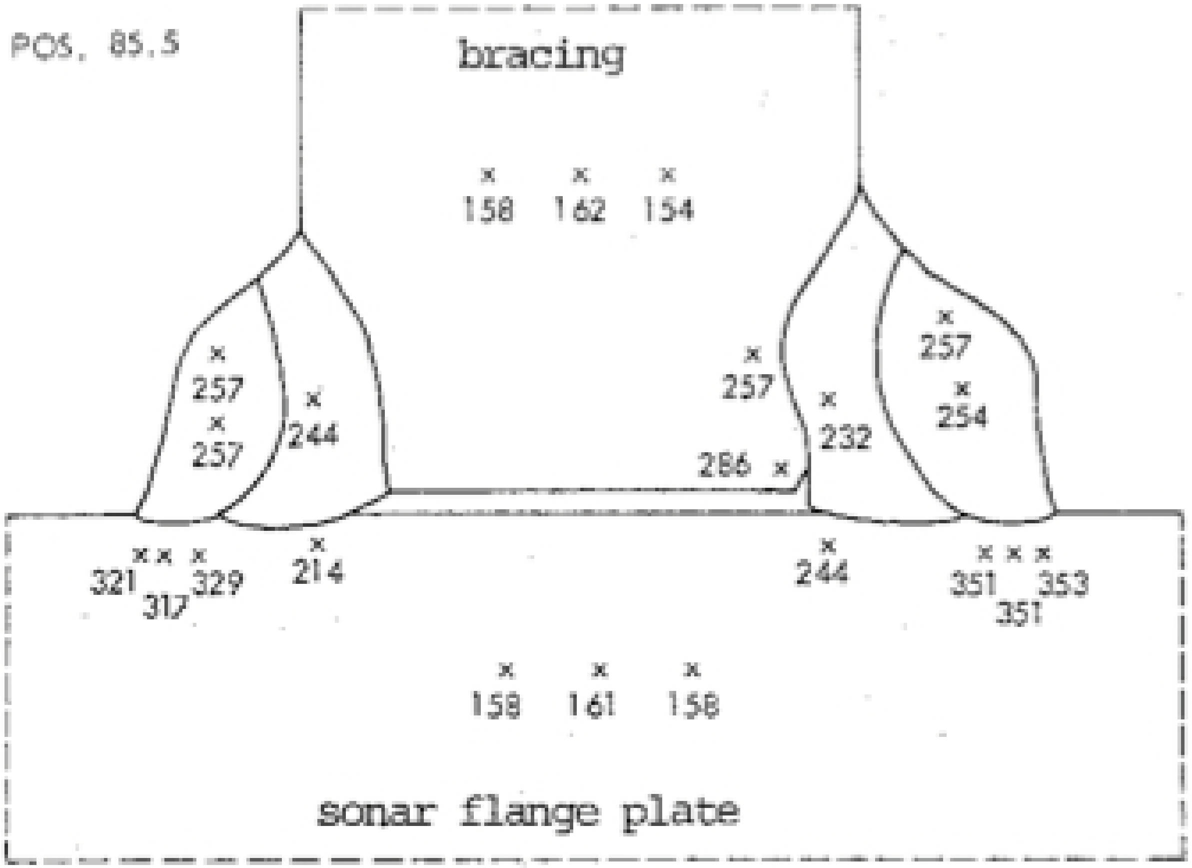

Figure 4.51 Hardness measurements (HVs) in the vicinity of the fillet weld between the flange plate and main bracing (ref. 37)

Summary of Failure Analysis

- Failure initially by HIC, fatigue and then overloading!
- What started the fatigue cracks?
  - Butt weld of sonar flange plate contained toe and root cracks; butt welds are poor
  - Secondary cracks between crossover between butt and fillet weld
- Possible reasons:
  - Quality of the fillet welds – not good uneven profile
  - Lamellar tearing in the flange plate and not in the brace plate
  - Cracks around fillet welds and main welds
  - Cold cracks were found close to the initiation point
  - These formed during construction itself!
  - Flange steels are not as good as “brace” steels
  - Stress concentration at the hole was high!

Case study 2: Cracking in Heavy Section Welds for Nuclear Application

- Crack Mitigation during Buttering and Cladding of a Low Alloy Steel Pipe

Yu-Ping Yang, Suresh Babu and Suhas Vaze
Edison Welding Institute
yyang@ewi.org

Joining Innovation

Jeffrey Kikel and David Dewees
Babcock and Wilcox
jmkikel@babcock.com

nuclear operations group

8th International Conference on Trends in Welding Research
Session 12 - Physical Processes in Weldiing II
June 3, 2008

Outline

- Background
- Experiment study
- Finite element modeling
- Crack mitigation
- Summary

Cracks in the Low-Alloy Steel Pipe during Cladding and Buttering

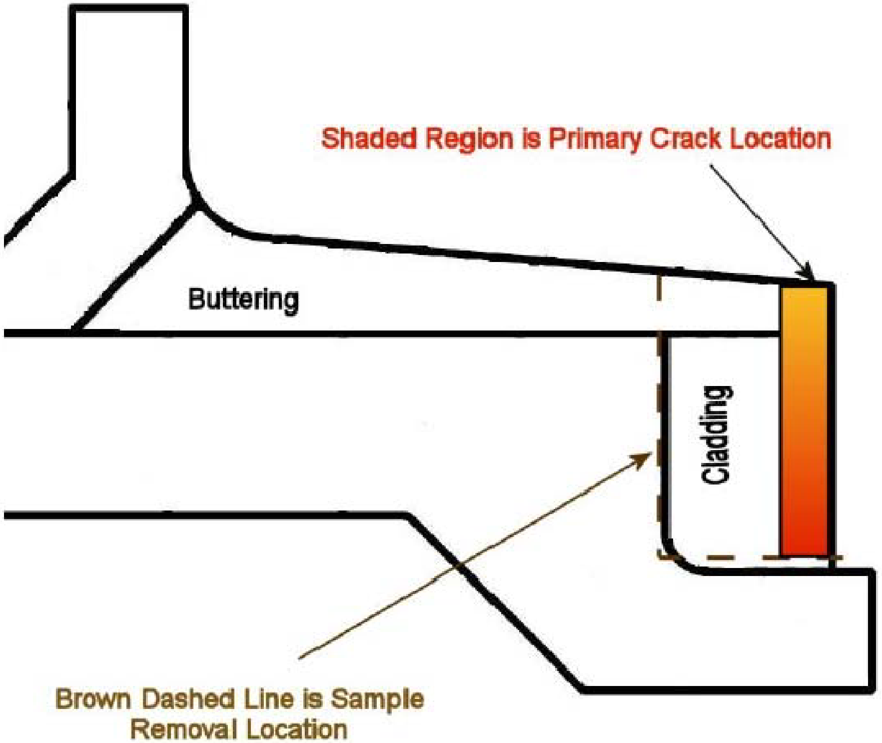

- Both Solidification and ductility dip cracking are found in the shaded region
- More cracks near the top (OD of pipe)
- Cracks also observed in the buttering region
- Cladding and Buttering deposited using Hot WIRE GTAW using Inconel Filler Metal 82

A Mockup Design

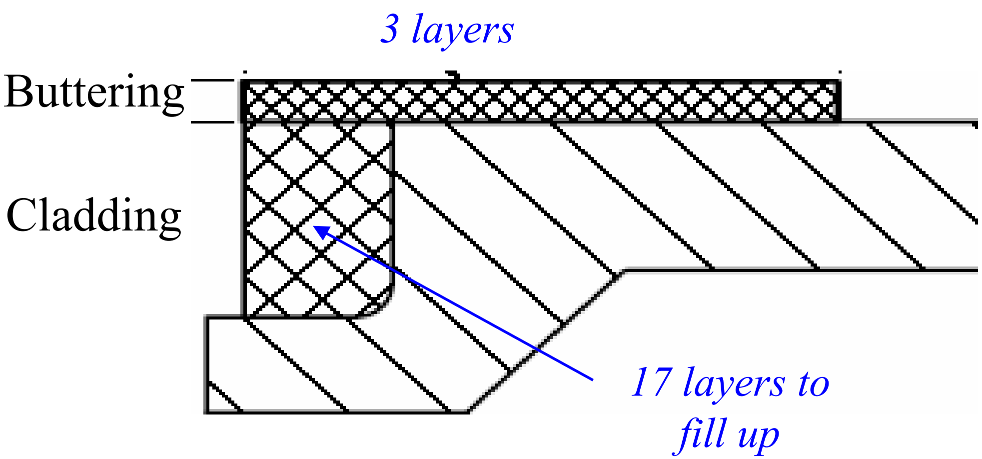

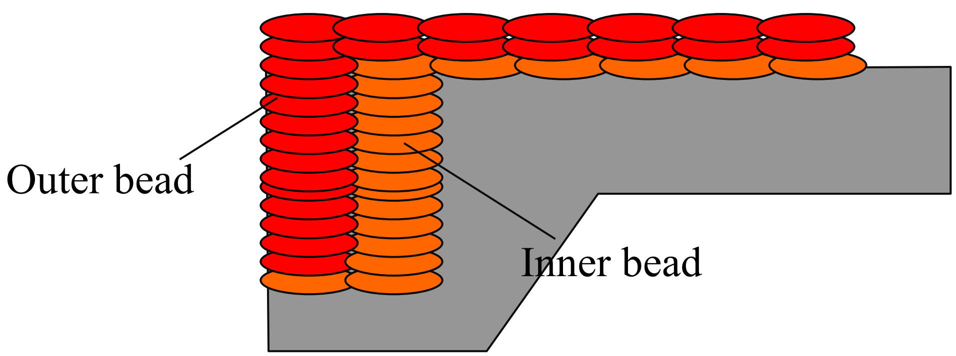

- A mockup was designed to investigate the cracking problem
- The mockup
  - Cladding
  - Buttering

Weld Parameters and Sequences

		Outer Bead	Overlap	Inner bead
Buttering Layer	3	a	ab	b
	2	a	ab	b
	1	a	ab	b
Clading Layer	17	b	ab	a
	16	b	ab	a
	15	b	ab	a
	14	b	ab	a
	13	b	ab	a
	12	b	ab	a
	11	b	ab	a
	10	b	ab	a
	9	b	ab	a
	8	b	ab	a

Steel

Steel

- Cladding
  - Welding Current
    - Weld: 300 A
    - Voltage: 13 V
  - Traveling Speed, 6.5 IPM
- Buttering
  - Welding Current
    - Weld: 300 A
    - Voltage: 16 V
  - Traveling Speed, 6.5 IPM

A Clad and Buttered Pipe

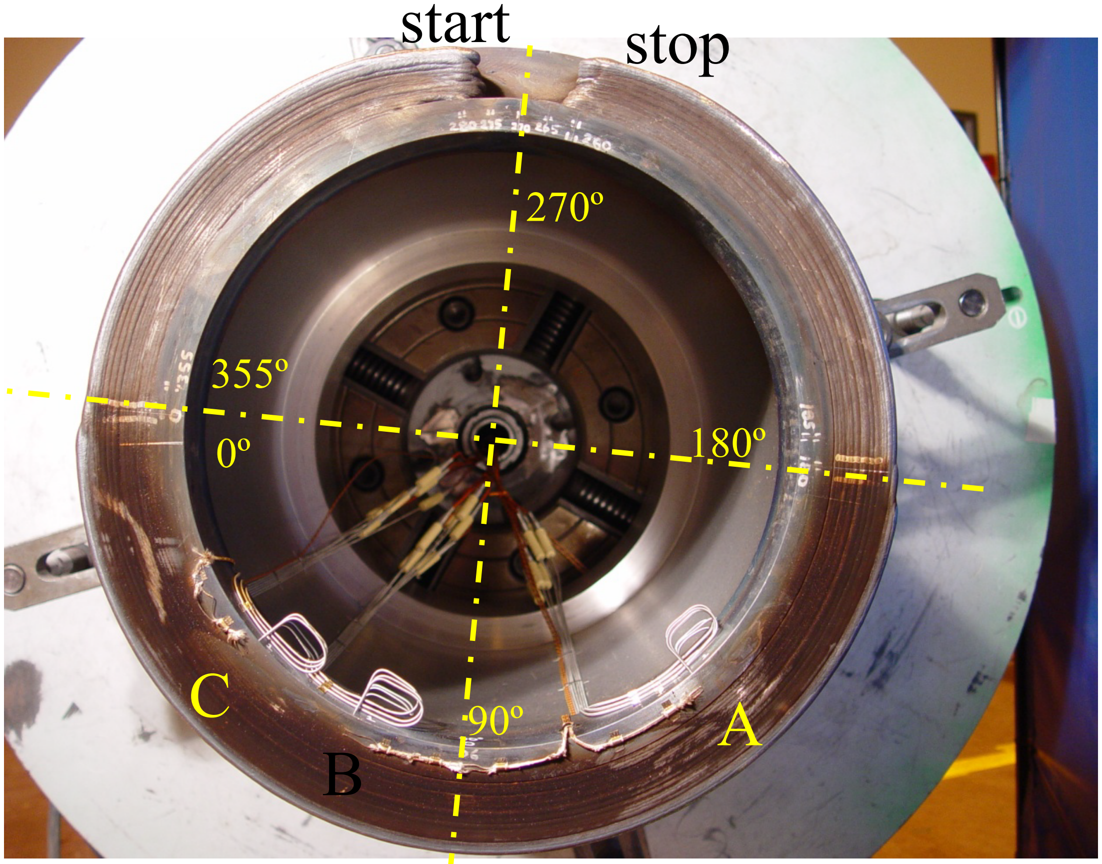

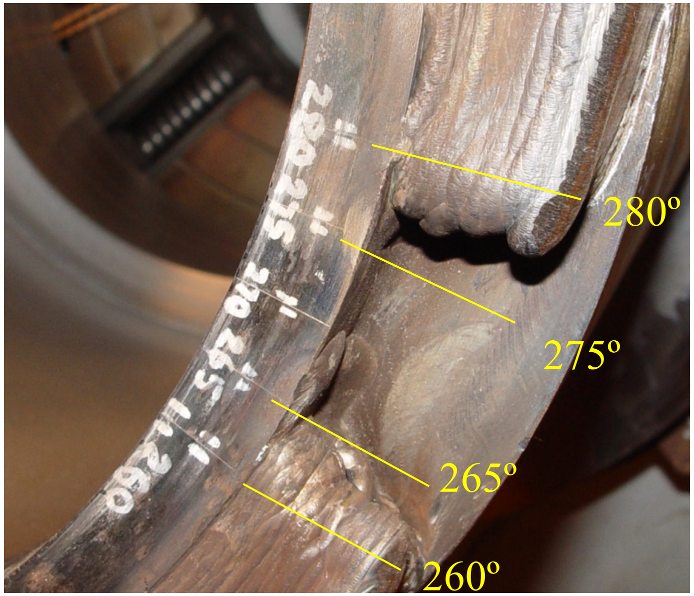

Non-cladding: 262.5º~277.5º

Etched Microstructures

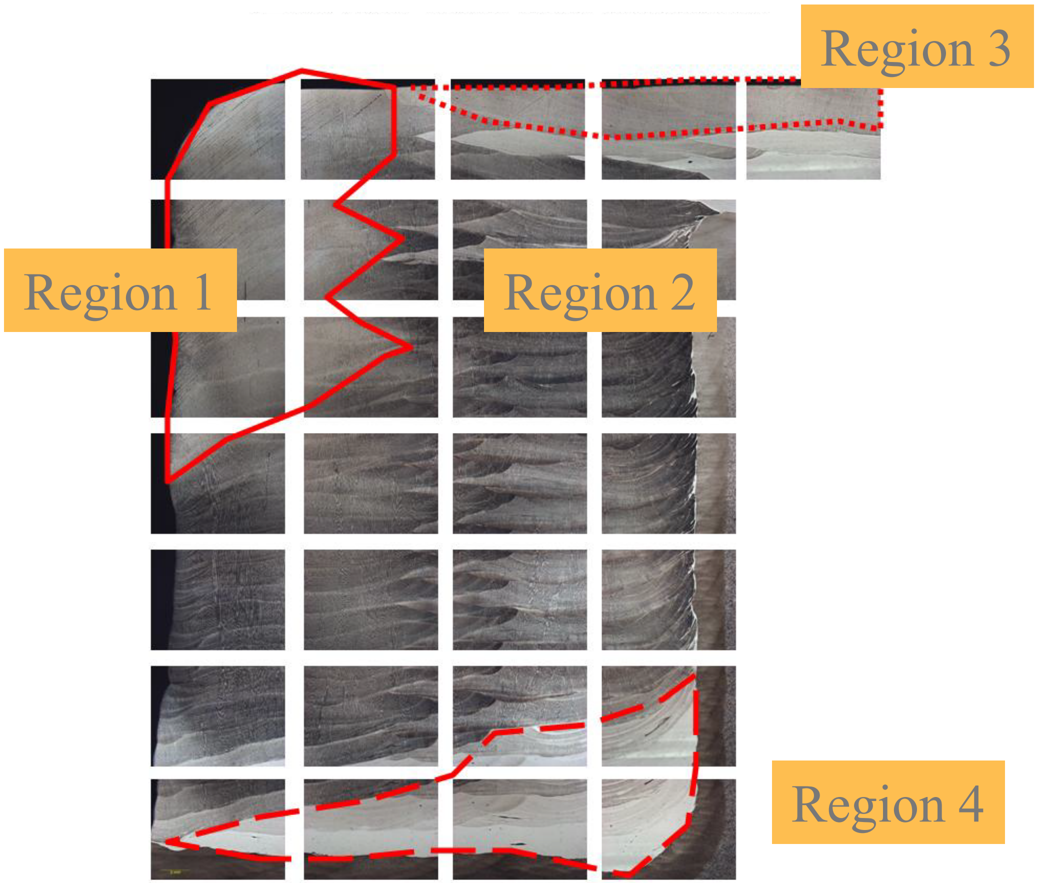

- Region 1
  - High cracking tendency
- Region 2
  - Reduced cracking tendency
- Region 3
  - Buttered region where cracks are observed
- Region 4
  - Mixed region

Summary of Experimental Study

- Experimental results show that the cracks are mainly located in the
  - outer bead region of cladding near the pipe OD surface
  - buttering region near the end of the pipe
- Finite element modeling was conducted to find the reason for the cracks

Modeling Process

- Model Validation
  - Predict fusion zone shape and size and compare with the experimental data
  - Predict temperature-time profiles and compare with the experimental data
- Model Prediction
  - Predict thermo-mechanical strain during solidification and during the following-on pass deposition

Modeling Approach

- Build a finite element model based on the mockup design and weld cross sections
- Thermal analysis and thermo-mechanical analysis performed with EWI weld FEA© software by inputting:
  - Temperature dependent thermal-physical and mechanical material properties
  - Cladding and buttering specifications
    - Preheating, interpass temperature, welding parameters, welding sequences, and torch weaving
  - Welding fixture

Finite Element Model

Three locations were modeled

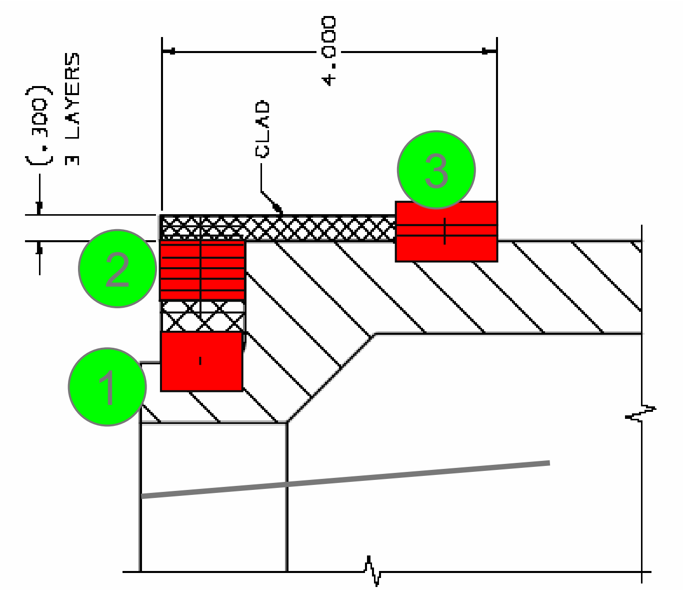

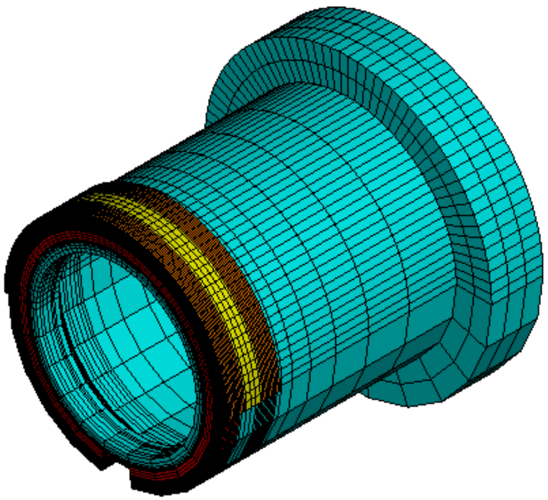

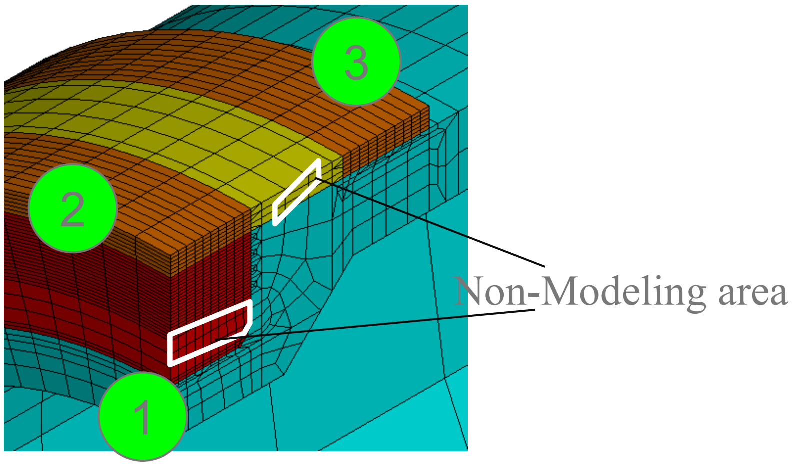

Fusion-Zone Comparison between Prediction and Experiment – Inner Bead of Cladding

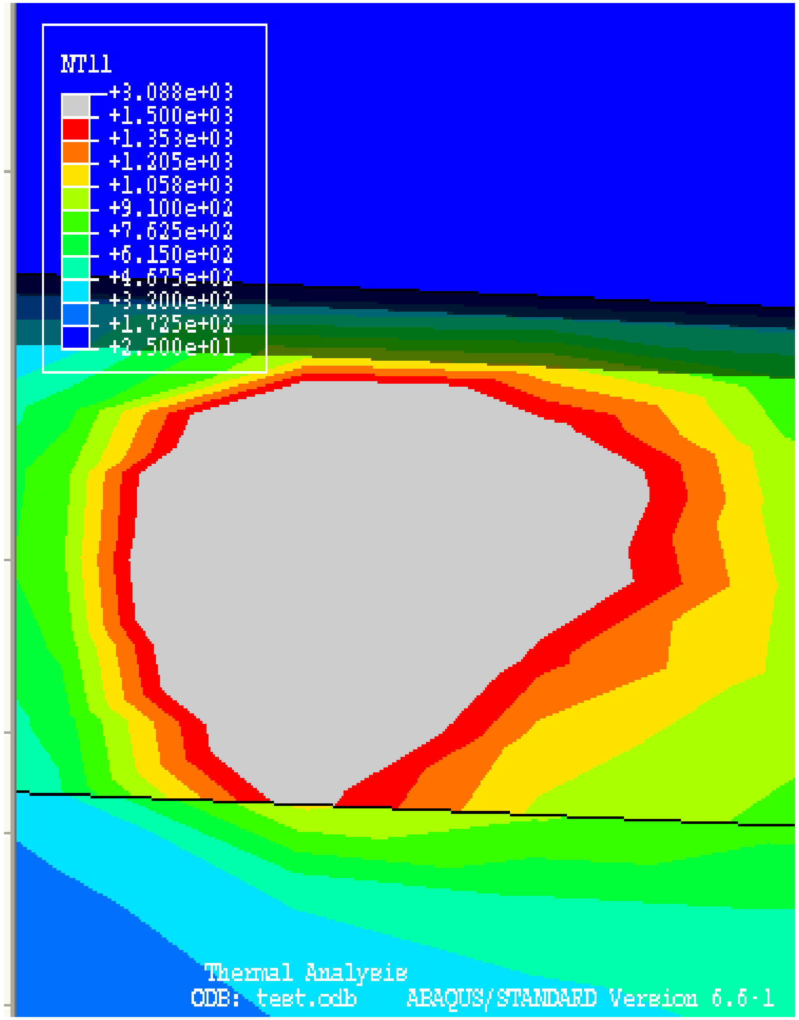

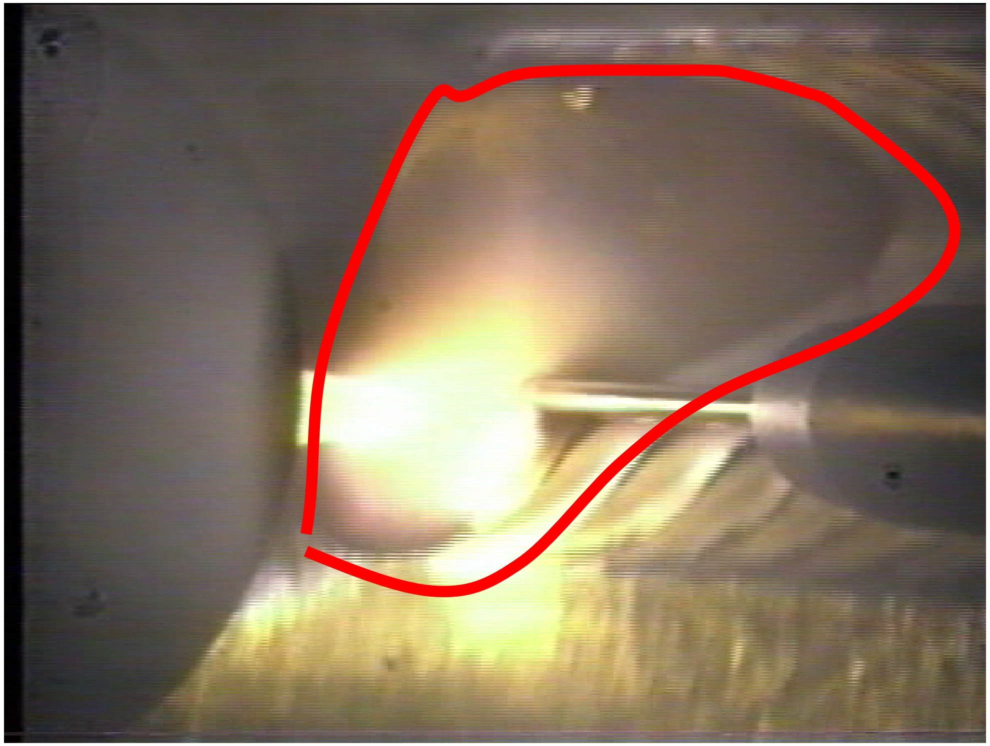

Fusion-Zone Comparison between Prediction and Experiment – Outer Bead of Cladding

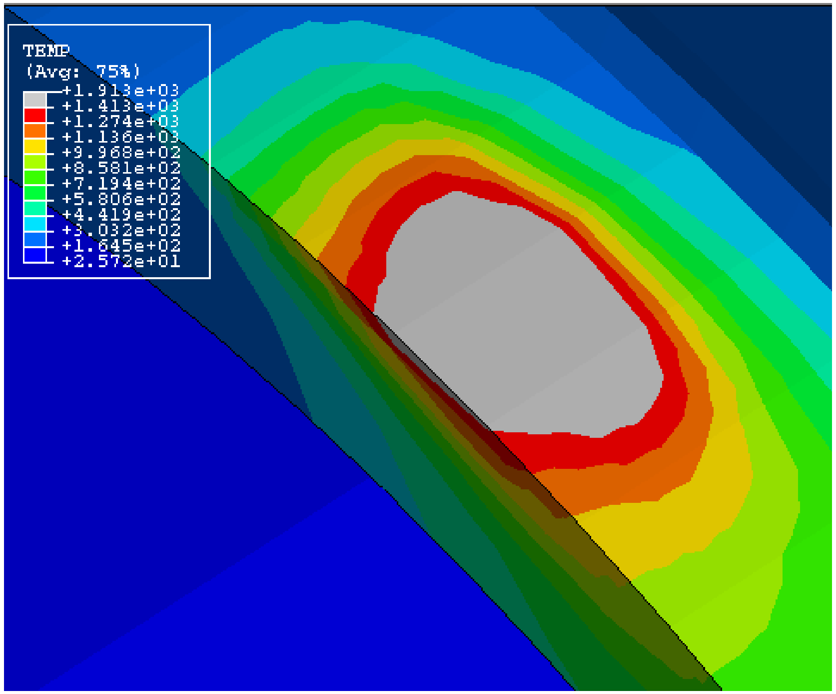

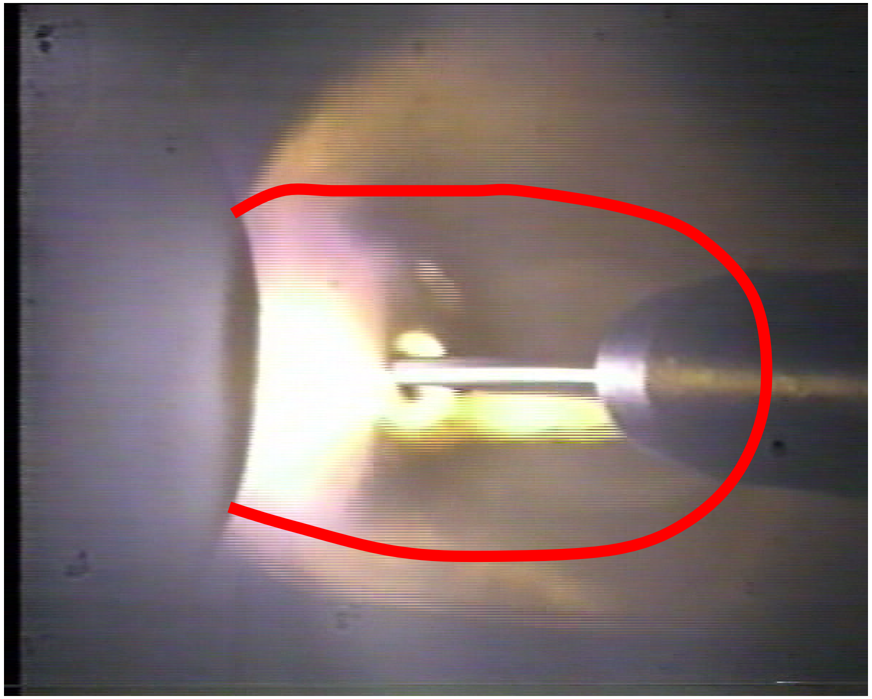

Bead 2 is a normal weld pool shape

Temperature Profile

Thermocouple Locations

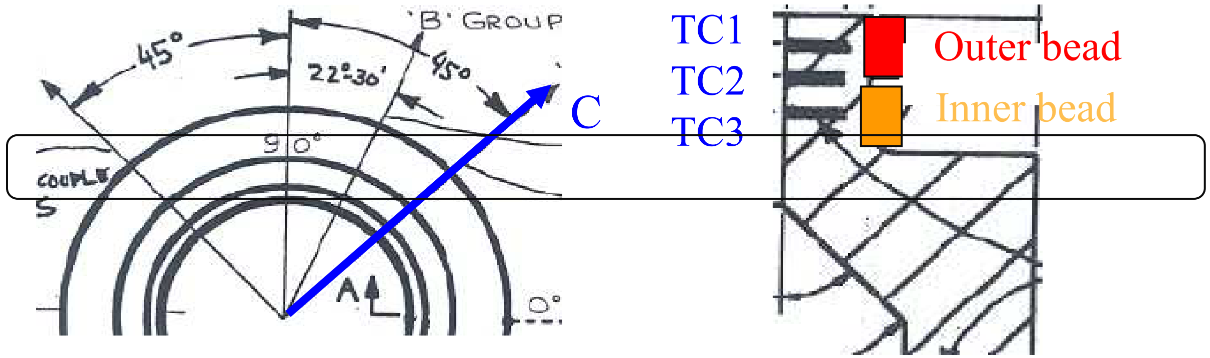

Thermocouple histories

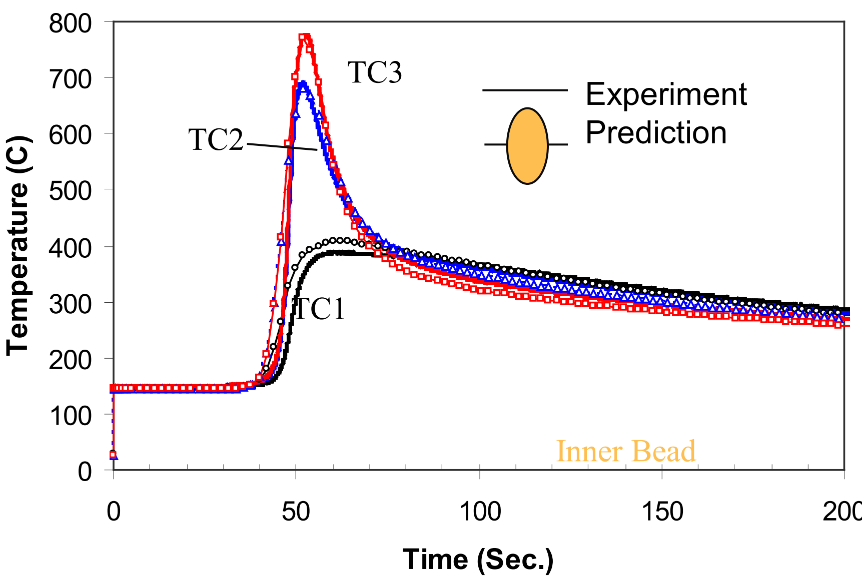

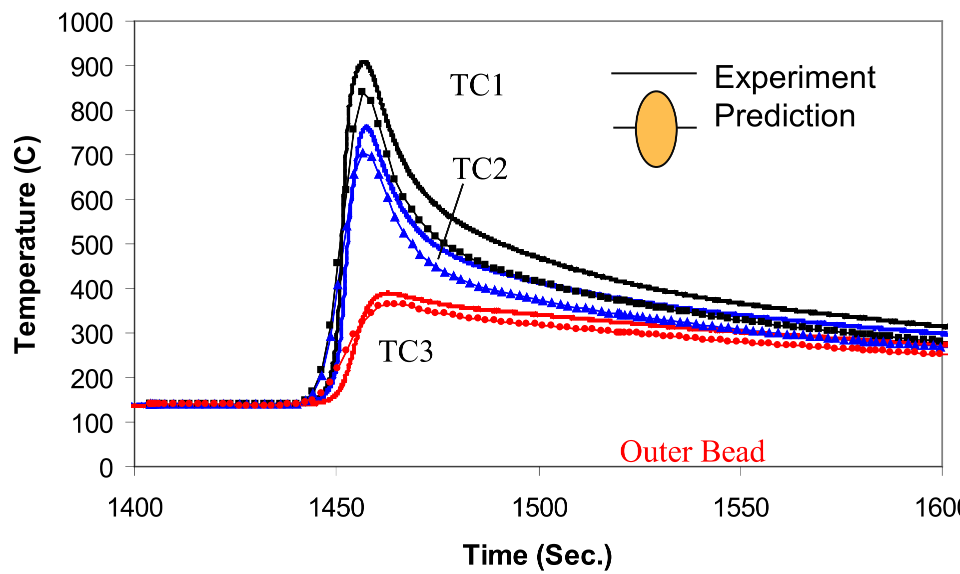

Maximum Temperature Comparison between Outer Bead and Inner Bead

Predicted maximum temperature

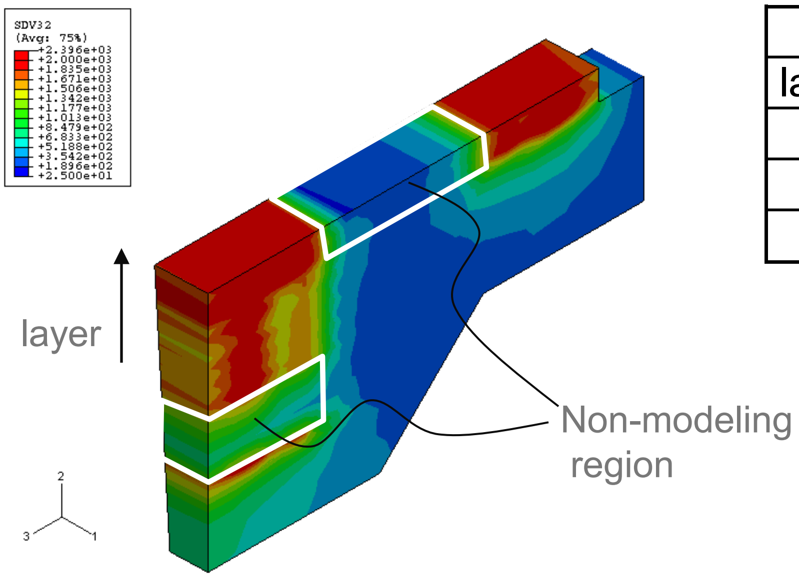

Experiments show that outer bead is always hotter.

	Maximum temperature, C		Temperature, C
layer	bead 1	bead 2	difference
1	765	898	133
2	548	728	180
3	438	637	199

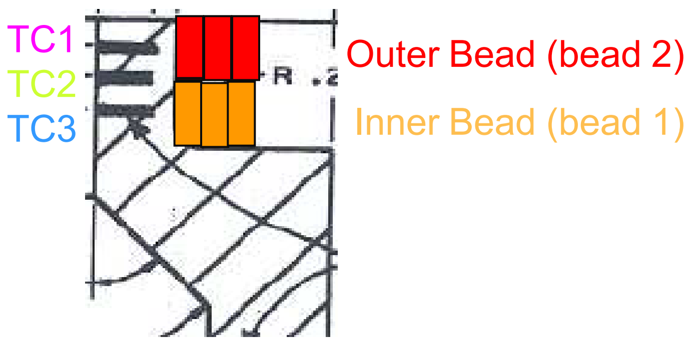

Temperature difference increasing between the outer bead and the inner bead as the layer number increases

Displacements Comparison between Experiment and Prediction

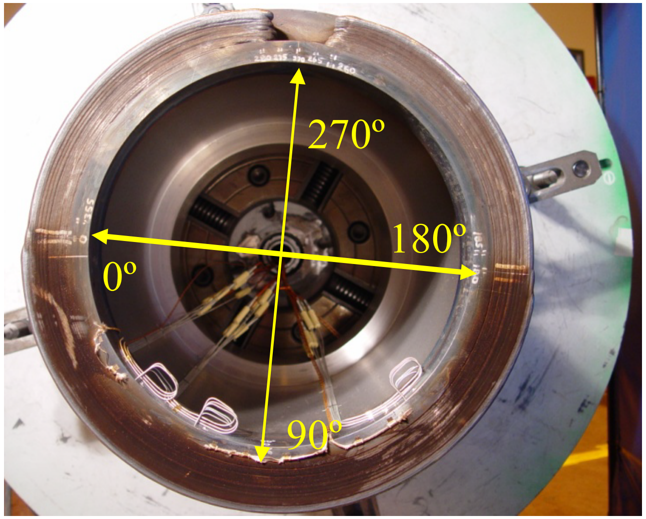

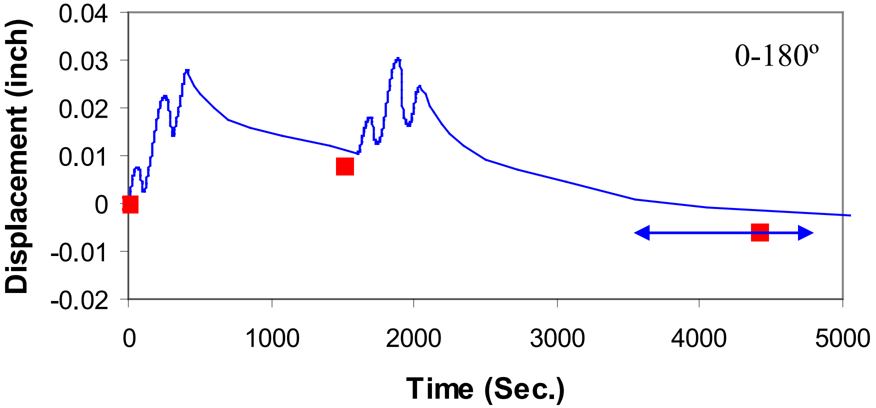

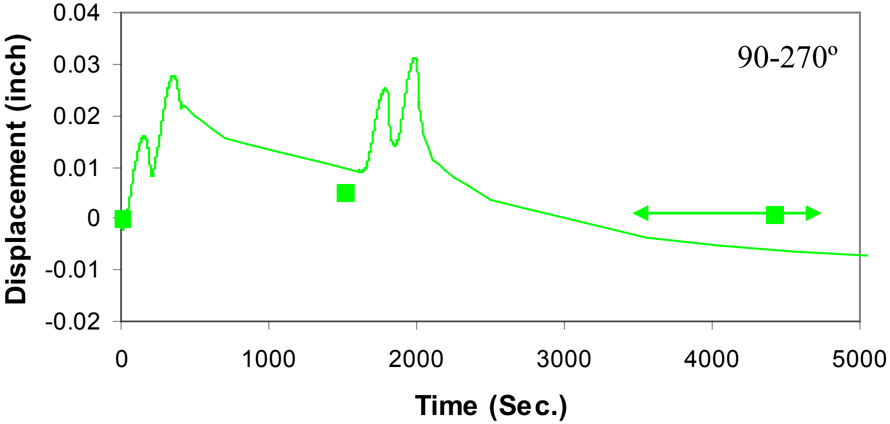

Summary of Model Validation

- Predicted fusion zone has a good agreement with experimental results.
- Predicted temperature-time history has a good agreement with experimental measured data.
- Higher temperature was observed at the outer bead by comparing with the inner bead from both experiment and modeling.

Crack Mitigation Studies

- Reduce the heat input of the outer region by 15%
- Original heat input
  - Cladding power input, 3900W
  - Buttering power input, 4800W
- New heat input
  - Cladding power input, 3315W
  - Buttering power input, 4080W
- Traveling Speed
  - 6.5 IPM

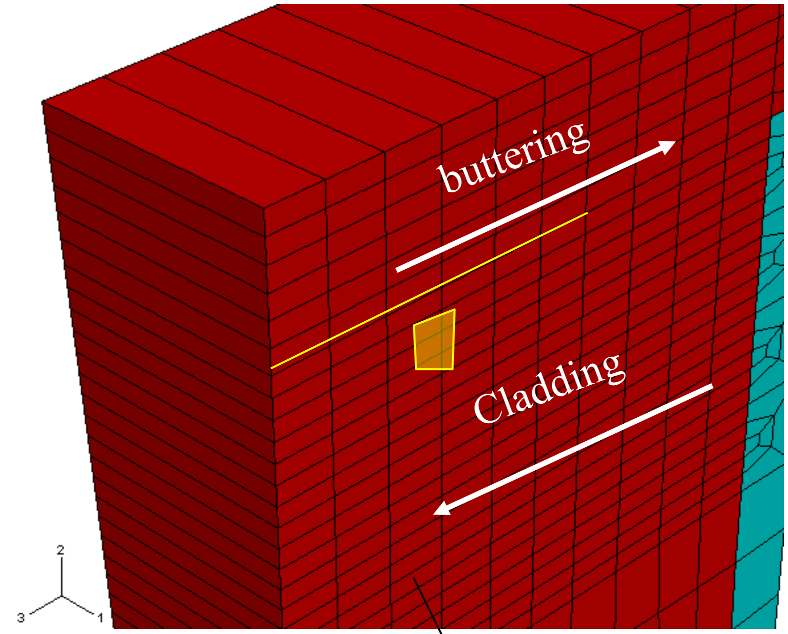

Heat input reduced area

Fusion-Zone Comparison between Two Heat Inputs

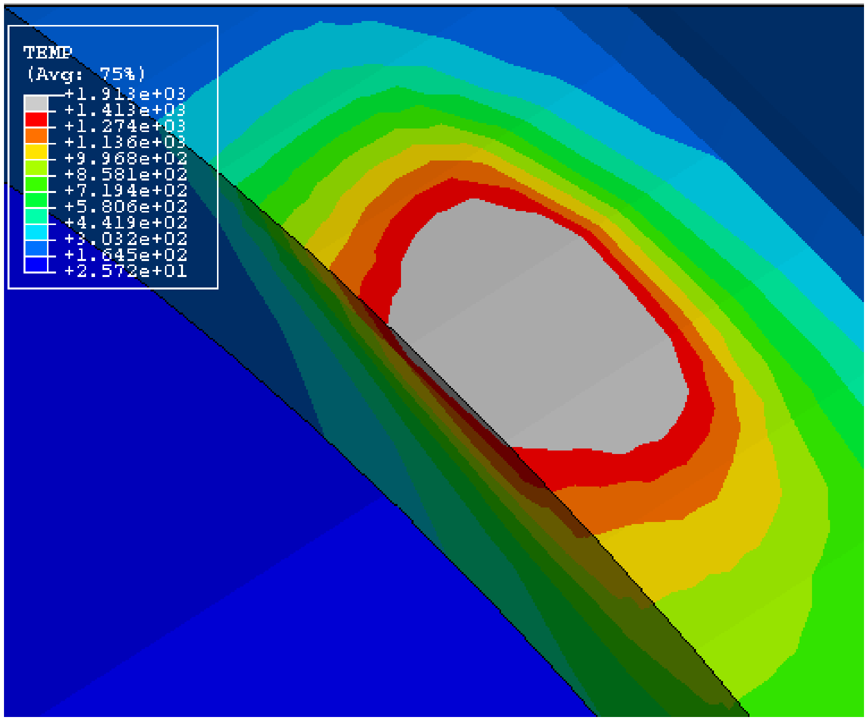

Normal Heat Input

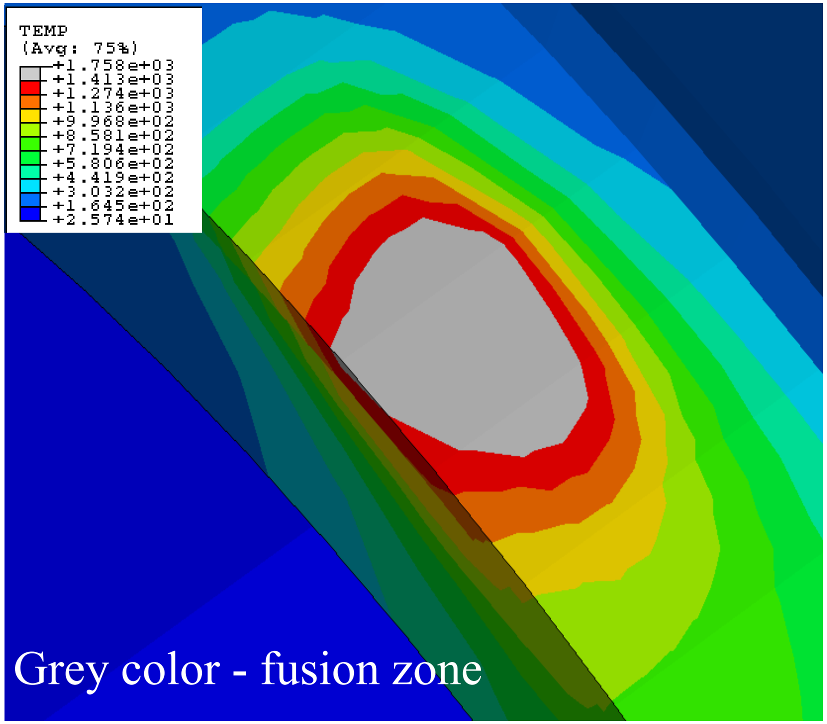

Reduced Power input by 15%

Temperature Comparison between Two Outer Bead Heat Inputs

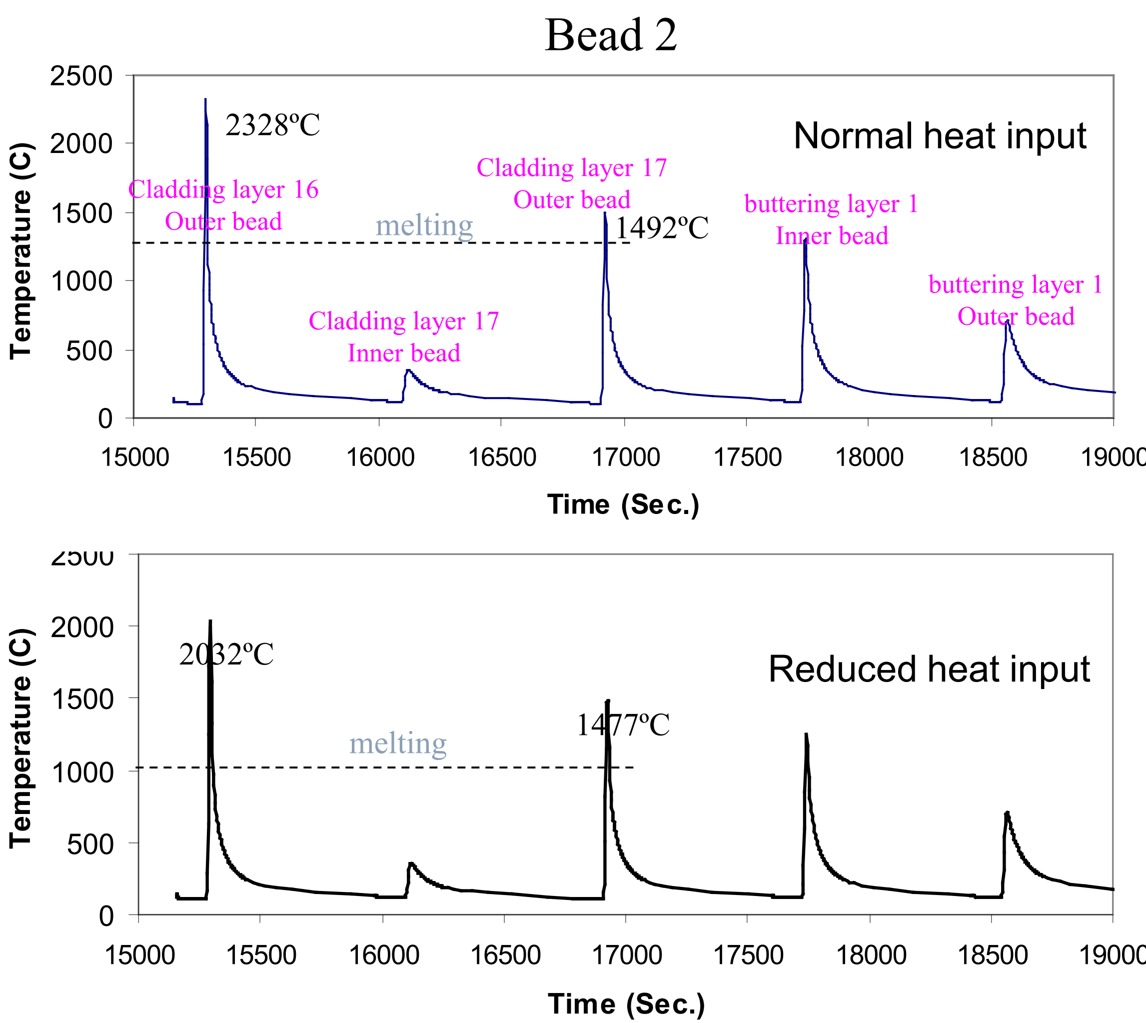

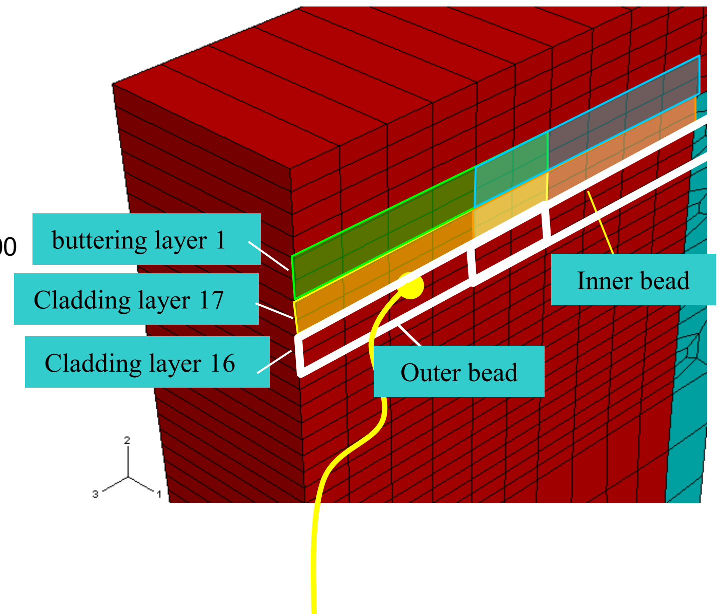

Result locations

Hoop Strain Comparison between Two Heat Inputs

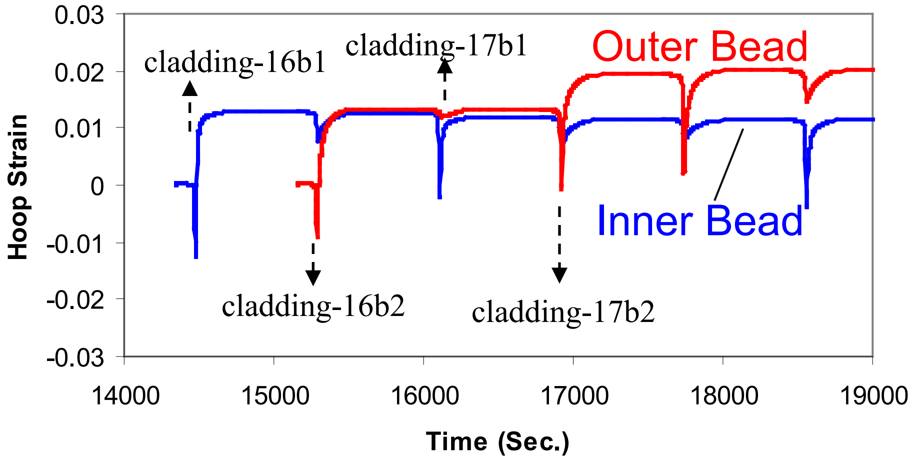

(a) Normal heat input

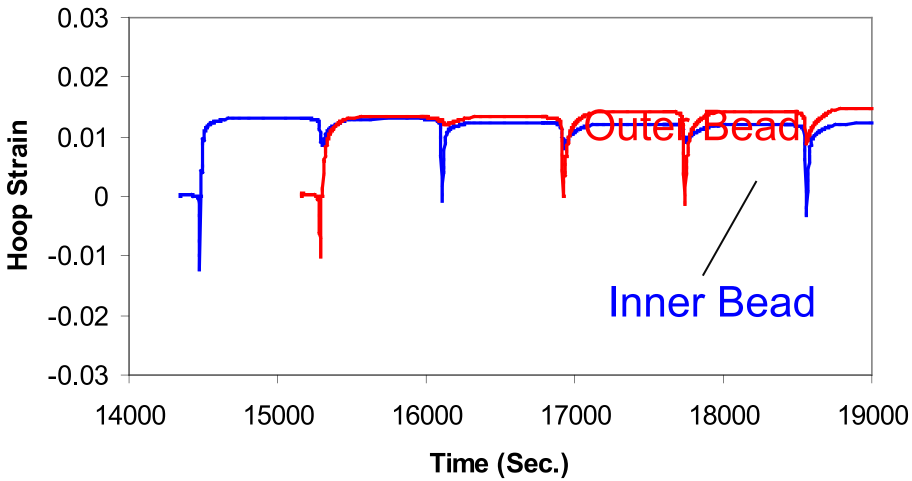

(b) Reduced heat input

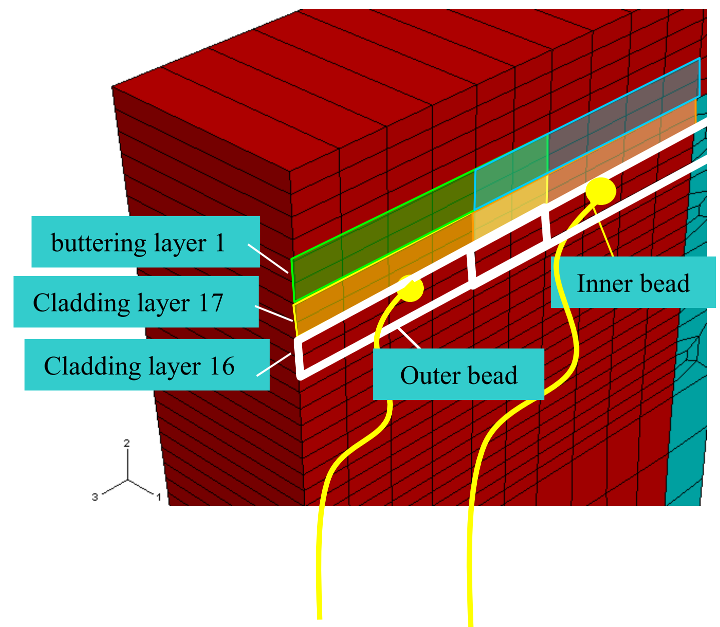

Result locations

Summary on Heat Input Study

- Predicted weld pool size using the reduced heat input is smaller than that using the normal heat input.
- The modeling results shows:
  - Thermo-mechanical strain is reduced by reducing heat input.
  - Reduced heat input may lead to reduced cracking tendency
- Production welding with reduced heat input has shown decreased susceptibility to cracking

Case Study 3: Replacement Steam Generator Divider Plate to Channel Head Weld Separation

- NRC Information Notice: 2010-7
- Released on April 5, 2010
- Title: welding defects in replacement steam generators

- Outline of the presentations
  - Circumstances
  - Failure Analyses
  - Root Cause Problem
  - Relevant to ASME Section X1; IWA-4461

Background

- The licensee, Southern California Edison (SCE), contracted Mitsubishi Heavy Industries (MHI), to manufacture four RSGs in Japan for installation at San Onofre Nuclear Generating Station (SONGS) Units 2 and 3.
- MHI completed manufacturing and testing of the first two RSGs in 2008 and shipped them to SONGS Unit 2 for scheduled installation in October 2009.
- MHI was scheduled to complete manufacturing and testing of the two RSGs for SONGS Unit 3 in 2009.

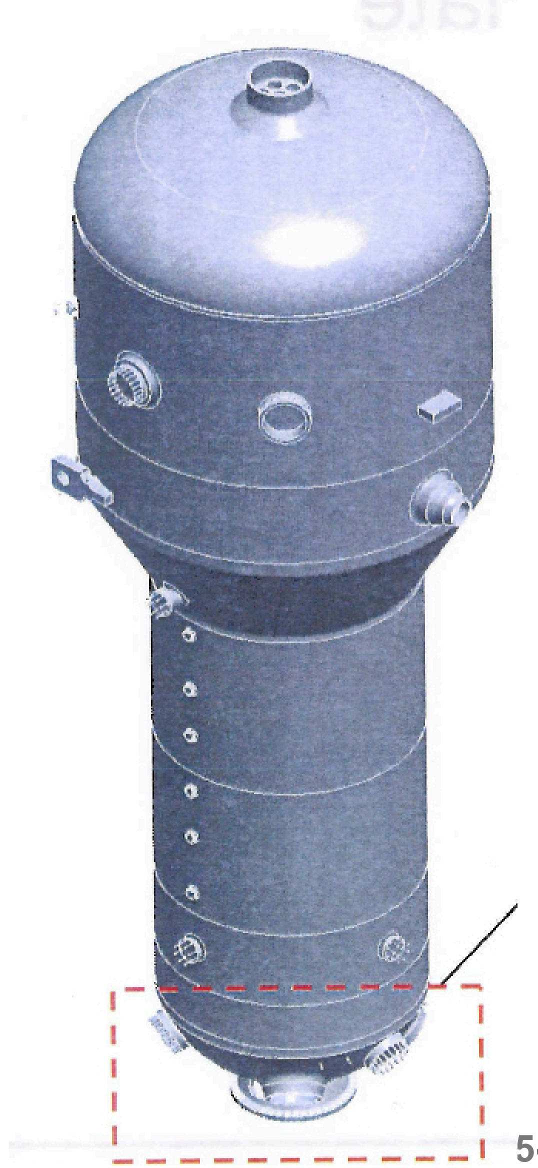

Routine Visual Inspection Showed a Crack

- After completion of the ASME Boiler and Pressure Vessel Code (ASME Code), Section III primary and secondary side hydrostatic pressure test on the SONGS Unit 3 “B” RSG.
- 5-inch long surface flaw (crack) in the dissimilar metal weld between the divider plate, made from Alloy 690, and the channel head, made from low-alloy steel (LAS).

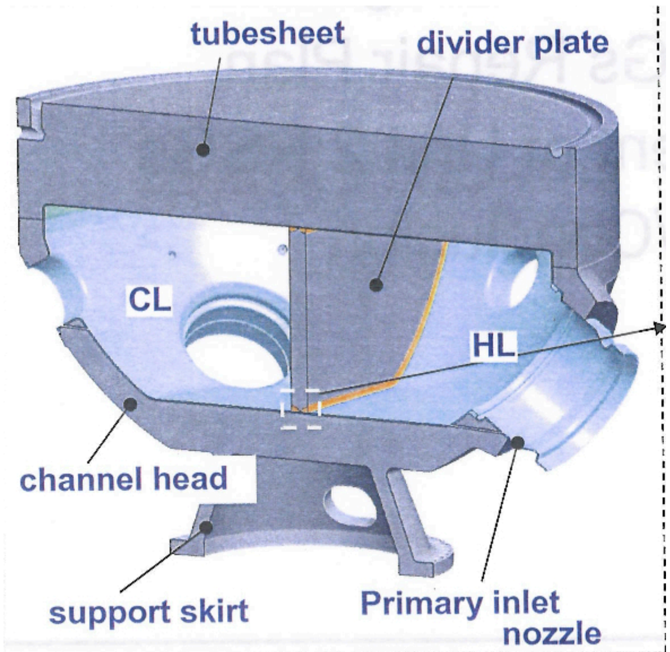

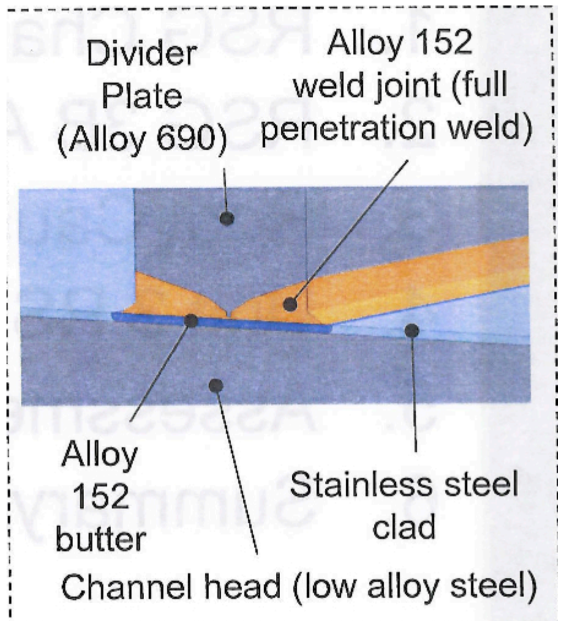

Flaw was observed in regions between the low-alloy-steel and alloy 152 layer

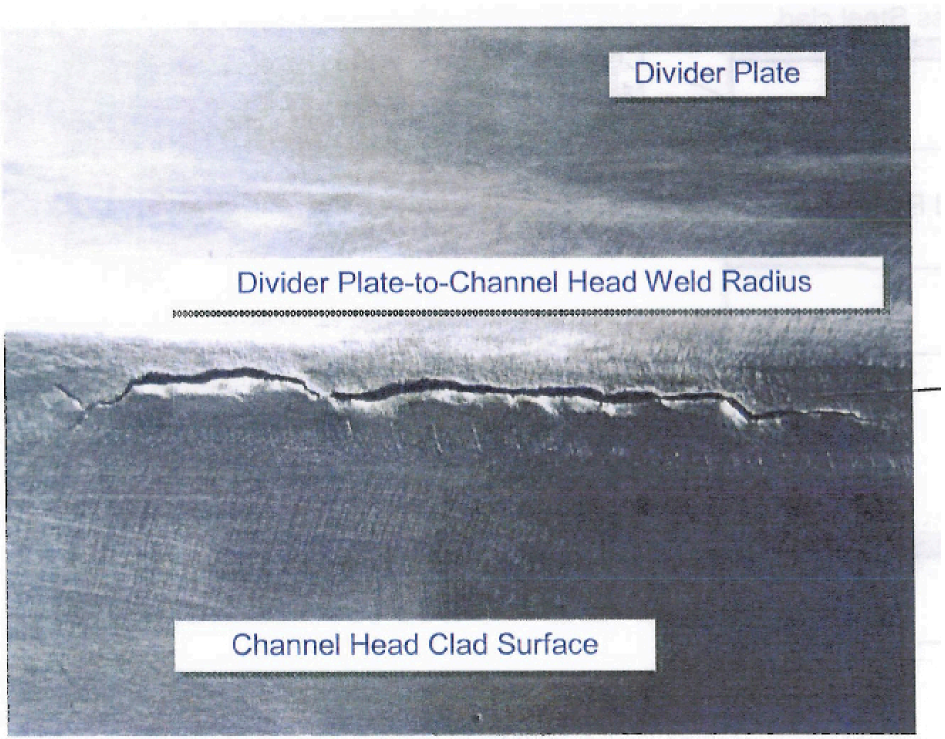

RSG 3B Cold-Side Crack in Divider Plate-to-Channel Head Weld

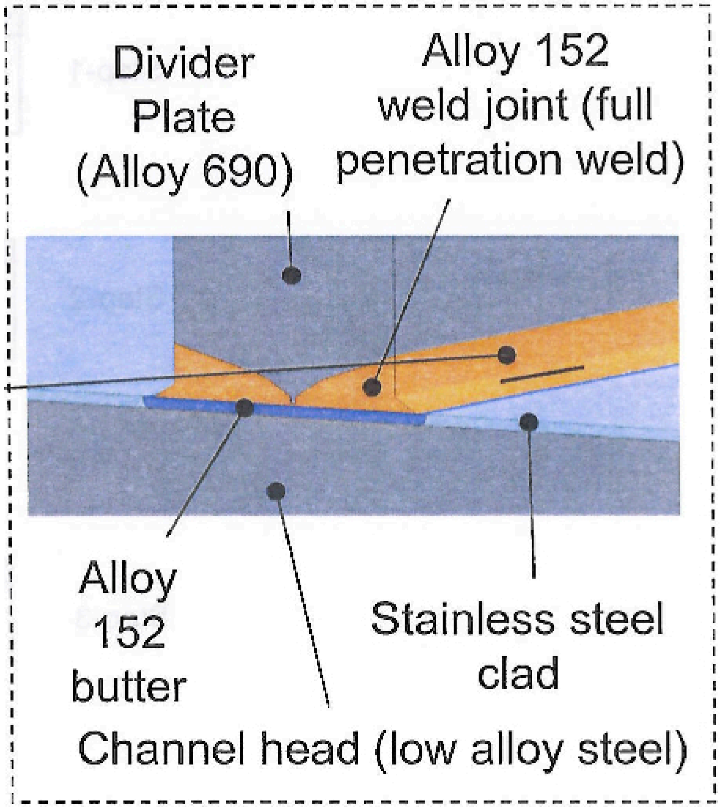

- Where and when did the crack start?

Fabrication Procedure

- Clad; carbon arc gouge and then butter;
- Surface cracks were observed after the clad removal
- Higher carbon content observed in the fusion zone
- Higher than expected hardness in the HAZ region of low-alloy steel

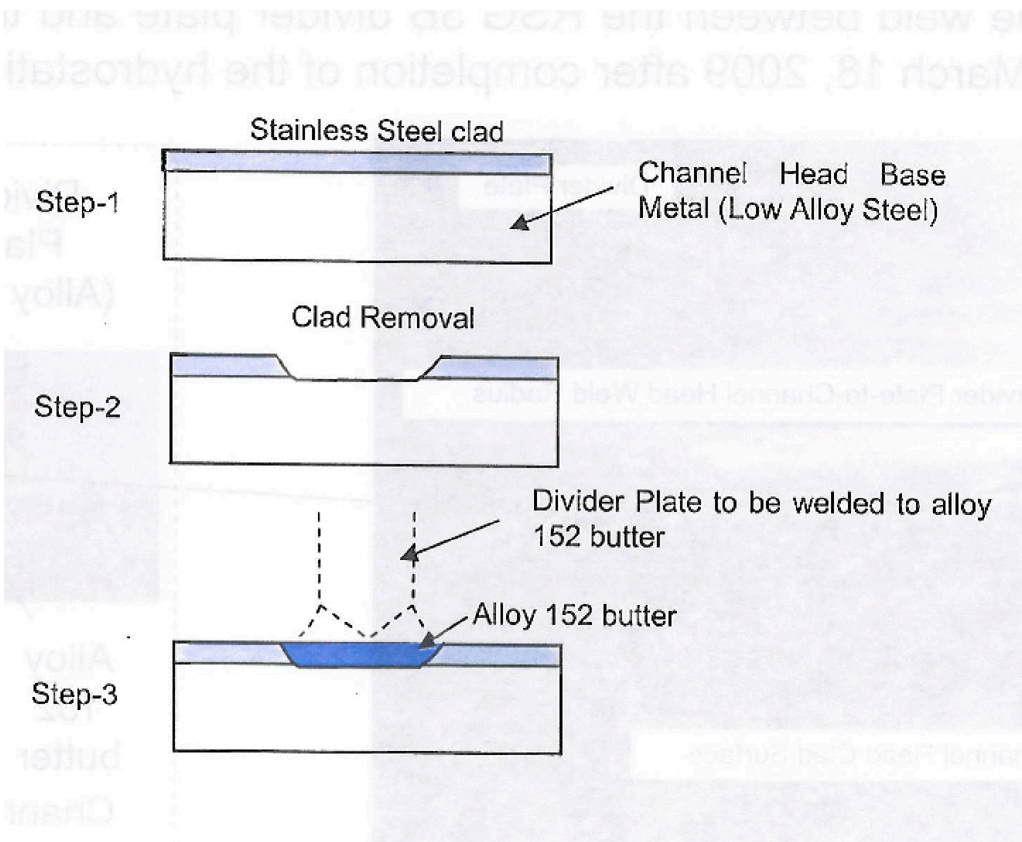

Results from Mock-up Confirm Brittle Regions

Mockup - gouging showing case hardening locations

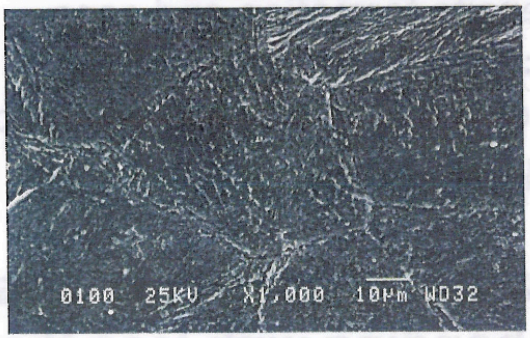

Boat Sample

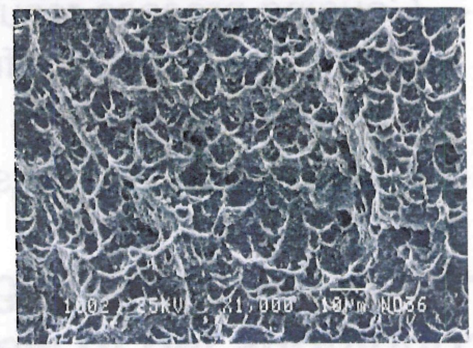

Poor bonding – flat, featureless surface at fusion boundary

Good bonding – ductile failure in weld

- Is there any other effect possible?

Hydrogen induced cracking cannot be eliminated

- Unable to completely exclude Hydrogen Induced Cracking (HIC)
  - Mockup tests with hydrogen added reproduced brittle failure
  - Gouging produces higher hardness
  - Higher stress provided by steeper weld joint edge (gouging)
- May leave the butter to base metal weld more vulnerable to hydrogen-induced cracking
- Speculation that welding rod controls may have contributed moisture

- Remember the three components for HIC cracking; stress, microstructure and hydrogen levels

Improper Air carbon arc gouging technique may lead to carbon pick up

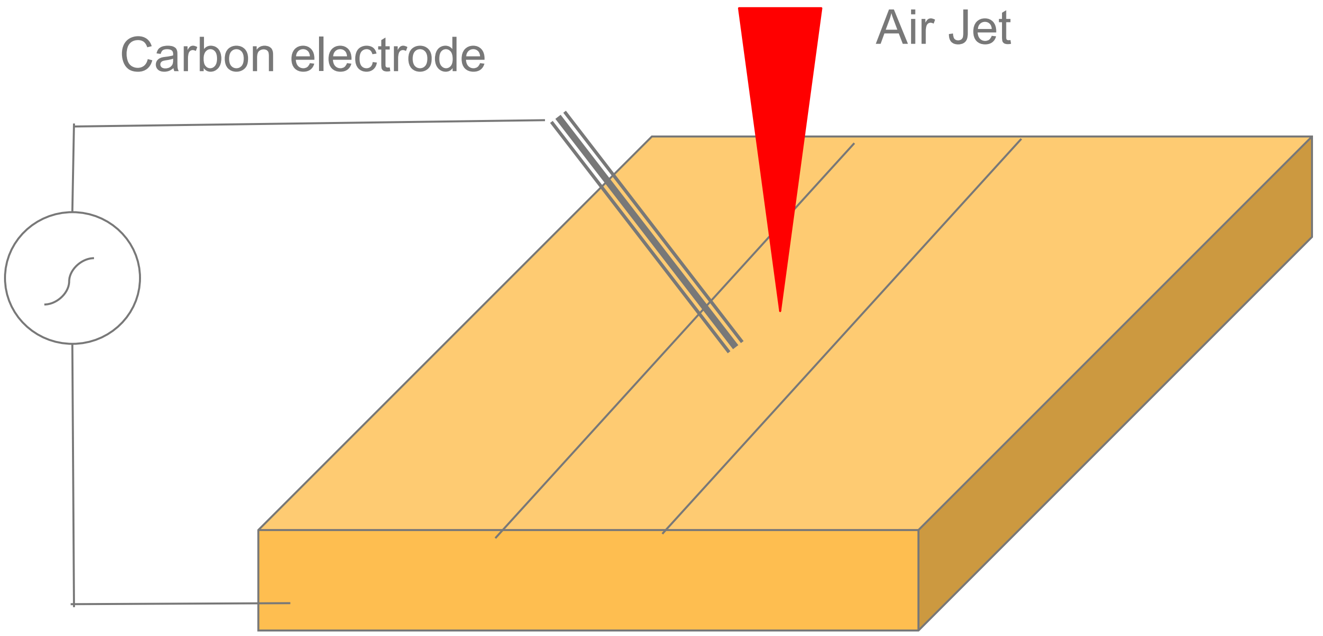

- Carbon is indeed consumed during this process. The air stream should remove carbon-rich metal from the groove to leave only minimal contamination of the sidewalls. Poor gouging technique or insufficient air flow will result in carbon pick-up!!! (See reference from TWI web page)
- Let us evaluate the sensitivity of rapid cooling and carbon pick up with CCT diagrams (calculations.ewi.org)

Effect of Carbon on Steel Phase Transformations

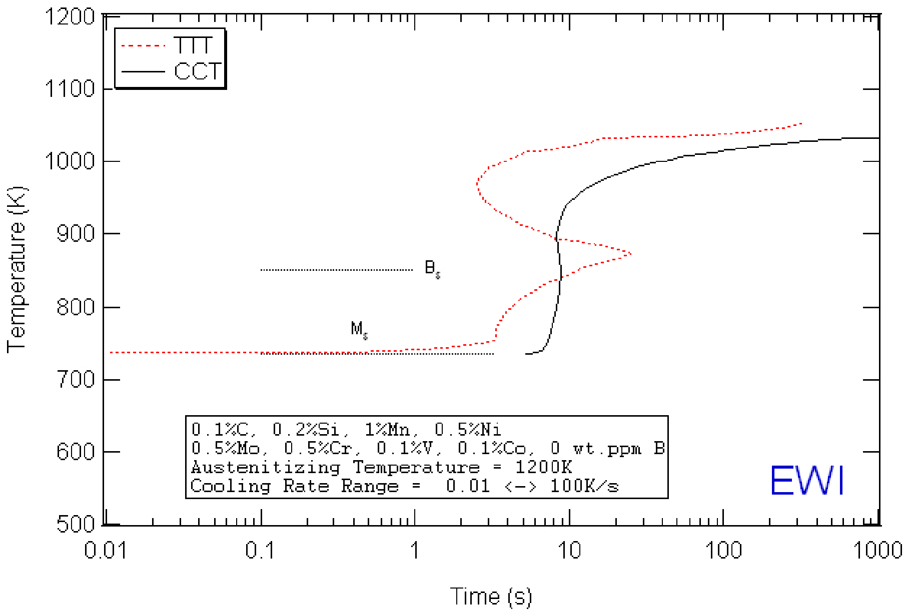

- Carbon pick up will make the steel more hardenable and will lead to cracking!

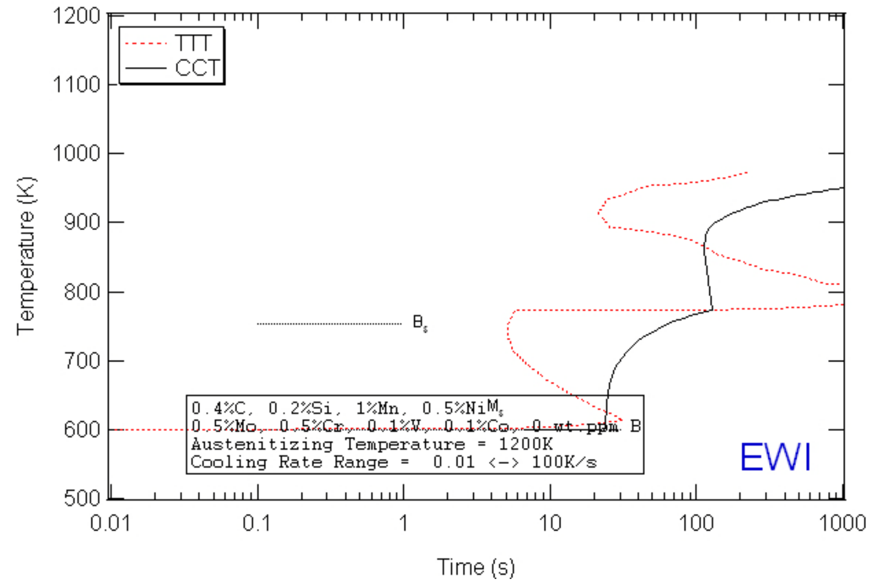

Remedial Action - Conclusions

- ACAG is not specifically covered in Section III of the ASME Code; however, ASME Code, Section XI, IWA-4461 covers the qualification and use of a thermal removal process like ACAG. In addition, 10 CFR 50.55a(b)(2)(xxiii) states:
- The use of provisions to eliminate the mechanical processing of thermally cut surfaces in IWA-4461.4.2 of Section XI, 2001 Edition through the latest edition and addenda incorporated by reference in paragraph (b)(2) of 10 CFR 50.55a are prohibited.
- Although all specific requirements or standards were met, this event illustrates that control over all aspects of welding ASME Code Class 1, 2, and 3 components can prevent welding defects like those found in the RSGs for SONGS Unit 3 from occurring.